PROFILING ESTER PRODRUG ACTIVATION: AN ACTIVITY BASED PROTEIN PROFILING (ABPP) APPROACH

By

Hao Xu

A dissertation submitted in partial fulfillment
of the requirements for the degree of
Doctor of Philosophy
(Medicinal Chemistry)
In the University of Michigan
2015

Doctoral Committee:

Professor Gordon L. Amidon, Co-Chair
Professor Hollis H. Showalter, Co-Chair
Professor George A. Garcia
Professor Anna K. Mapp
Assistant Professor Brent R. Martin

DEDICATION

To my family,
To my father, Xu Kesheng, and my mother, Li Xiujuan,
who raised me up and shaped my character.

ACKNOWLEDGEMENT

Too much appreciation needs to be expressed along this most important part of my life. I would like to thank Dr. Gordon L. Amidon for offering me the chance to be his student, to work and study with him, the opportunity that many people dream of. From the excellent working environment Dr. Amidon provided, I learned not only experimental techniques through various research experiences, but also ways of collaborating with different people, exploring the unknown world and the art of sciences. His treatment of people with sincerity and genuine consideration has been of such influence during my training that it will carry through to my future endeavors, and it is a great treasure I will possess for the rest of my life.

One benefit of being trained under co-mentorship is that every aspect learned and experienced is doubled. Dr. Hollis H. Showalter, as my co-advisor, gave me the warmest and most unforgettable welcome to his group and VMCC synthesis core when I joined Department of Medicinal Chemistry in the early days. He guided me through the tough first two years of training like a grandfather, and dramatically expanded my knowledge of organic synthesis and medicinal chemistry. His insightful advice on the general synthetic scheme, concise suggestions on detailed experimental manipulation and marvelous choice of specific reaction conditions all together form the basis for my successfully synthesized compounds.

I am also appreciative of the efforts of my committee members, Drs. George Garcia, Anna Mapp, and Brent Martin. Their advice and many discussions through years have always been

constructive and enlightening. I would specifically thank Dr. Brent Martin for his scientific guidance which was invaluable in the success of my activity-based protein profiling project. Dr. Jaimeen Majmudar and Dahvid Davda from Dr. Martin's lab are appreciated for their generous help on proteomic and enzymatic studies.

I am so fortunate to have so many great people in the lab to work with. I thank Drs. Chester Provoda and Yasuhiro Tsume. It is their occasional jokes through email and daily "cupping competition" that highlights my everyday bench work. I also thank Dr. Kefeng Sun for his advices to me, Ki H. Kim for his great help of sharing my lab works. I also thank Laura Radecki, Jing Sun, Brain J. Krieg, Deanna Mudie, Arjang Talattof, Takeuchi Susumu, Kazuki Matsui, Juhee Lee, Oluseyi Adeniyi, Allison Matyas, Longsheng Lai and also my friends from VMCC: Yafei Jin, Rod Sorenson, Allen Brooks, Fardokht Abulwerdi. Their friendship, encouragement, tolerance, and presence will be invaluable memories in the future.

I am particularly grateful to Gail Benninghoff for her kind and efficient assistance on scheduling my appointments with Dr. Amidon and preparing administrative documents. I also would like to thank Pat Greeley, L.D. Hieber, Pamela Armstrong, Antoinette Hopper, Elaine Griffin for their tremendous help on administrative affairs in the College of Pharmacy.

Lastly, I need to thank my mother and father for their encouragement and continuous support as I studied abroad, and for their unconditional love and care.

TABLE OF CONTENTS

LIST OF FIGURES

LIST OF TABLES

LIST OF SCHEMES

LIST OF APPENDICES

LIST OF ABBREVIATIONS

ABPP - activity-based protein profiling

ACN - acetonitrile

ADMET - absorption, distribution, metabolism, elimination, toxicity

ABESF - 4-(2-Aminoethyl) benzenesulfonyl fluoride hydrochloride

AUC - area under the curve

BCA - bicinchoninic acid assay

BCS - biopharmaceutical classification system

BNPP - bis-(4-nitrophenyl) phosphate

BPHL - biphenyl hydrolase-like (serine hydrolase)

Caco-2 - human epithelial colorectal adenocarcinoma cells

$CDCl_3$ - deuterated chloroform

DDI - drug-drug interaction

CD_3OD - deuterated methanol

DE - dabigatran etexilate

CES - carboxylesterase

DAST - (diethylamino)sulfur trifluoride

DFP - diisopropyl fluorophosphonate

DIPEA - *N*,*N*-diisopropylethylamine

DMEM - Dulbecco's modified eagle medium

DMF – *N*,*N*-dimethylformamide

DMSO - dimethyl sulfoxide

DTT - dithiothreitol

EDC·HCl - 1-ethyl-3-[3-dimethylaminopropyl]carbodiimide hydrochloride

FAAH - fatty acid amide hydrolase

FBS - fetal bovine serum

FDA - Food and Drug administration

FP - fluorophosphonate

GI - gastrointestinal

GIS - gastrointestinal simulator

GSTO1 - glutathione S-transferase omega-1

Hep G2 - human liver carcinoma cell line

HI - human small intestinal tissue

HOBt - *N*-hydroxybenzotriazole

HP - human pancreatic tissue

HPLC - high performance liquid chromatography

HRMS - high resolution mass spectrometry

kD - kilodalton

KI - potassium iodide

KOH - potassium hydroxide

LC/MS - liquid chromatography/mass spectrometry

MAGL - monoacylglycerol lipase

MDR - multidrug-resistant

MgSO4 - magnesium sulfate

MIF - mouse intestinal fluid

MTB - mycobacterium tuberculosis

Na2S2O3 - sodium thiosulfate

NMR - nuclear magnetic resonance

O.C. - oseltamivir carboxylate

PAGE - polyacrylamide gel electrophoresis

PD - pharmacodynamics

PEG - polyethylene glycols

P-gp - P-glycoprotein

PMSF - phenylmethanesulfonyl fluoride

PK - pharmacokinetics

PVDF - polyvinylidene fluoride

rh - rhodamine

RLZ - rifalazil

RMP - rifampin

SDS - sodium dodecyl sulfate

SH - serine hydrolase

SILAC - stable isotope labeling of amino acids in cell culture

TB - tuberculosis

TBS - tert-Butyldimethylsilyl

THF - tetrahydrofuran

TFA - trifluoroacetic acid

TLC - thin layer chromatography

TPI1 - triosephosphate isomerase

Tris - tris(hydroxymethyl)aminomethane

UPLC - ultra Performance Liquid Chromatography

USP - United States Pharmacopeia

UV- ultraviolet

WHO - World Health Organization

XDR - extensively drug-resistant

Chapter 1

INTRODUCTION

1.1 Prodrug approach

Advances in modern genomics and proteomics technologies make drug discovery much more complex than decades ago. Although the identification of new drug substances by high-throughput screening has provided medicinal chemists a powerful tool of exploring more chemical scaffolds for better efficacy, the pharmaceutical parameters of a new molecule with satisfying physicochemical properties make small-molecule drug design more and more challenging. Compounds are generally built with proper structural features that will meet pharmacokinetic (PK) and pharmacodynamic (PD) criteria, as well as maintain efficacy and safety. However, when good biological activity unavoidably leads to problematic pharmaceutical or pharmacokinetic properties, resulting in a situation that is unsolvable by structural modification of a targeted scaffold, a prodrug approach is often considered.[1]

The prodrug concept was introduced in 1958 by Adrien Albert[2] to describe pharmacologically inactive therapeutics which then can be transformed *in vivo* to active metabolites after being absorbed. Prodrugs are designed to improve undesirable properties, such as poor ADMET (absorption, distribution, metabolism, elimination, toxicity) of pharmacologically active compounds. Historically, the design of a prodrug strategy was "an act of desperation"; it was considered only when structure-activity relationship studies could not bridge the incompatibility

between pharmacological activity and non-optimal pharmaceutical parameters.[3] Many prodrug examples have been found to improve the drugs aqueous solubility, enhance passive intestinal absorption, and protect again fast metabolism, etc.[4] Other prodrugs with efforts beyond the modification of physicochemical properties have also been reported targeting an intestinal transporter, such as valacyclovir.[5, 6] Nevertheless, with the exploration of pharmaceutical sciences at the molecular level, drug delivery technologies facilitated by prodrug approaches can be extended to many other aspects. In recent years prodrugs designed for tissue-selective delivery have become an interesting area of study in addition to increasing the overall bioavailability.[7] By attaching specific pro-moieties, drugs could be locally concentrated by the corresponding transporter (Levodopa[8]) /surface antigens (Gemtuzunab ozogamicin[9]) or special pro-moieties could be hydrolyzed by unique enzymes in targeted areas by selective activation.[7] These approaches are able to significantly reduce the concentration of parent drugs in the whole body circulation, thus reduce their toxicity.

1.2 Activating Enzymes

The prodrug approach has been successful in many therapeutic areas such as marketed anticancer, antiviral, anti-inflammatory agents and angiotensin-converting-enzyme inhibitors.[4, 10] However, various challenges still exist and work is needed in preclinical and clinical studies to understand the mechanisms of enzymatic activation of prodrugs. After achieving the desire site of delivery, prodrugs must be converted to the active form either enzymatically or chemically prior to eliciting their pharmacological effect. When prodrugs are chemically activated, the effects from enzymatic variations are negligible. But there are only very few reported prodrugs relying purely on chemical activation[11, 12] likely due to stability issues and the uncertainty of activation sites.

Most marketed prodrugs are activated enzymatically. There are many advantages of enzymatic prodrug activation although disadvantages such as interspecies differences, drug-drug interactions, and enzymatic polymorphisms have posed great challenges for prodrug design.

The most common prodrugs utilize ester bonds to link the drugs to alkyls, amino acids, and phosphates as the pro-moieties, which are then hydrolyzed by esterases, peptidases, phosphatases, and other similar metabolizing enzymes after the prodrugs have been absorbed. Even though prodrugs contribute a clear benefit to drug development, the application of the strategy is still being debated as it introduces extra complexity due to the requirement of enzymatic activation. This activation is greatly challenged by interspecies (differences of activating ability between mice, dog, human)[13] and intraspecies (genetic polymorphism of activating enzymes) variabilities.[14] Thus these activating enzymes and associated mechanisms present pivotal obstacles toward a broader application of prodrugs. Unfortunately, the activation mechanisms have been lagging compared to the commercialization of many prodrugs. For example, the activating enzyme valacyclovirase (BPHL) for valacyclovir, which was approved by FDA in 1995, was not identified until 2003.[15] Dabigatran etexilate was approved in 2010 and its PK and pharmacodynamic parameters have been characterized in detail,[16, 17] but its activating enzymes were not reported until recently.[18] These examples highlight the present challenges and need in developing a mechanistic understanding of prodrug activation in drug delivery.

1.3 Activity-Based Protein Profiling (ABPP)

Activity-based protein profiling is a powerful chemical proteomic tool which is able to annotate the functions of different classes of enzymes.[19-21] Specific chemical compounds as ABPP probes

are designed to target certain enzyme subclasses on an active-site-directed basis in proteomic samples from cell lines or animal tissues (Figure 1.1).[22-26]

ABPP chemical probes essentially consist of three building blocks: a reactive group, a spacer/linker, and an analytical tag. The reactive groups with different chemical scaffolds covalently bind to certain subclasses of enzymes with similar functions.[27-30] Reactive groups are designed and selected based on the aim of maintaining coverage for a manageable number of intra-class enzymes but minimizing cross-linkage with extra-class enzymes. Over the last two decades, many probes targeting different enzyme classes have been synthesized and used to characterize enzymatic functions. For example, there are fluorophosphonate probes for serine hydrolases,[31-33] epoxide probes for the papain family of cysteine proteases,[23, 34] and photoreactive probes for metalloproteases.[35] All of these target tens to hundreds of enzymes in their subclasses and are differentiated by their enzymatic activity. Another element in an ABPP probe is the analytical tag, which can be a fluorophore for fluorescence visualization, biotin for streptavidin isolation in LC/MS identification approaches, and azide or alkyne handles for detection through click chemistry.[32, 36, 37] Profiling results can be reported out in the form of images from a fluorescence scanner or peptide sequence data by LC-LC/MS identification[38] depending on which tags are used in the probe. Platforms for high-throughput screening of ABPP analysis have also been reported for the identification of enzyme inhibitors.[39, 40] Reactive groups and analytical tags are linked together by a spacer, which can be alkyl chains, polyethylene glycols (PEG) or peptide sequences. Alkyl and PEG spacers will change the hydrophobicity of the probe, thus resulting in altered binding preferences and kinetics.[31, 41] When a specific peptide sequence is used as a spacer, it usually behaves as a substrate for the

corresponding protease, and is enzymatically cleaved to separate the binding group and analytical tag.[42]

Amongst these probes, the fluorophosphonate (FP) is especially effective in the study of the active serine hydrolase (SH) class of enzymes[43] which includes the activating enzymes of ester prodrugs.[44] In our studies, we have utilized FP-PEG-rhodamine and FP-PEG-biotin probes (Figure 1.2) for the identification of ethyl ester prodrug activating enzymes.

1.4 Carboxylesterases

Human carboxylesterases belong to a well-conserved multigene family of α,β-hydrolase fold proteins, and they catalyze the hydrolysis of a variety of endogenous and exogenous compounds including toxins and drugs.[45] There are at least five gene families among all of the identified carboxylesterases,[46] the majority of which fall into carboxylesterase 1 (CES1) and carboxylesterase 2 (CES2). Human CES1 and CES2 are differentiated by their substrate specificity and tissue distribution. Both CES1 and CES2 have large catalytic binding sites that can accommodate various substrates. CES1 prefers to hydrolyze esters with small alcohol and large acyl groups[47] while CES2 hydrolyzes esters of large alcohol and small acyl groups with higher efficiency.[48] CES1 is highly expressed in liver and is also detectable in other tissues. CES1 has been reported as the activating enzyme of oseltamivir and many other ester prodrugs.[49, 50] Newly identified variants of CES1 and polymorphs have been reported recently to affect substrate activation.[51-54] Thus, taking oseltamivir as a case study, we looked to develop a general approach to rapidly profile its activating enzymes, provide information on how CES1 activates oseltamivir and whether there are any other activating hydrolases in humans.

1.5 Objectives

Due to its potential for pharmacokinetic and pharmacodynamic advantages, prodrug development has received increased attention. Many successful prodrugs are known to be activated via the hydrolysis of an ester bond by serine esterases. Our goal is to develop a general method by which to identify activating enzymes of various prodrugs and apply this method to profile the activating enzymes in different human cell lines. Towards this goal, we plan to utilize oseltamivir as an example to compete with FP probes in human cell lines and validate the competitive ABPP approach. We will then confirm the activities of the identified enzymes by comparison with their recombinantly overexpressed pure forms.

In our first aim, a serine hydrolase labeling reagent, FP-PEG-Biotin was synthesized via a novel and safe route. A biotinylated fluorophosphonate (FP-PEG-biotin) was previously synthesized as an effective probe for activity-based protein profiling (ABPP).[31] The reactive group, fluorophosphonate, specifically targets active serine hydrolases and is inactive towards denatured proteins. The biotin group, which is attached to FP group by a PEG linker, can pull down the labeled proteins by interacting with streptavidin. This probe was synthesized via a novel route proceeding by first building up a biotin-PEG-phosphonate linker fragment, and then completing it by modifying the phosphonate ester to a fluorophosphonate in the last step. This route has the capability to provide sufficient quantities of the FP-PEG-biotin probe, which can be utilized in the identification and purification of enzymes.

The second aim is to validate competitive ABPP between prodrugs and the FP probe, visualizing the interactions via 1D SDS-PAGE and identifying the activating enzyme via mass spectrometry, as illustrated in figure 1.3. FP probes are capable of binding non-specifically to serine hydrolases

in a Caco-2 cell homogenate. However, if the homogenate is treated first with prodrugs, such as oseltamivir, the FP binding of activating enzymes will be greatly reduced due to a competition between the prodrug and probe. The degree of reduction as reflected in the change of band intensities can be visualized by fluorescence imaging. The targeted enzyme could then be subjected to mass spectrometry analysis for identification.

Thirdly, we confirmed enzymatic activation with corresponding recombinantly overexpressed enzymes. A selective CES1 inhibitor, WWL50, was characterized by an advanced technology "ABPP-SILAC". The enzymatic hydrolysis of several ethyl ester prodrugs was totally inhibited in human cell homogenates with WWL50 pre-treatment, confirming that CES1 is the predominant activating enzyme for ethyl ester prodrugs.

The proteomic strategy outlined in this study should help us elucidate the activation process of ester prodrugs and in turn accelerate the development of prodrug activation mechanism studies that contribute to the design of effective drug delivery systems.

1.6 Figures

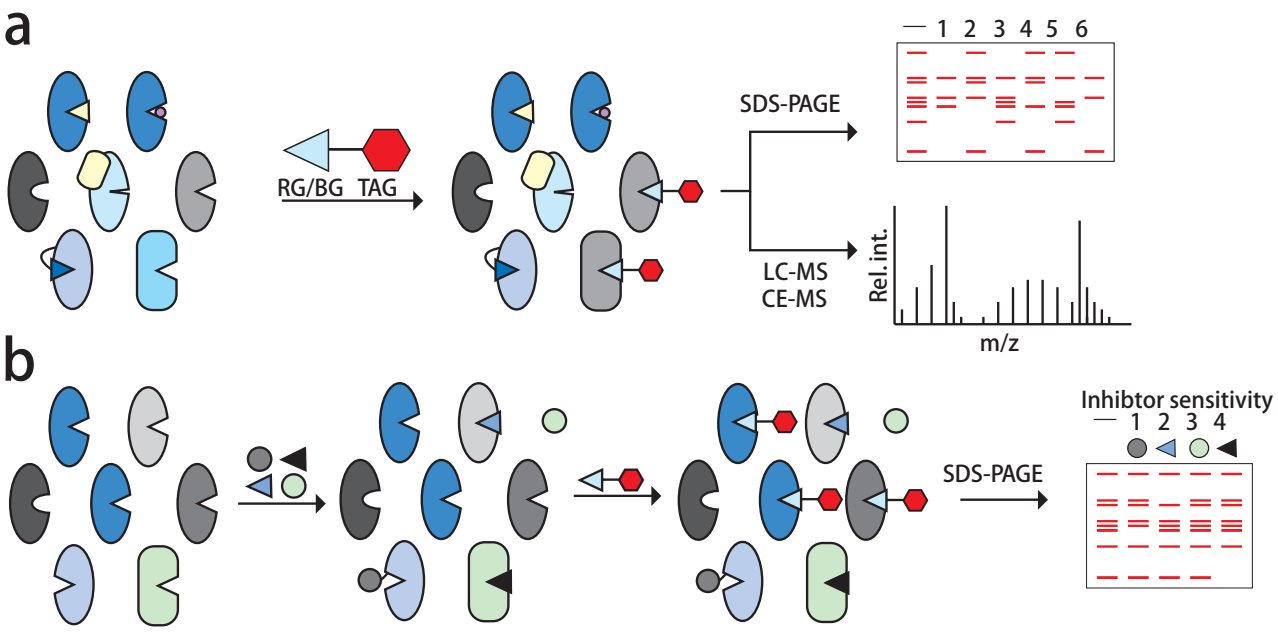

Figure 1.1 Schematic diagram of the mechanism of ABPP. (a) General strategy of profiling enzymes by LC-LC/MS in specific subclasses with similar activity. RG, reactive group; BG, binding group; TAG, analytical tage, biotin or rhodamine. (b) Inhibitor discovery and selectivity profiling in whole proteome samples (adopted from Saghatelian and Cravatt 2005.[20]).

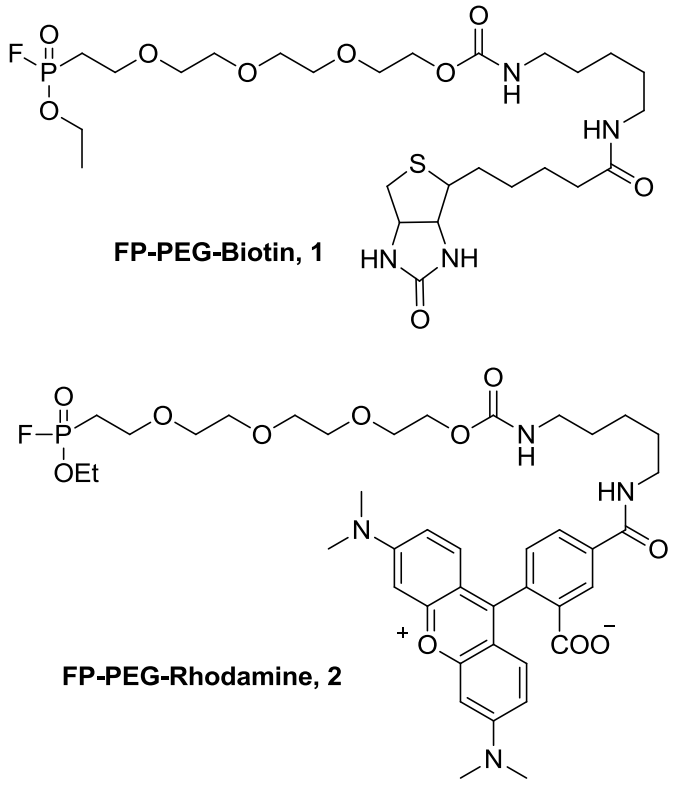

Figure 1.2. Chemical structures of serine hydrolase probes.

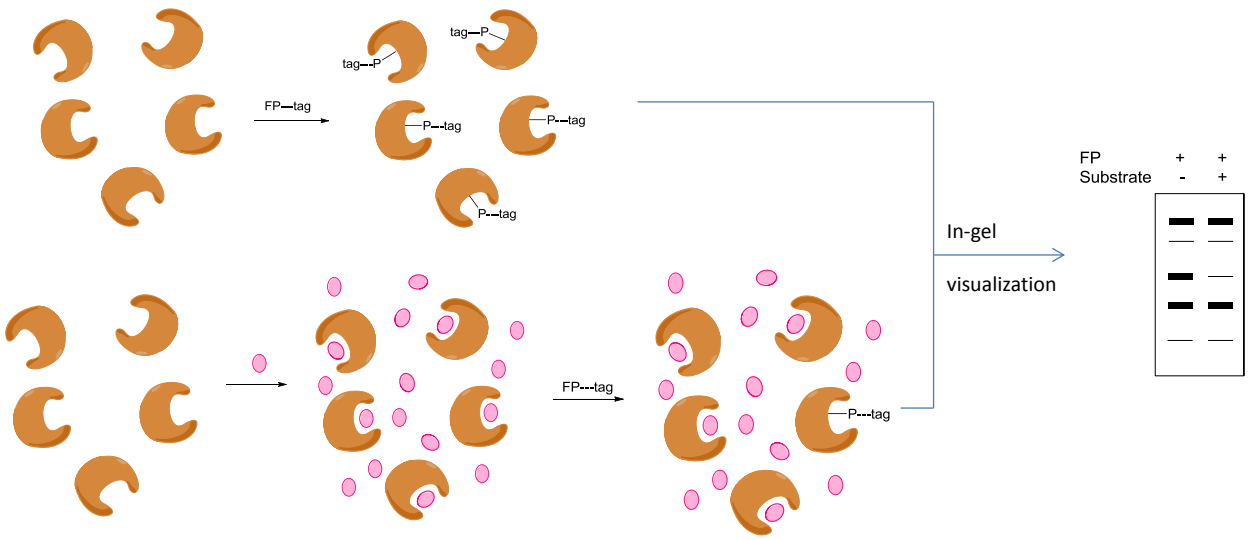

Figure 1.3 Competitive ABPP between FP probes and prodrugs. The enzymatic binding of FP probe is kinetically competed by the catalytic reactions of enzymatic substrate.

1.7 References

1. Ettmayer, P.; Amidon, G. L.; Clement, B.; Testa, B. Lessons learned from marketed and investigational prodrugs. *J Med Chem* **2004,** *47*, (10), 2393-404.
2. Albert, A. Chemical aspects of selective toxicity. *Nature* **1958,** *182*, (4633), 421-2.
3. Stella, V. J. Prodrugs: Some thoughts and current issues. *J Pharm Sci* **2010,** *99*, (12), 4755-65.
4. Landis, M. S. Physicochemical property trends of marketed prodrugs. *Therapeutic delivery* **2013,** *4*, (2), 225-37.
5. Balimane, P. V.; Tamai, I.; Guo, A.; Nakanishi, T.; Kitada, H.; Leibach, F. H.; Tsuji, A.; Sinko, P. J. Direct evidence for peptide transporter (PepT1)-mediated uptake of a nonpeptide prodrug, valacyclovir. *Biochemical and biophysical research communications* **1998,** *250*, (2), 246-51.
6. Sinko, P. J.; Balimane, P. V. Carrier-mediated intestinal absorption of valacyclovir, the L-valyl ester prodrug of acyclovir: 1. Interactions with peptides, organic anions and organic cations in rats. *Biopharmaceutics & drug disposition* **1998,** *19*, (4), 209-17.
7. Rooseboom, M.; Commandeur, J. N.; Vermeulen, N. P. Enzyme-catalyzed activation of anticancer prodrugs. *Pharmacol Rev* **2004,** *56*, (1), 53-102.
8. del Amo, E. M.; Urtti, A.; Yliperttula, M. Pharmacokinetic role of L-type amino acid transporters LAT1 and LAT2. *European journal of pharmaceutical sciences : official journal of the European Federation for Pharmaceutical Sciences* **2008,** *35*, (3), 161-74.
9. Giles, F.; Estey, E.; O'Brien, S. Gemtuzumab ozogamicin in the treatment of acute myeloid leukemia. *Cancer* **2003,** *98*, (10), 2095-104.
10. Huttunen, K. M.; Raunio, H.; Rautio, J. Prodrugs--from serendipity to rational design. *Pharmacol Rev* **2011,** *63*, (3), 750-71.
11. Hochdorffer, K.; Abu Ajaj, K.; Schafer-Obodozie, C.; Kratz, F. Development of novel bisphosphonate prodrugs of doxorubicin for targeting bone metastases that are cleaved pH dependently or by cathepsin B: synthesis, cleavage properties, and binding properties to hydroxyapatite as well as bone matrix. *J Med Chem* **2012,** *55*, (17), 7502-15.
12. Sohma, Y.; Hayashi, Y.; Ito, T.; Matsumoto, H.; Kimura, T.; Kiso, Y. Development of water-soluble prodrugs of the HIV-1 protease inhibitor KNI-727: importance of the conversion time for higher gastrointestinal absorption of prodrugs based on spontaneous chemical cleavage. *J Med Chem* **2003,** *46*, (19), 4124-35.
13. Hosokawa, M.; Maki, T.; Satoh, T. Characterization of molecular species of liver microsomal carboxylesterases of several animal species and humans. *Arch Biochem Biophys* **1990,** *277*, (2), 219-27.
14. Imai, T. Human carboxylesterase isozymes: catalytic properties and rational drug design. *Drug Metab Pharmacokinet* **2006,** *21*, (3), 173-85.
15. Kim, I.; Chu, X. Y.; Kim, S.; Provoda, C. J.; Lee, K. D.; Amidon, G. L. Identification of a human valacyclovirase: biphenyl hydrolase-like protein as valacyclovir hydrolase. *The Journal of biological chemistry* **2003,** *278*, (28), 25348-56.
16. Blech, S.; Ebner, T.; Ludwig-Schwellinger, E.; Stangier, J.; Roth, W. The metabolism and disposition of the oral direct thrombin inhibitor, dabigatran, in humans. *Drug metabolism and disposition: the biological fate of chemicals* **2008,** *36*, (2), 386-99.
17. Stangier, J.; Rathgen, K.; Stahle, H.; Gansser, D.; Roth, W. The pharmacokinetics, pharmacodynamics and tolerability of dabigatran etexilate, a new oral direct thrombin inhibitor, in healthy male subjects. *Br J Clin Pharmacol* **2007,** *64*, (3), 292-303.

18. Laizure, S. C.; Parker, R. B.; Herring, V. L.; Hu, Z. Y. Identification of carboxylesterase-dependent dabigatran etexilate hydrolysis. *Drug metabolism and disposition: the biological fate of chemicals* **2014,** *42*, (2), 201-6.
19. Barglow, K. T.; Cravatt, B. F. Activity-based protein profiling for the functional annotation of enzymes. *Nat Methods* **2007,** *4*, (10), 822-7.
20. Saghatelian, A.; Cravatt, B. F. Assignment of protein function in the postgenomic era. *Nature chemical biology* **2005,** *1*, (3), 130-42.
21. Cravatt, B. F.; Wright, A. T.; Kozarich, J. W. Activity-based protein profiling: from enzyme chemistry to proteomic chemistry. *Annu Rev Biochem* **2008,** *77*, 383-414.
22. Berger, A. B.; Vitorino, P. M.; Bogyo, M. Activity-based protein profiling: applications to biomarker discovery, in vivo imaging and drug discovery. *Am J Pharmacogenomics* **2004,** *4*, (6), 371-81.
23. Greenbaum, D.; Baruch, A.; Hayrapetian, L.; Darula, Z.; Burlingame, A.; Medzihradszky, K. F.; Bogyo, M. Chemical approaches for functionally probing the proteome. *Molecular & cellular proteomics : MCP* **2002,** *1*, (1), 60-8.
24. Fonovic, M.; Bogyo, M. Activity based probes for proteases: applications to biomarker discovery, molecular imaging and drug screening. *Current pharmaceutical design* **2007,** *13*, (3), 253-61.
25. Speers, A. E.; Cravatt, B. F. Chemical strategies for activity-based proteomics. *Chembiochem : a European journal of chemical biology* **2004,** *5*, (1), 41-7.
26. Simon, G. M.; Niphakis, M. J.; Cravatt, B. F. Determining target engagement in living systems. *Nature chemical biology* **2013,** *9*, (4), 200-5.
27. Shannon, D. A.; Gu, C.; McLaughlin, C. J.; Kaiser, M.; van der Hoorn, R. A.; Weerapana, E. Sulfonyl fluoride analogues as activity-based probes for serine proteases. *Chembiochem : a European journal of chemical biology* **2012,** *13*, (16), 2327-30.
28. Gu, C.; Shannon, D. A.; Colby, T.; Wang, Z.; Shabab, M.; Kumari, S.; Villamor, J. G.; McLaughlin, C. J.; Weerapana, E.; Kaiser, M.; Cravatt, B. F.; van der Hoorn, R. A. Chemical proteomics with sulfonyl fluoride probes reveals selective labeling of functional tyrosines in glutathione transferases. *Chemistry & biology* **2013,** *20*, (4), 541-8.
29. Harris, J. L.; Backes, B. J.; Leonetti, F.; Mahrus, S.; Ellman, J. A.; Craik, C. S. Rapid and general profiling of protease specificity by using combinatorial fluorogenic substrate libraries. *Proceedings of the National Academy of Sciences of the United States of America* **2000,** *97*, (14), 7754-9.
30. Kato, D.; Boatright, K. M.; Berger, A. B.; Nazif, T.; Blum, G.; Ryan, C.; Chehade, K. A.; Salvesen, G. S.; Bogyo, M. Activity-based probes that target diverse cysteine protease families. *Nature chemical biology* **2005,** *1*, (1), 33-8.
31. Kidd, D.; Liu, Y.; Cravatt, B. F. Profiling serine hydrolase activities in complex proteomes. *Biochemistry* **2001,** *40*, (13), 4005-15.
32. Gillet, L. C.; Namoto, K.; Ruchti, A.; Hoving, S.; Boesch, D.; Inverardi, B.; Mueller, D.; Coulot, M.; Schindler, P.; Schweigler, P.; Bernardi, A.; Gil-Parrado, S. In-cell selectivity profiling of serine protease inhibitors by activity-based proteomics. *Molecular & cellular proteomics : MCP* **2008,** *7*, (7), 1241-53.
33. Liu, Y.; Patricelli, M. P.; Cravatt, B. F. Activity-based protein profiling: the serine hydrolases. *Proceedings of the National Academy of Sciences of the United States of America* **1999,** *96*, (26), 14694-9.
34. Greenbaum, D.; Medzihradszky, K. F.; Burlingame, A.; Bogyo, M. Epoxide electrophiles as activity-dependent cysteine protease profiling and discovery tools. *Chemistry & biology* **2000,** *7*, (8), 569-81.
35. Chan, E. W.; Chattopadhaya, S.; Panicker, R. C.; Huang, X.; Yao, S. Q. Developing photoactive affinity probes for proteomic profiling: hydroxamate-based probes for metalloproteases. *Journal of the American Chemical Society* **2004,** *126*, (44), 14435-46.

36. Lone, A. M.; Bachovchin, D. A.; Westwood, D. B.; Speers, A. E.; Spicer, T. P.; Fernandez-Vega, V.; Chase, P.; Hodder, P. S.; Rosen, H.; Cravatt, B. F.; Saghatelian, A. A substrate-free activity-based protein profiling screen for the discovery of selective PREPL inhibitors. *Journal of the American Chemical Society* **2011,** *133*, (30), 11665-74.
37. Martin, B. R.; Wang, C.; Adibekian, A.; Tully, S. E.; Cravatt, B. F. Global profiling of dynamic protein palmitoylation. *Nat Methods* **2012,** *9*, (1), 84-9.
38. Everley, P. A.; Gartner, C. A.; Haas, W.; Saghatelian, A.; Elias, J. E.; Cravatt, B. F.; Zetter, B. R.; Gygi, S. P. Assessing enzyme activities using stable isotope labeling and mass spectrometry. *Molecular & cellular proteomics : MCP* **2007,** *6*, (10), 1771-7.
39. Sieber, S. A.; Mondala, T. S.; Head, S. R.; Cravatt, B. F. Microarray platform for profiling enzyme activities in complex proteomes. *Journal of the American Chemical Society* **2004,** *126*, (48), 15640-1.
40. Bachovchin, D. A.; Brown, S. J.; Rosen, H.; Cravatt, B. F. Identification of selective inhibitors of uncharacterized enzymes by high-throughput screening with fluorescent activity-based probes. *Nature biotechnology* **2009,** *27*, (4), 387-94.
41. Adibekian, A.; Martin, B. R.; Chang, J. W.; Hsu, K. L.; Tsuboi, K.; Bachovchin, D. A.; Speers, A. E.; Brown, S. J.; Spicer, T.; Fernandez-Vega, V.; Ferguson, J.; Hodder, P. S.; Rosen, H.; Cravatt, B. F. Confirming target engagement for reversible inhibitors in vivo by kinetically tuned activity-based probes. *Journal of the American Chemical Society* **2012,** *134*, (25), 10345-8.
42. Speers, A. E.; Cravatt, B. F. A tandem orthogonal proteolysis strategy for high-content chemical proteomics. *Journal of the American Chemical Society* **2005,** *127*, (28), 10018-9.
43. Simon, G. M.; Cravatt, B. F. Activity-based proteomics of enzyme superfamilies: serine hydrolases as a case study. *The Journal of biological chemistry* **2010,** *285*, (15), 11051-5.
44. Bachovchin, D. A.; Cravatt, B. F. The pharmacological landscape and therapeutic potential of serine hydrolases. *Nat Rev Drug Discov* **2012,** *11*, (1), 52-68.
45. Hosokawa, M. Structure and catalytic properties of carboxylesterase isozymes involved in metabolic activation of prodrugs. *Molecules* **2008,** *13*, (2), 412-31.
46. Holmes, R. S.; Wright, M. W.; Laulederkind, S. J.; Cox, L. A.; Hosokawa, M.; Imai, T.; Ishibashi, S.; Lehner, R.; Miyazaki, M.; Perkins, E. J.; Potter, P. M.; Redinbo, M. R.; Robert, J.; Satoh, T.; Yamashita, T.; Yan, B.; Yokoi, T.; Zechner, R.; Maltais, L. J. Recommended nomenclature for five mammalian carboxylesterase gene families: human, mouse, and rat genes and proteins. *Mamm Genome* **2010,** *21*, (9-10), 427-41.
47. Imai, T.; Imoto, M.; Sakamoto, H.; Hashimoto, M. Identification of esterases expressed in Caco-2 cells and effects of their hydrolyzing activity in predicting human intestinal absorption. *Drug metabolism and disposition: the biological fate of chemicals* **2005,** *33*, (8), 1185-90.
48. Kobayashi, Y.; Fukami, T.; Shimizu, M.; Nakajima, M.; Yokoi, T. Contributions of arylacetamide deacetylase and carboxylesterase 2 to flutamide hydrolysis in human liver. *Drug metabolism and disposition: the biological fate of chemicals* **2012,** *40*, (6), 1080-4.
49. Zhu, H. J.; Wang, X.; Gawronski, B. E.; Brinda, B. J.; Angiolillo, D. J.; Markowitz, J. S. Carboxylesterase 1 as a determinant of clopidogrel metabolism and activation. *J Pharmacol Exp Ther* **2013,** *344*, (3), 665-72.
50. Shi, D.; Yang, J.; Yang, D.; LeCluyse, E. L.; Black, C.; You, L.; Akhlaghi, F.; Yan, B. Anti-influenza prodrug oseltamivir is activated by carboxylesterase human carboxylesterase 1, and the activation is inhibited by antiplatelet agent clopidogrel. *J Pharmacol Exp Ther* **2006,** *319*, (3), 1477-84.
51. Zhu, H. J.; Markowitz, J. S. Carboxylesterase 1 (CES1) genetic polymorphisms and oseltamivir activation. *European journal of clinical pharmacology* **2013,** *69*, (3), 733-4.
52. Zhu, H. J.; Patrick, K. S.; Yuan, H. J.; Wang, J. S.; Donovan, J. L.; DeVane, C. L.; Malcolm, R.; Johnson, J. A.; Youngblood, G. L.; Sweet, D. H.; Langaee, T. Y.; Markowitz, J. S. Two CES1 gene mutations

lead to dysfunctional carboxylesterase 1 activity in man: clinical significance and molecular basis. *American journal of human genetics* **2008,** *82*, (6), 1241-8.
53. Zhu, H. J.; Markowitz, J. S. Activation of the antiviral prodrug oseltamivir is impaired by two newly identified carboxylesterase 1 variants. *Drug metabolism and disposition: the biological fate of chemicals* **2009,** *37*, (2), 264-7.
54. Tarkiainen, E. K.; Backman, J. T.; Neuvonen, M.; Neuvonen, P. J.; Schwab, M.; Niemi, M. Carboxylesterase 1 polymorphism impairs oseltamivir bioactivation in humans. *Clin Pharmacol Ther* **2012,** *92*, (1), 68-71.
55. Ross, M. K.; Borazjani, A.; Wang, R.; Crow, J. A.; Xie, S. Examination of the carboxylesterase phenotype in human liver. *Arch Biochem Biophys* **2012,** *522*, (1), 44-56.
56. Hosokawa, M.; Furihata, T.; Yaginuma, Y.; Yamamoto, N.; Koyano, N.; Fujii, A.; Nagahara, Y.; Satoh, T.; Chiba, K. Genomic structure and transcriptional regulation of the rat, mouse, and human carboxylesterase genes. *Drug metabolism reviews* **2007,** *39*, (1), 1-15.
57. Yamada, S.; Richardson, K.; Tang, M.; Halaschek-Wiener, J.; Cook, V. J.; Fitzgerald, J. M.; Elwood, K.; Marra, F.; Brooks-Wilson, A. Genetic variation in carboxylesterase genes and susceptibility to isoniazid-induced hepatotoxicity. *Pharmacogenomics J* **2010,** *10*, (6), 524-36.

Chapter 2

SYNTHESIS OF FLUOROPHOSPHONATE – POLYETHYLENEGLYCOL – BIOTIN

2.1 Introduction

One of the goals of chemical biology is to develop small molecule and biomolecule-based probes to interrogate biological processes. In this regard, fluorophosphonate (FP) probes have been extensively used in activity-based protein profiling (ABPP) in proteomic studies.[1, 2] FP probes, specifically designed to target serine hydrolases, originated from diisopropyl fluorophosphonate (DFP).[3, 4] DFP is a serine hydrolase covalent inhibitor and from it have evolved analytical tools in which "handles", such as biotin, rhodamine, and alkyne have been appended via a variety of linking chains.[5-8] These FP analogues have proven to be powerful tools in the profiling of complex proteome samples[9] and in the identification of selective inhibitors.[10, 11] However, very few cases have been published in which these probes have been utilized in the study of enzymes with reversible substrates. These substrates are usually endogenous or exogenous organic molecules of small molecular weight, like ethyl ester prodrugs, exhibiting enzymatic kinetic properties different from other inhibitors due to their high turnover rates. Thus, competition assays between substrates and FP probes are more difficult to perform due to the rapid kinetics and covalent binding properties of the probes.

The FP-PEG-biotin compound **1**, shown in figure 2.1, was first synthesized by the Cravatt group and utilized for affinity isolation of enzymes by pull-down with avidin beads followed by mass

spectrometry analysis.[12] Our interest in generating **1** on a larger scale to use in our research led us to consider an alternative and more expeditious synthetic route. This was driven by several concerns of the original route including (a) a poor overall yield (b) challenges in the chromatographic purification of some intermediates due to their hydrophilicity and lack of a UV chromophore, and (c) generating and then carrying the fluorophosphonate moiety through two steps with an attendant concern of its high reactivity and potential for toxicity to the laboratory chemist.[12, 13] In our efforts to address those shortcomings, we report a novel synthetic route to FP-PEG-biotin **1**, and in its following validation in which this probe was utilized in competitive ABPP experiments with ethyl ester prodrug.

2.2 Results

Synthesis

The route to target probe **1** is delineated in scheme 2.1 Monobenzylation of tetraethylene glycol **2** was carried out by the procedure of Jiang et al.[14] to give ether **3** in 78% yield. This was then subjected to a two-step procedure to provide the novel iodo-ether **4b**. Thus, tosylation of **3** utilizing a slight modification of literature conditions[15] gave **4a**, which was subjected to Finkelstein conditions utilizing a procedure reported for a related compound[16] to afford **4b** in a combined 90% yield. The phosphonate moiety was installed under standard Arbuzov conditions by refluxing **4b** in neat triethyl phosphite for 1 h to provide novel intermediate **5** in 92% yield following purification by column chromatography. Clean removal of the benzyl protecting group under standard conditions of catalytic hydrogenolysis provided in 96% yield the known phosphonate polyether alcohol **6**, the synthesis of which had been accomplished earlier by a different route.[17] Activation of the alcohol moiety of **6** to the succinimidyl carbonate **7** was

carried out under standard conditions in 87% yield following chromatographic purification. Coupling of **7** to the *in situ* generated 5-(biotinamido)pentaneamine fragment **12**, made from Boc-protected diamine **10** in a known two-step process,[18] was carried out under mild conditions to provide novel precursor **8** in 76% yield following purification. The stage was now set for a two-step modification of the phosphonate moiety. Reaction of **8** with lithium azide in hot DMF, under conditions developed for the monodealkylation of phosphonic acid dialkyl esters of nucleosides,[19] provided the novel monoethyl ester **9** in 87% yield following purification by a two-stage chromatographic procedure. Penultimate intermediate **9** was then cleanly converted to the fluorophosphonate utilizing the standard fluoridating reagent (DAST in dichloromethane) at -42 ºC. Workup provided the FP probe **1** [20] in 80% yield, which was pure enough to use directly in biological studies. Due to the absence of a UV chromophore, the purity of FP-PEG-biotin **1** could not be determined by HPLC. TLC analysis was also problematic due to its reactivity with the highly polar solvent mixture required to move it up a plate. Nevertheless, we deem **1** to be of high purity due to the cleanliness of its NMR spectra (^{1}H, ^{13}C, ^{19}F, ^{31}P). The structural assignments of all compounds were supported by diagnostic peaks in the ^{1}H and ^{13}C NMR spectra and by mass spectrometry.

Kinetic study of FP probe labelling activity

An incubation time control study is key toward successfully monitoring competition between FP-PEG-biotin **1** and a prodrug as a reversible substrate with a high turnover rate. Hence, over a long incubation time, the prodrug will be competed out with the active enzyme covalently linked to the FP probe even though the concentration of added prodrug is high compared to the probe. Enzymes present different kinetic properties in the same proteome sample, and a single enzyme can have different preferences for FP probes with different linkers.[21] Thus it is important to

perform kinetic studies on a specific tissue or cell line before the start of competition assays. Toward this end, Caco-2 cell homogenate samples were prepared and incubated with FP-PEG-biotin **1** over different time courses ranging from 1- 30 minutes (Figure 2.2). The sample from each trial was then separated by SDS-PAGE and blotted by alkaline phosphatase conjugated streptavidin. A proteome sample was also incubated with DMSO for 10 minutes as a control. As all competitive exchanges between the FP probe and prodrugs occur within less than a 15 minute window, data collection was limited to 30 minutes.

The band intensities from endogenous streptavidin-binding proteins, indicated in the control lane, did not change with incubation time. Neither did the intensity of the band around 64-kD (thin arrow), suggesting that this protein bound to the FP probe very fast (~50% within 1 minute). In contrast, the 49-kD enzyme band (hollow arrow) showed a clear time-dependent reaction. Due to their lower expression levels, reaction of **1** with other enzymes (dark arrows) could not be detected until 10 minutes incubation time. Therefore, depending on the type and expression levels of serine hydrolase being investigated, different incubation times are required in order to observe a clear signal.

Competition study

To assess the possibility and potency of utilizing FP-PEG-biotin in the identification of prodrug activating enzymes, oseltamivir was chosen as an example to compete with **1**. Oseltamivir (Tamiflu®) is a commercially available prodrug, which is converted to oseltamivir carboxylate (O.C.) after being absorbed in gastrointestinal tract. Carboxylesterase 1 (CES1),[22] a common esterase existing in multiple human tissues, has been shown to be active in the oseltamivir hydrolysis.[23] Caco-2 cell homogenate (1 mg/mL) in Tris buffer (50 mM, pH 7.4) was treated with oseltamivir (10 mM final) or vehicle (as control) for 10 min at room temperature and then

treated with FP-PEG-biotin (concentration as noted in figure 2.3) for 1 or 5 min. Western blot analysis showed a clear reduction in band intensity around 60-70 kDa due to oseltamivir competition while signals from the rest of the protein bands remained the same. The reduced band intensity suggested the feasibility of applying FP-PEG-biotin **1** to the study of prodrug activating enzymes identification.

2.3 Discussion

Fluorophosphonate probes with different analytical handles, such as rhodamine and alkyne, are being used to identify and characterize the proteome samples from cell or animal tissue.[8] Biotin-based probes that bind to streptavidin play an essential role in isolating and analysing serine hydrolases. In our studies with FP-PEG-biotin probe **1**, we required sufficient enough quantities that we decided to re-engineer the original synthesis of Kidd et al.[6] Our major modifications involved (a) introduction of a benzyl protecting group (in place of the TBS of the original synthesis) onto the PEG moiety to facilitate the early stages of the synthesis by providing a UV active chromophore for easy detection; (b) introduction of a high yielding two-step iodination process, which avoids chromatography; (c) reversing the sequence of fluoridation and amidation reactions such that the reactive FP moiety can be introduced in the last step. Overall, these modifications make for a more scalable, higher yielding synthetic scheme and importantly isolates the handling of reactive and potentially toxic FP compounds to a single step, namely the last one.

FP probes have been used mostly in the enzymatic annotation and development of covalent inhibitors for pharmacologically interesting serine hydrolases due to their strong binding and rapid labelling properties. We have shown that for serine hydrolases with reversible substrates,

FP probes can be useful tools if their concentration and incubation times are properly controlled, as demonstrated in the competitive ABPP between oseltamivir (10 mM) and FP-PEG-biotin probe in Caco-2 cell line.

In summary, several steps of the original synthesis of FP-PEG-biotin probe **1** have been modified, leading to a higher overall yield and easier manipulation. Starting from common precursor **2**, our synthesis requires only four chromatographic purifications over nine steps and provides a 28.5% overall yield of **1**. In contrast, the Cravatt sequence requires six chromatographic purifications over eight steps with an overall yield of 1%. The subsequent kinetic study and competition of probe **1** with oseltamivir have shown that FP probes can be utilized for investigation of prodrug activating enzymes as long as sufficient control is taken to kinetically tune the time and probe concentration of reaction.

2.4 Experimental Methods

All reagents were commercially available and used without further purification. ^{1}H and ^{13}C NMR spectra were obtained on Bruker 300 or Bruker 500 MHz spectrometers with $CDCl_3$, d_6-DMSO, or d_4-methanol as solvent, and chemical shifts are reported relative to the residual solvent peak in δ (ppm). Mass spectrometry analysis was performed using a Waters LCT time-of-flight mass spectrometry instrument. Flash column chromatography was performed with silica gel (220-240 mesh). Thin-layer chromatography (TLC) was performed on silica gel GHLF plates (250 microns) purchased from Analtech. Developed TLC plates were visualized with a UV lamp at 254 nm or by iodine staining. Extraction solutions were dried over $MgSO_4$ prior to concentration.

1-Phenyl-2,5,8,11-tetraoxatridecan-13-yl 4-methylbenzenesulfonate (4a)

This compound was made by a slight modification of the literature procedure.[15] An ice-cold solution of tetraethylene glycol monobenzyl ether (**3**; 13.9 g, 48.9 mmol; made by the procedure of Jiang et al.[14]) in 70 mL of THF was treated with KOH (9.85 g, 171.1 mmol) dissolved in 50 mL of water. A solution of *p*-toluenesulfonyl chloride (11.18 g, 58.7 mmol) in 36 mL of THF was added dropwise to the reaction mixture, which was then gradually warmed to room temperature and stirred overnight. The reaction mixture was poured into sat. aq. ammonium chloride and extracted with dichloromethane (3x). The combined extracts were dried and concentrated to leave 21.11 g (98%) of **4a** as a light yellow oil: R_f 0.26 (hexanes : ethyl acetate, 1 : 1); ^{1}H NMR ($CDCl_3$, 300 MHz) δ 7.77-7.80 (d, *J* = 8 Hz, 2H), 7.26-7.34 (m, 7H), 4.56 (s, 2H), 4.14 (t, *J* = 4.5 Hz, 2H), 3.58-3.69 (m, 14 H), 2.44 (s, 3H); ^{13}C NMR ($CDCl_3$, 75 MHz) δ 144.8, 138.2, 132.9, 129.8, 128.4, 128.0, 127.7, 127.6, 73.2, 70.7, 70.6, 70.5, 69.4, 69.2, 68.6, 21.7; MS *m/z* 461.0 $(M+Na)^+$.

13-iodo-1-phenyl-2,5,8,11-tetraoxatridecane (4b)

The synthesis of **4b** utilized a procedure reported for a related compound.[16] A mixture of KI (23.97 g, 144.4 mmol) and sulfonate ester **4a** (21.11 g, 48.14 mmol) in 250 mL of acetone was refluxed for 18 h. After cooling to room temperature, the reaction mixture was filtered and the collected salts were rinsed with acetone. The filtrate was concentrated to an oil that was diluted with dichloromethane. The solution was washed sequentially with sat. aq. $Na_2S_2O_3$ and brine, dried, and concentrated to give 17.44 g (92%) of **4b** as a clear oil: R_f 0.37 (hexanes : ethyl acetate, 2 : 1) ; ^{1}H NMR ($CDCl_3$, 300 MHz) δ 7.26-7.35 (m, 5H), 4.57 (s, 2H), 3.63-3.77 (m, 14H), 3:.24(t, *J* = 6.5 Hz, 2H); ^{13}C NMR ($CDCl_3$, 75 MHz) δ 138.3, 128.4, 127.7, 127.6, 73.2, 72.0, 70.7, 70.68, 70.63, 70.2, 69.4, 3.0; MS *m/z* 416.9 $(M+Na)^+$.

Diethyl (1-phenyl-2,5,8,11-tetraoxatridecan-13-yl)phosphonate (5)

Iodo benzyl polyether **4b** (17.44 g, 44.23 mmol) and triethyl phosphite (32 mL, 183.9 mmol) were mixed in an oven-dried round-bottom flask, and refluxed for 1 h. Excess triethyl phosphite was removed under vacuum and the reaction mixture was directly loaded onto a silica gel column, which was eluted with ethyl acetate and then methanol : ethyl acetate (5 : 95). Product fractions were combined and concentrated to give 16.5 g (92%) of **5** as a light yellow oil: R_f 0.11 (ethyl acetate); ^{1}H NMR ($CDCl_3$, 500 MHz) δ 7.27-7.33 (m, 5H), 4.55 (s, 2H), 4.06 (q, *J* = 7 Hz, 4H), 3.6 (m, 14H), 2.05-2.16 (m, 2H), 1.30 (t, *J* = 7 Hz, 6H); ^{13}C NMR ($CDCl_3$, 125 MHz) δ 138.2, 128.4, 127.7, 127.6, 73.2, 70.66, 70.63, 70.4, 70.2, 69.4, 65.1, 61.65, 61.60, 27.5, 26.5, 16.46, 16.42; MS *m/z* 405.1 $(M+Na)^+$.

Diethyl (2-(2-(2-(2-hydroxyethoxy)ethoxy)ethoxy)ethyl)phosphonate (6)

A mixture of diethylphosphonate polyether **5** (3g, 7.4 mmol), 10% Pd/C (0.3 g) and 100 mL ethanol in a 250 mL hydrogenation vessel was hydrogenated at 40 psi H_2 for ~ 20 h. The reaction mixture was rapidly filtered over Celite, and concentrated under reduced pressure to give 2.23 g (96 %) of **6** as a clear oil: The ^{1}H and ^{13}C NMR are the same as previously reported for **6** made by a different procedure;[17] MS *m/z* 315.1 $(M+H)^+$.

2-(2-(2-(2-(Diethoxyphosphoryl)ethoxy)ethoxy)ethoxy)ethyl (2,5-dioxopyrrolidin-1-yl) carbonate (7)

A mixture of diethylphosphonate polyether alcohol **6** (0.5 g, 1.6 mmol), *N*, *N*-disuccinimidyl carbonate (2.04 g, 8 mmol), triethylamine (1.1 mL, 8 mmol), and anhydrous acetonitrile (4.5 mL) was stirred at room temperature for 12 h. The mixture was concentrated to an oil that was

distributed between dichloromethane and water. The organic phase was dried and concentrated to a yellow oil that was then purified by silica gel chromatography. Elution with dichloromethane : methanol (98 : 2 to 95 : 5) followed by pooling and concentration of product fractions provided 0.64 g (87%) of **7** as a light brown oil: The ^{1}H and ^{13}C NMR are the same as previously reported for **7** made by a different procedure;[17] MS *m/z* 456.1 $(M+H)^{+}$.

2-(2-(2-(2-(Diethoxyphosphoryl)ethoxy)ethoxy)ethoxy)ethyl (5-(5-((3a*S*,4*S*,6a*R*)-2-oxohexahydro-1*H*-thieno[3,4-*d*]imidazol-4-yl)pentanamido)pentyl)carbamate (8)

A solution of *in situ* synthesized 5-(biotinamido)pentaneamine, trifluoroacetic acid salt, **12** (see below) in 2 mL of DMF was treated with triethylamine (0.4 mL) at 0 ºC and stirred at room temperature for 10 min. Diethylphosphonate polyether succinimidyl carbonate **7** (145 mg, 0.31 mmol) was then added and the solution was stirred at room temperature overnight. The reaction mixture was distributed between ethyl acetate and brine, and the organic phase was dried. Concentration left a brown oil that was purified by silica gel chromatography eluting with dichloromethane : methanol: NH_4OH (92 : 8 : 0.5 to 90 : 10 : 1). Product fractions were pooled and concentrated to leave 324 mg (76%) of **8** as a pale white solid: ^{1}H NMR ($CDCl_3$, 500 MHz) δ 6.66 (br s, 1H), 6.61 (br s, 1H), 6.03 (br s, 1H), 5.42 (br s, 1H), 4.46 (t, *J* = 6 Hz, 1H), 4.26 (t, *J* = 6 Hz, 1H), 4.14-4.12 (m, 2H), 4.06-4.02 (m, 4H), 3.64-3.58 (m, 12H), 3.15-3.06 (m, 7H), 2.84 (dd, *J* = 5 Hz, 13 Hz, 1H), 2.69 (d, *J* = 13 Hz, 1H), 2.13 (t, *J* = 7.3 Hz, 2H), 2.10-2.05 (m, 2H), 1.63-1.59 (m, 4H), 1.45-1.37 (m, 6H), 1.29-1.25 (m, 6H); ^{13}C NMR ($CDCl_3$, 125 MHz) δ 173.4, 164.2, 156.6, 70.5, 70.4, 70.1, 69.6, 65.0, 63.7, 61.8, 61.7, 61.6, 60.2, 55.7, 40.6, 40.5, 39.2, 35.8, 29.5, 28.9, 28.2, 28.0, 27.4, 26.3, 25.7, 23.9, 16.4, 16.3; MS *m/z* 669.2 $(M+H)^{+}$.

2-(2-(2-(2-(Ethoxy(hydroxy)phosphoryl)ethoxy)ethoxy)ethoxy)ethyl (5-(5-((3a*S*,4*S*,6a*R*)-2-oxohexahydro-1*H*-thieno[3,4-*d*]imidazol-4-yl)pentanamido)pentyl)carbamate (9)

A mixture of lithium azide (200 mg, 4.1 mmol), diethylphosphonate polyether carbamate **8** (150 mg, 0.22 mmol), and 2 mL of DMF was stirred at 95 ºC for 18 h. DMF was removed under vacuum to leave a yellow oil, which was diluted with water and loaded onto a column of Amberlite – IR120 (H^+) resin. The column was eluted with DI water and the collected eluate was evacuated at 30 mm/Hg with stirring for 30 min at rt (to draw off hydrazoic acid), and then lyopholized to leave a crude yellow residue that was purified by flash chromatography. Gradient elution with dichloromethane : methanol : NH_4OH (70 : 30 : 2 and then 80:20:1) followed by pooling and concentration of product fractions left 0.125 g (87%) of **9** as a colorless solid: ^{1}H NMR (CD_3OD, 500 MHz) δ 4.50-4.53 (m, 1H), 4.31-4.34 (m, 1H), 4.18 (t, *J* = 4.6 Hz, 2H), 3.89-3.95 (m, 2H), 3.76-3.62 (m, 12H), 3.18-3.28 (m, 3H), 3.12 (t, *J* = 7 Hz, 2H), 2.95 (dd, *J* = 4.9 Hz, 12.9 Hz, 1H), 2.73 (d, *J* = 12.9 Hz, 1H), 2.22 (t, *J* = 7.3 Hz, 2H), 1.97-1.91 (m, 2H), 1.80-1.37 (m, 12H), 1.26 (t, *J* = 7 Hz, 3H); ^{13}C NMR (CD_3OD, 125 MHz) δ 174.5, 164.7, 157.3, 69.8, 69.7, 69.5, 69.2, 66.7, 63.4, 62.0, 60.2, 59.6, 55.6, 40.3, 39.7, 38.9, 35.5, 29.2, 28.7, 28.4, 28.1, 28.0, 25.6, 23.8, 15.9, 15.8; MS *m/z* 641.2 $(M+H)^+$.

2-(2-(2-(2-(Ethoxyfluorophosphoryl)ethoxy)ethoxy)ethoxy)ethyl (5-(5-((3a*S*,4*S*,6a*R*)-2-oxohexahydro-1*H*-thieno[3,4-*d*]imidazol-4-yl)pentanamido)pentyl)carbamate (FP-PEG-biotin; 1)

To a solution of monoethylphosphonate polyether carbamate **9** (46 mg, 0.072 mmol) in 1 mL of anhydrous dichloromethane at -42 ºC was added (diethylamino)sulfur trifluoride (DAST; 26.4μL, 0.022 mmol). The mixture was stirred for 30 min and quenched with water at -42ºC.

After stirring at room temperature for 10 min, the mixture was extracted with dichloromethane (3x). The organic phase was dried and concentrated to a yellow oil that was evacuated under high vacuum to leave 32 mg (70%) of **1**, which was used directly in biological studies: ^{1}H NMR ($CDCl_3$, 500 MHz) δ 6.38 (br s, 1H), 5.60 (br s, 1H), 5.36 (br s, 1H), 5.29 (bs, 1H), 4.51 (m, 1H), 4.40-4.21 (m, 5H), 3.90-3.55 (m,12H), 3.30-3.11 (m, 5H), 2.92 (dd, *J* = 4.9, 12.9 Hz, 1H), 2.74 (d, *J* = 12.9 Hz, 1H), 2.35-2.18 (m, 4H), 1.85-1.40(m, 12H); 1.31 (t, *J* = 6.0 Hz, 3H); ^{13}C NMR ($CDCl_3$, 125 MHz) δ 173.3, 163.9, 156.6, 70.5, 70.4, 69.6, 64.2, 63.7, 63.6, 63.5, 61.8, 60.2 55.7, 40.6, 39.2, 35.8, 29.5, 28.9, 28.1, 28.0, 26.8, 25.7, 24.9, 23.8, 16.4, 16.3; ^{19}F NMR ($CDCl_3$, 282 MHz) δ -59.4, -63.2; ^{31}P NMR ($CDCl_3$, 121 MHz) δ 32.8, 24.0; MS *m/z* 643.2 $(M+H)^+$.

tert-Butyl (5-(5-((3a*S*,4*S*,6a*R*)-2-oxohexahydro-1*H*-thieno[3,4-*d*]imidazol-4-yl)pentanamido)pentyl) carbamate (11)

This compound was made by the procedure of Konoki et al.[18] from *tert*-butyl (5-aminopentyl) carbamate (**10**; made by the procedure of Kaur et al[24]) and D-biotin. The ^{1}H NMR spectrum is the same as previously reported;[18] ^{13}C NMR ($CDCl_3$, 125 MHz) δ 173.3, 164.2, 156.2, 79.1, 61.8, 60.2, 55.8, 40.5, 40.3, 39.2, 36.0, 29.7, 29.1, 28.4, 28.2, 28.0, 25.8, 23.9; MS *m/z* 451.1 $(M+Na)^+$.

***N*-(5-Aminopentyl)-5-((3a*S*,4*S*,6a*R*)-2-oxohexahydro-1*H*-thieno[3,4-*d*]imidazol-4-yl)pentanamide (12)**

This compound was made similar to the procedure of Konoki et al.[18] To an ice-cold solution of *t*-butyl 5-(biotinamidopentyl)carbamate (**11**; 136 mg, 0.32 mmol) in dichloromethane (2.0 mL)

was added dropwise trifluoroacetic acid (1.0 mL). The cooling bath was removed and the mixture was stirred for 2 h. The solution was concentrated *in vacuo* to a yellow oil, which was used in the next step without further purification: ^{1}H NMR (CD_3OD, 300 MHz) δ 4.45 (dd, *J* = 8.0, 5.5 Hz, 1H), 4.26 (dd, *J* = 7.5, 4.5 Hz, 1H), 3.15-3.11 (m, 3H), 2.90-2.85 (m, 1H), 2.67-2.61 (m, 3H), 2.16 (t, *J* = 7.5 Hz, 2H), 1.71-1.48 (m, 4H), 1.42-1.33 (m, 8H); MS *m/z* 329.1 $(M+H)^+$.

Material for Biological Experiments

Oseltamivir was purchased from Allichem LLC. Cell culture reagents were obtained from Invitrogen (Rockville, MD), and the cell culture supplies were obtained from Corning (Corning, NY) and Falcon (Lincoln Park, NJ).

Preparation of cell proteome samples

The human colon carcinoma cell line, Caco-2 (from ATCC, HTB-37), was grown in complete medium (DMEM with 1% nonessential amino acid and 10% FBS) in 100 mm tissue culture dishes in an atmosphere of 5% CO_2 at 37 °C. The cells were grown until 13-14 days post-confluence before harvest. Caco-2 cells were collected in ice-cold 50 mM Tris buffer (pH 7.4), and immediately Dounce homogenized and sonicated at 0 °C. The resulting sample was centrifuged for 45 min at high speed (100,000 x g at 4 °C). The supernatant was removed and kept at 0 °C, and then the pellet was sonicated in a small amount of Tris buffer at 0 °C and centrifuged again (100,000 x g at 4 °C for 45 min). The washing step was repeated twice and all the supernatants were combined and saved as a cytosolic proteome fraction. The final pellet was resuspended by sonication in 50 mM Tris buffer containing 0.25 M sucrose and saved as

membrane proteome fraction. Protein concentration was determined by the BCA assay and aliquots of the proteome were stored at -80 °C.

Competitive ABPP Between FP-PEG-biotin and Oseltamivir

Caco-2 cytosol fraction (1 mg/mL) in 50 mM Tris buffer (pH 7.4) was incubated with oseltamivir (10 mM) for 10 min at room temperature. FP-peg-biotin (0.1, 0.5, 2 μM) or vehicle was then added to the sample and incubated for 1 or 5 min before being quenched with 5 x sample loading buffer, followed by subsequent heating at 85 °C for 5 min. The treated samples were subjected to 4-20% sodium dodecyl sulfate-polyacrylamide gel electrophoresis (SDS-PAGE; Invitrogen Corporation) at 125 v for 90 min. The gel was then electrophoretically transferred onto a Hybond PVDF membrane (Amersham, UK). The membrane was blocked in Tris buffer saline with 0.1% tween-20 (TBS-T) containing 1% casein for 1 h at room temperature, followed by incubation with streptavidin alkaline phosphatase (1:2500 dilution) (R & D, Minneapolis, MN) in TBS-T at room temperature for 1 h. The membrane was washed with TBS-T three times, 10 min for each washing. The blot was subsequently visualized with ECF substrate (GE Healthcare, NJ) on a Typhoon 9200 Variable Mode Imager (GE Healthcare, NJ).

2.5 Figures

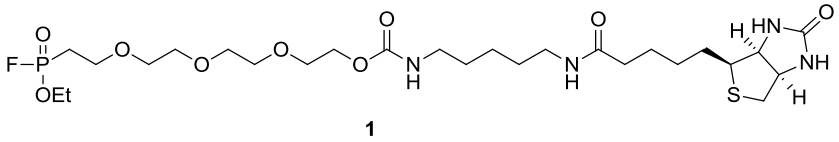

1

Figure 2.1. Structure of FP-PEG-biotin 1.

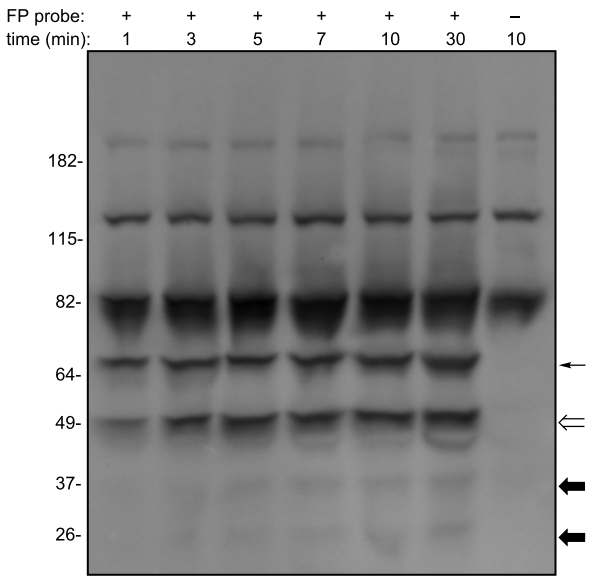

Figure 2.2. Kinetic study on FP labelling reactions. Caco-2 cell homogenates (1 mg/mL) were treated at room temperature with FP-PEG-biotin **1** (4 μM) for the indicated times, followed by the termination of reaction with 5x SDS-PAGE loading buffer. The results were analysed by 4-20% SDS-PAGE gel and streptavidin blotting. Serine hydrolases which reacted with the FP probe in a time-dependent manner are highlighted (thin, hollow and dark arrows, respectively).

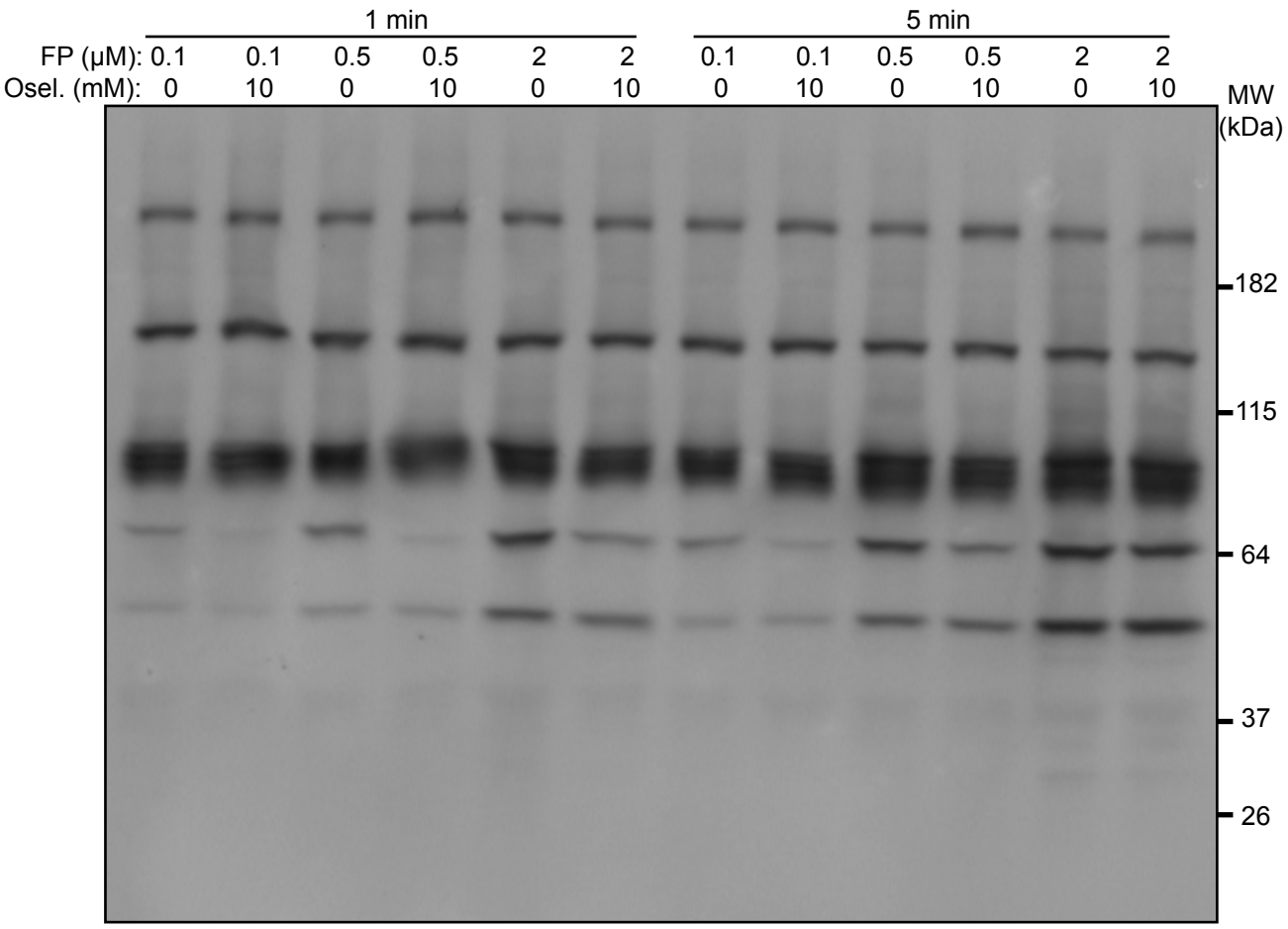

Figure 2.3. Western blot of oseltamivir competition assay with FP-PEG-biotin. Caco-2 cell homogenate was treated with tris buffer or oseltamivir solution (10 mM in tris buffer) for 10 min at room temperature, following the addition of FP-PEG-biotin (0.1, 0.5 or 2 μM) and was incubated for another 1 or 5 min. The sample was separated by SDS-PAGE, transferred to PVDF membrane, blocked by alkaline phosphotase-strepavidin. The competition was visualized by monitoring the fluorescent signal after treated with ECF.

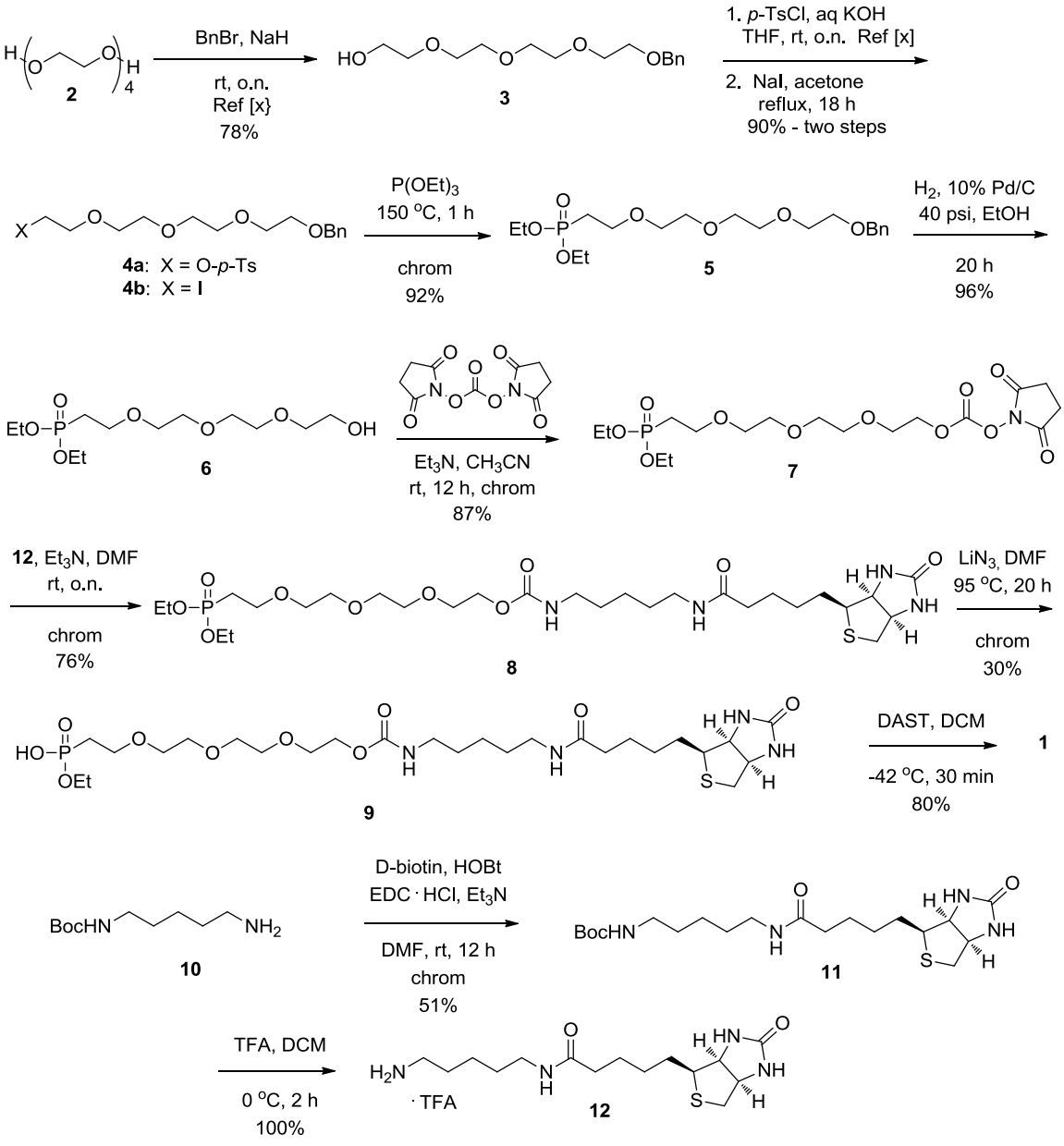

Scheme 2.1. Synthetic route of FP-PEG-biotin probe 1

2.6 References

1. Saghatelian, A.; Cravatt, B. F. Assignment of protein function in the postgenomic era. *Nature chemical biology* **2005,** *1*, (3), 130-42.
2. Berger, A. B.; Vitorino, P. M.; Bogyo, M. Activity-based protein profiling: applications to biomarker discovery, in vivo imaging and drug discovery. *Am J Pharmacogenomics* **2004,** *4*, (6), 371-81.
3. Walsh, C., *Enzymatic Reaction Mechanisms*. W. H. Freeman and Co.: 1979; p 978 pp.
4. Creighton, T. E., *Proteins. Structure and Molecular Principles. 2nd Ed*. Freeman: 1993; p 507 pp.
5. Liu, Y.; Patricelli, M. P.; Cravatt, B. F. Activity-based protein profiling: the serine hydrolases. *Proceedings of the National Academy of Sciences of the United States of America* **1999,** *96*, (26), 14694-9.
6. Kidd, D.; Liu, Y.; Cravatt, B. F. Profiling serine hydrolase activities in complex proteomes. *Biochemistry* **2001,** *40*, (13), 4005-15.
7. Patricelli, M. P.; Giang, D. K.; Stamp, L. M.; Burbaum, J. J. Direct visualization of serine hydrolase activities in complex proteomes using fluorescent active site-directed probes. *Proteomics* **2001,** *1*, (9), 1067-1071.
8. Gillet, L. C.; Namoto, K.; Ruchti, A.; Hoving, S.; Boesch, D.; Inverardi, B.; Mueller, D.; Coulot, M.; Schindler, P.; Schweigler, P.; Bernardi, A.; Gil-Parrado, S. In-cell selectivity profiling of serine protease inhibitors by activity-based proteomics. *Molecular & cellular proteomics : MCP* **2008,** *7*, (7), 1241-53.
9. Jessani, N.; Liu, Y.; Humphrey, M.; Cravatt, B. F. Enzyme activity profiles of the secreted and membrane proteome that depict cancer cell invasiveness. *Proc. Natl. Acad. Sci. U. S. A.* **2002,** *99*, (16), 10335-10340.
10. Leung, D.; Hardouin, C.; Boger, D. L.; Cravatt, B. F. Discovering potent and selective reversible inhibitors of enzymes in complex proteomes. *Nat. Biotechnol.* **2003,** *21*, (6), 687-691.
11. Bachovchin, D. A.; Brown, S. J.; Rosen, H.; Cravatt, B. F. Identification of selective inhibitors of uncharacterized enzymes by high-throughput screening with fluorescent activity-based probes. *Nature biotechnology* **2009,** *27*, (4), 387-94.
12. Sivalingam, N.; Basivireddy, J.; Pulimood, A. B.; Balasubramanian, K. A.; Jacob, M. Activation of phospholipase A2 is involved in indomethacin-induced damage in Caco-2 cells. *Toxicol. in Vitro* **2009,** *23*, (5), 887-896.
13. Quistad, G. B.; Klintenberg, R.; Casida, J. E. Blood Acylpeptide Hydrolase Activity Is a Sensitive Marker for Exposure to Some Organophosphate Toxicants. *Toxicol. Sci.* **2005,** *86*, (2), 291-299.
14. Jiang, Z.-X.; Yu, Y. B. The design and synthesis of highly branched and spherically symmetric fluorinated macrocyclic chelators. *Synthesis* **2008**, (2), 215-220.
15. Shan, M.; Bujotzek, A.; Abendroth, F.; Wellner, A.; Gust, R.; Seitz, O.; Weber, M.; Haag, R. Conformational Analysis of Bivalent Estrogen Receptor Ligands: From Intramolecular to Intermolecular Binding. *Chembiochem : a European journal of chemical biology* **2011,** *12*, (17), 2587-2598.
16. Bar-Nir, B. B.-A.; Kadla, J. F. Synthesis and structural characterization of 3-O-ethylene glycol functionalized cellulose derivatives. *Carbohydr. Polym.* **2009,** *76*, (1), 60-67.
17. Nickel, S.; Kaschani, F.; Colby, T.; van der Hoorn, R. A. L.; Kaiser, M. A para-nitrophenol phosphonate probe labels distinct serine hydrolases of Arabidopsis. *Bioorg. Med. Chem.* **2012,** *20*, (2), 601-606.
18. Konoki, K.; Sugiyama, N.; Murata, M.; Tachibana, K.; Hatanaka, Y. Development of Biotin-Avidin Technology to Investigate Okadaic Acid-Promoted Cell Signaling Pathway. *Tetrahedron* **2000,** *56*, (46), 9003-9014.
19. Holy, A. Simple method for cleavage of phosphonic acid diesters to monoesters. *Synthesis* **1998**, (4), 381-385.

20. Cravatt, B. F.; Sorensen, E.; Patricelli, M.; Lovato, M.; Adam, G. Methods for proteomic analysis using activity based probes for target proteins. WO2001077684A2, 2001.
21. Ross, M. K.; Borazjani, A.; Wang, R.; Crow, J. A.; Xie, S. Examination of the carboxylesterase phenotype in human liver. *Arch Biochem Biophys* **2012,** *522*, (1), 44-56.
22. Larmour, I.; Jackson, B.; Cubela, R.; Johnston, C. I. Enalapril (MK421) activation in man: importance of liver status. *Br. J. Clin. Pharmacol.* **1985,** *19*, (5), 701-704.
23. Shi, D.; Yang, J.; Yang, D.; LeCluyse, E. L.; Black, C.; You, L.; Akhlaghi, F.; Yan, B. Anti-influenza prodrug oseltamivir is activated by carboxylesterase human carboxylesterase 1, and the activation is inhibited by antiplatelet agent clopidogrel. *J Pharmacol Exp Ther* **2006,** *319*, (3), 1477-84.
24. Kaur, N.; Zhou, B.; Breitbeil, F.; Hardy, K.; Kraft, K. S.; Trantcheva, I.; Phanstiel, O. A Delineation of Diketopiperazine Self-Assembly Processes: Understanding the Molecular Events Involved in Nε-(Fumaroyl)diketopiperazine of L-Lys (FDKP) Interactions. *Mol. Pharmaceutics* **2008,** *5*, (2), 294-315.

CHAPTER 3

VALIDATION OF ABPP APPROACH IN THE IDENTIDICATION OF OSELTAMIVIR ACTIVATING ENZYMES

3.1 Introduction

Activity-based protein profiling (ABPP) is able to identify various classes of enzymes through the use of chemical probes.[1-3] Chemical probes have been designed for different enzyme classes and have been used for the characterization of selective inhibitors[4-7] and enzyme annotation.[8-11] Among these, the fluorophosphonate (FP) probes are especially effective in the study of the active serine hydrolases (SHs).[12] Competition experiments between FPs and inhibitors have been extensively reported, however only a few have dealt with competitive ABPP between FPs and substrates with high turnover rates.[13] In this chapter we performed competitive assays between FP-PEG-rhodamine (FP-PEG-rh) and oseltamivir, an ethyl ester prodrug. The competitive ABPP approach for the identification of ethyl ester prodrug activating enzymes was validated using oseltamivir as a case study.

The prodrug activation step, typically hydrolysis, is achieved enzymatically by hydrolases. There are ~240 serine hydrolases (SHs) in the human genome;[14] even for the carboxylesterases (CESs), there are several different families.[15] With such an enormous number of enzymes, the prodrug activation pathways have been investigated in case by case studies. Prodrug development would best be done with early knowledge of the specific activation pathways, i.e. specific enzymes

involved with the prodrug activation. The development of the ABPP approach to rapidly and extensively identify prodrug activating enzymes would aid prodrug optimization and development.

Oseltamivir was selected as a representative classical ethyl ester prodrug (Figure 1) for our studies. Transforming the parent molecule, oseltamivir carboxylate (O.C.), to the ethyl ester significantly increases the oral bioavailability from < 5% to 80%.[16] Human liver Carboxylesterase 1 (CES1) has been reported as the activating enzyme of oseltamivir.[17] Here we assayed the concentration and incubation time of FP-PEG-rh with oseltamivir in on-gel competitive ABPP experiments and from these derived a kinetic mechanism. After a broad survey of Caco-2 cell homogenates, CES1 was identified as one of the binding enzymes of oseltamivir by LC-LC/MS.

3.2 Results

FP-PEG-rh Inhibits Oseltamivir Hydrolysis to Buffer Hydrolysis Level

To successfully identify hydrolases utilizing the competitive ABPP approach, it is necessary to choose the right molecular probes. Although many hydrolases are recognized as SHs, it is essential to verify that the FP-PEG-rh probe can target all of the hydrolases capable of activating oseltamivir in whole cell homogenates. The human intestine is considered as the first site where prodrug hydrolysis occurs; we therefore chose the human colorectal adenocarcinoma (Caco-2) cell line to start our studies. Following pre-incubation with or without FP-PEG-rh for 30 min, we monitored the hydrolysis of oseltamivir in cytosolic and membrane fractions of Caco-2 lysate (2 mg/mL). As illustrated in figure 3.1, oseltamivir hydrolysis in Caco-2 cytosolic and membrane

fractions was reduced to buffer level by pre-treatment with FP-PEG-rh. The results indicated that all of the oseltamivir hydrolases can be bound by FP-PEG-rh.

Identification of CES1 as One Binding Enzyme by Competitive ABPP

Oseltamivir, a good enzyme substrate with rapid on/off kinetics, was used to compete with an FP probe which covalently links to enzymes. A longer incubation time or higher concentration of the probe will readily lead to the disappearance of the substrate competition signal. Thus a time and concentration dependent kinetic study is necessary to observe the most significant competition between prodrug and probe. In addition, different probes may exhibit different binding kinetics toward different enzymes. Therefore, a competition study at different time and concentration conditions between probes and substrates is critical for this approach to be successful.

We initially evaluated the competition in Caco-2 cytosolic and membrane fractions (Figure 3.2A and 3.2B). The best conditions showing a clear competition was with the FP probe (0.25 μM) incubating for 1 min, which would minimize the appearance of other low expressing enzymes. Longer FP incubation times showed more protein bands on the gel, and eventually abolished the competition signal. Thus, there is always a balance between the observance of all the protein bands and the most significant competition signal. Three protein bands (A, B and C), showing the most pronounced signal differences, are labeled by red arrows in figure 3. Protein bands A and C were competed for by oseltamivir in the Caco-2 cytosolic fraction. Band A was rapidly labeled by the FP probe upon increasing the probe incubation time or concentration; however band C was still observable even with a 5 min FP incubation time. This suggests that band A exhibits a higher turnover rate against oseltamivir than band C. The fluorescence signal of band

B binding to the FP probe was surprisingly enhanced by the binding of oseltamivir. This "reversed competition" or enhancement of signal was more prominent in the membrane fraction (Figure 3.2B).

The oseltamivir concentration-dependence study was then performed under the optimized conditions using the FP (0.25 μM) for 1 min (Figure 3.2C). Oseltamivir at 20 mM readily abolished the signals of bands A and C, while enhancing that of band B. The competition was observable even at 5 mM oseltamivir.

In order to identify bands A, B and C, we treated the proteome sample with FP-PEG-biotin, pulled down the proteins with streptavidin agarose beads (Thermo Scientific), separated the accumulated serine hydrolases (SHs) by SDS-PAGE (Figure 3.3), excised the bands, and analyzed each by LC-MS/MS. Band A was identified as a mixture of human liver carboxylesterase 1 (CES1) and carboxylesterase 2 (CES2) (Table 3.1). Based on a previous report[17] and our experiments (data not shown), CES2 is not the activating enzyme of oseltamivir. Thus CES1 was identified as one of the potential activating enzymes of oseltamivir. Interestingly, however, bands B and C could not be isolated as described above even after several large scale trials. This result was consistent with the western-blot competition assay. Possible reasons for this are (a) the proteins were bound by FP-PEG-biotin non-covalently, and were washed off by the buffer after the FP probe was linked to streptavidin and (b) the expressed quantities of bands B and C were too low to be observed on SDS-PAGE after isolation (although unlikely considering the strength of the fluorescence signal in the competition assay).

Band B and C was excised from the gel directly without serine hydrolase isolation and analyzed by LC/MS as a mixture of different proteins. No serine hydrolases around 30 kD were detected from bands B and C.

Kinetic Mechanism of FP competition with enzymatic substrate

Since CES1 has already been reported as an activating enzyme of oseltamivir,[17] it is thus a more attractive and feasible target for the mechanism-based study of the enzymatic competition kinetics between oseltamivir and FP-PEG-rh. Parameters of K_M and V_{max} were determined by the hydrolysis study of oseltamivir in pure recombinant hCES1 (160 nM; Corning®, Tewksbury, MA). The hydrolysis rate was plotted as a function of substrate concentrations (0.2 - 5 mM) and non-linearly fitted to Michealis-Menten equation by GraphPad Prism 6 (Figure 3.4). The K_M and V_{max} values are 2.984 mM and 7.204 μM/min, respectively. The calculated k_{cat} / K_M value is 251.34 $s^{-1} \cdot M^{-1}$.

The pseudo-first-order rate constant (k_{obs}) of FP-PEG-rh (1 μM) to CES1 was determined on-gel based on the fluorescent signals over different time points (Figure 3.5a). The binding rate demonstrated from the gel is very fast such that a strong fluorescent signal could be observed 5 sec after the initiation of the reaction and the inactivation reached essential completion after 30 sec. However, the fast binding from FP-PEG-rh alone could be impacted by the competition of oseltamivir. At the same condition when CES1 (100 nM) was preincubated with oseltamivir (10 mM) for 8 min, followed by the initiation of reaction with FP-PEG-rh (1 μM), the complete binding of the probe to CES1 was reached at 2 min (Figure 3.5b). The competition signals at the first several time points were also clearly observable from the comparison with the corresponding time points of FP-PEG-rh binding.

Fluorescence intensities from on-gel study were quantified and normalized by the average of their highest intensities. The fractionated intensities were then plotted exponentially over time as shown in figure 3.6 (k_{obs}(s) are represented as K in the figure). The apparent binding rate of FP-PEG-rh (k_{obs}) is reduced by about 4-fold due to the competition of oseltamivir (k'_{obs}).
The calculated inactivation rate ($k_{obs}/[I]$) of FP-PEG-rh is 4.0 x 10^6 $s^{-1}\cdot M^{-1}$, which is about 10,000-fold faster than the turnover rate of oseltamivir (k_{cat}/K_M = 251.34 $s^{-1}\cdot M^{-1}$). By using 10 mM of prodrug to compete with 1 μM of FP-PEG-rh, the binding rate (k_{obs}) was decreased by 4-fold, to an observable time frame.

Generally, oseltamivir binding enzymes were broadly surveyed among the serine hydrolases in Caco-2 whole cell proteome samples with the kinetically tuned competitive ABPP approach. The specific enzyme kinetics study on CES1 unveiled the fact that the covalent binding of FP probe could be slowed down through interference of reversible substrates. The competitive binding signal could only be observed within a short time frame, which is determined by the parameters of the applied probes (K_I and k_{inact}) and prodrugs (K_M). In on-gel competition assays, the competitive binding rate (k'_{obs}) of the probe could further be reduced by either decreasing probe concentration or increasing substrate concentration as shown in our case. This validated approach can potentially be applied to the detection of competitive binding between prodrugs and corresponding probes; in addition, confirmation of enzymatic activations have to be verified in follow up experiments with specific binding enzymes in over-expressed form.

3.3 Discussion

Identifying prodrug-activating enzymes is essential to understanding the factors that contribute to drug delivery and drug efficacy, yet this analysis tends to occur at a later stage or as an

afterthought in the drug development process. This lag is partly a result of the typically late stage implementation of prodrug moieties to modify biopharmaceutical properties and the time-consuming biochemical separations and assays required for validation. In this chapter, we have adopted ABPP to compete the chemical probes and prodrugs toward identifying potential prodrug activating enzymes. This method combined tuned kinetic competition studies with LC-MS protein identification to identify several oseltamivir binding enzymes. Despite the utility of the method, the competition between probes and substrates with high enzymatic turnover rate has some limitations: (i) a short incubation time with the probe can obscure low expressing proteins compared to background (ii) a long time incubation with probe can lead to complete probe binding to hydrolyzing enzymes, thus completely abolishing the competition signal. These limitations can be overcome by an in-gel competitive kinetic study, which involves screening with different incubation times and probe concentrations.

This method can also be applied to activating mechanism studies of prodrugs with a selective activation function. Since different tissues show different degrees of serine hydrolase expression,[12] SHs are expected to exist at higher levels in some tissues and lower in others. In this case, a given SH may potentially be targeted for selective hydrolysis of prodrugs in a specific tissue. Dozens of new chemical probes targeting most of the metabolizing enzymes have been developed over the last ten years, which enables most of the prodrug activating enzymes to be associated with a functional proteomic probe. Thus, researchers have the possibility of choosing the right probe for the study of corresponding types of prodrugs activation.

In summary, we have validated a rapid and practical method for the identification of potential prodrug activating enzymes through activity-based protein profiling competition between FP-

PEG-rh and oseltamivir. The strategy outlined here has the advantage of surveying almost the entire class of serine hydrolase enzymes and could potentially accelerate process of identifying prodrug activating enzymes.

3.4 Experimental Methods

Materials

Oseltamivir phosphate (Osel.) was purchased from Allichem LLC. Enalapril maleate salt was purchased from Sigma-Aldrich. Tazarotene and benazepril HCl were purchased from Selleckchem. FP-PEG-rhodamine was prepared as previously described.[11]

Prodrug hydrolysis assay

Caco-2 cytosolic and membrane fractions (2 mg/mL) in 50 mM Tris buffer (pH 7.6) were treated with DMSO (0.5%) as control, FP-PEG-rhodamine (5 μM) for 30 min at room temperature, and then oseltamivir (1 mM) was added. The reactions were incubated at 37 °C for 20 min, 50 min, 80 min and 120 min before being terminated by two volume equivalents of acetonitrile (ACN) with 0.1% TFA. After centrifugation at 13,200 x g for 3 min at room temperature, the supernatant was filtered with Microplate PVDF filter. The filtrates were analyzed by an Agilent 1100 HPLC system. Briefly, chromatography was performed on a 4.6 x 150 mm 3.5 micron ZORBAX Eclipse XDB-C18 column (Agilent), and samples were eluted with an 11 min gradient of 2%- 90% buffer B (Buffer A: H_2O with 0.1% TFA; Buffer B: ACN with 0.1% TFA). The percentages of products generated were calculated based on the relative areas under the curve of the prodrugs and products.

Competition assays

Competition assays of cytosolic and membrane fractions were performed in 50 mM Tris buffer (pH 7.4) in a total volume of 50 μL by first incubating proteome aliquots (1 mg/mL final), osel. (various concentrations as noted in figures) for 10 min at room temperature. Then FP-PEG-rh (1 μM, 0.5 μM or 0.25 μM final) was added and incubated for 1 min, 3 min, or 5 min at room temperature. Competition reaction was quenched by adding 5x sample loading buffer (12.5 μL), heated at 85 °C for 5 min, subjected to SDS-PAGE (4% - 20%, Tris-Glycine) and visualized on-gel in a Typhoon 9200 fluorescence imager.

Serine hydrolases isolation by streptavidin beads

Caco-2 cytosolic fraction (2 mg/ml, 1.5 mL) was incubated with FP-PEG-biotin (10 μM final) at room temperature for 1 h with occasional vortexing. Methanol (6 mL, 4 volumes) was added and vortexing, followed by the addition of chloroform (2.25 mL, 1.5 volumes) and vortexing, and then the addition of water (4.5 mL, 3 volumes) and vortexing to homogeneity. The mixture was centrifuged (10,000 x g) at room temperature for 10 min in a swinging bucket rotor to separate the aqueous and organic phases. The top aqueous phase was carefully removed and discarded and then 3 volumes of methanol (4.5 mL) were added and mixed gently, trying not to completely disrupt the pancake-like protein interface. The protein precipitate was centrifuged (10,000 x g, 2 min) and the liquid was removed. The resulting protein precipitate was mixed with 4 volumes of methanol (6 mL) and sonicated at 4 °C until homogenous. The protein precipitate was centrifuged (10,000 x g, 10 min) and air dried for 2-3 min after removing the methanol. The resulting protein was resuspended in 500 μL of 6M urea / 25 mM NH_4CO_3H buffer, with the addition of 140 μL of 10% SDS, and was incubated at 65 °C for 5 min to re-solubilize protein. The protein solution was diluted with 6.5 mL PBS buffer and cooled to room temperature. Strepavidin agarose resin (Thermo Scientific, 50% slurry, 200 μL) was added and the mixture

incubated at room temperature for 1.5 h with rotation. The resin was centrifuged (3,000 x g, 2 min) to a pellet and the supernatant was removed. The resin was then washed three times each by 1% SDS in PBS buffer (200 μL) and in PBS buffer only (200 μL), respectively by vortexing, centrifuging, and removing supernatant. After washing buffer was removed, sample loading buffer (2x, 50 μL) was added to the resin and the mixture was boiled at 85 °C for 5 min. The resulting solution was loaded to SDS-PAGE and separated, and the corresponding protein bands were excised and identified by LC/MS.

Enzymatic kinetics study on CES1

Recombinant pure human carboxylesterase 1 (6.25 mg/L, 100 nM) was incubated with oseltamivir (10 min) or vehicle for 8 min at room temperature in TBS-F127 buffer (50mM Tris, 150mM NaCl, 0.5g/L Pluronic F127, pH 7.4), followed by the addition of FP-PEG-rh (1 μM) with vortex. At the indicated time points, 20 μL of reaction mixture was taken and inactivated with 5 μL of 5 x Laemmli sample buffer, heated at 95ºC, for 5 min. Mixtures were separated by 15% of 1:29 bis:mono acrylamide SDS gel (Figure b1, 1 ug protein/lane) and 4%-20% precasted Tris-Glycine gel (Invitrogen; Figure b2, 1.5 ug protein/lane). Fluoroescence intensity was quantified with ImageJ.

3.5 Figures

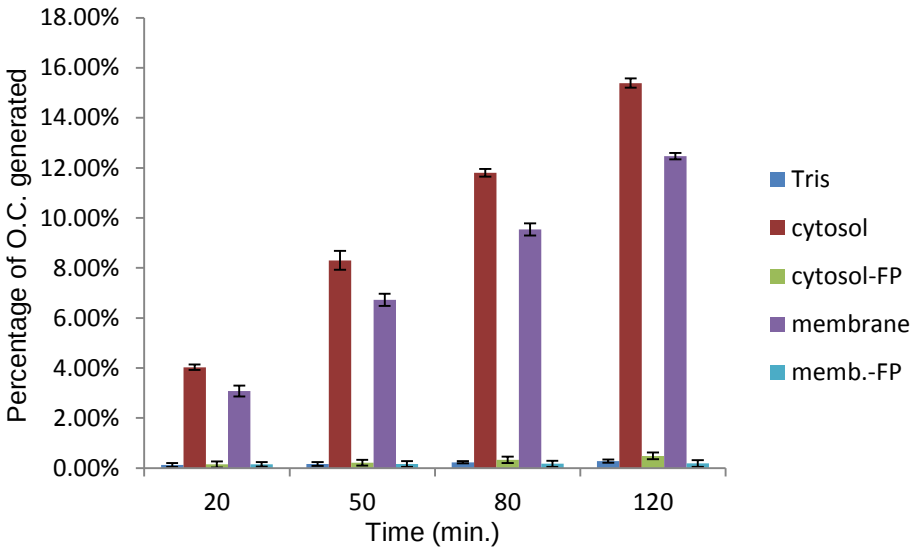

Figure 3.1. Inhibition of oseltamivir hydrolysis. The hydrolase activity in Caco-2 cells was measured under the following conditions: Proteome samples (2 mg/mL, 200 µL reaction volume) were incubated with DMSO (control), or FP-PEG-rh (5 µM) for 30 min at room temperature and then with oseltamivir (1 mM) at 37 °C for 20 min, 50 min, 80 min or 120 min. The percentage of oseltamivir carboxylate generated in each reaction was monitored by HPLC. Results are represented as the average ± SEM of 2-3 individual experiments. *, $p < 0.001$.

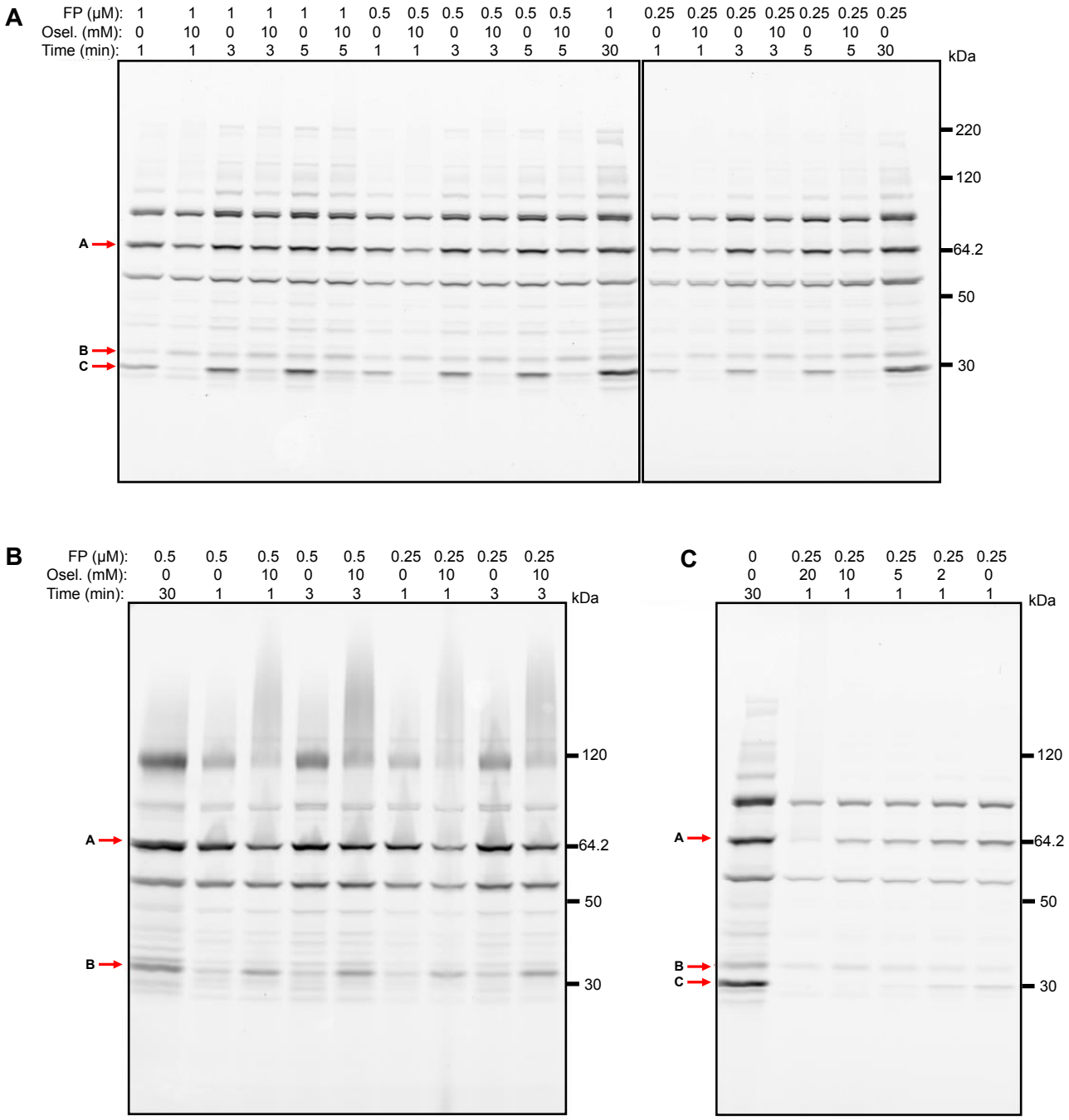

Figure 3.2. Time vs. concentration study for oseltamivir competing with FP-PEG-rh in Caco-2 lysates. Caco-2 cytosolic (A) and membrane (B) proteome samples (1 mg/mL final) were treated with oseltamivir (10 mM final) for 10 min at room temperature and then FP-PEG-rh (1 μM, 0.5 μM or 0.25 μM) for 1 min, 3 min or 5 min. Protein samples were then treated with sample loading buffer, heated at 85 °C for 5 min, separated by SDS-PAGE, and scanned by Typhoon imager. (C) Caco-2 cytosolic proteome samples (1 mg/mL) were treated with 20 mM, 10 mM, 5 mM, 2 mM, or 0 mM of oseltamivir for 10 min and then FP-PEG-rh (0.25 μM) for 1 min at room temperature. Protein samples were then treated with sample loading buffer, heated

at 85 °C for 5 min, and monitored as described above. Protein bands with the most prominent competition signals are labeled by red arrows as A, B, and C.

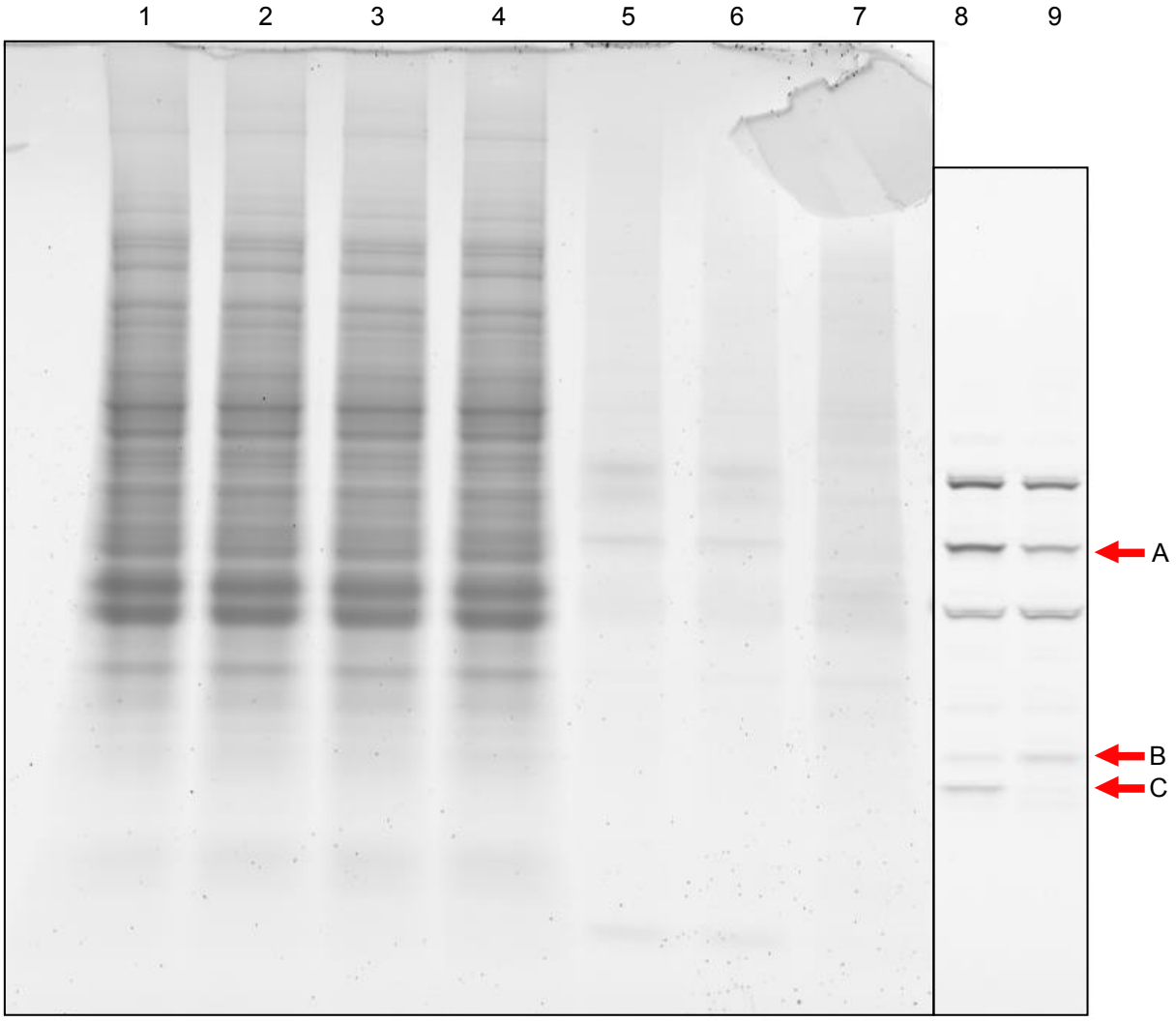

Figure 3.3. Serine hydrolases isolation by FP-PEG-biotin and streptavidin agarose beads. Lane 1 to Lane 4 were samples for competition assay to be monitored by fluorescent signal. Lane 5 and 6 were the results from serine hydrolases isolation. Lane 7 was control group (samples with DMSO instead of FP-PEG-biotin). Lane 8 and 9 were competition results for comparison. The gel was stained by coomassie blue.

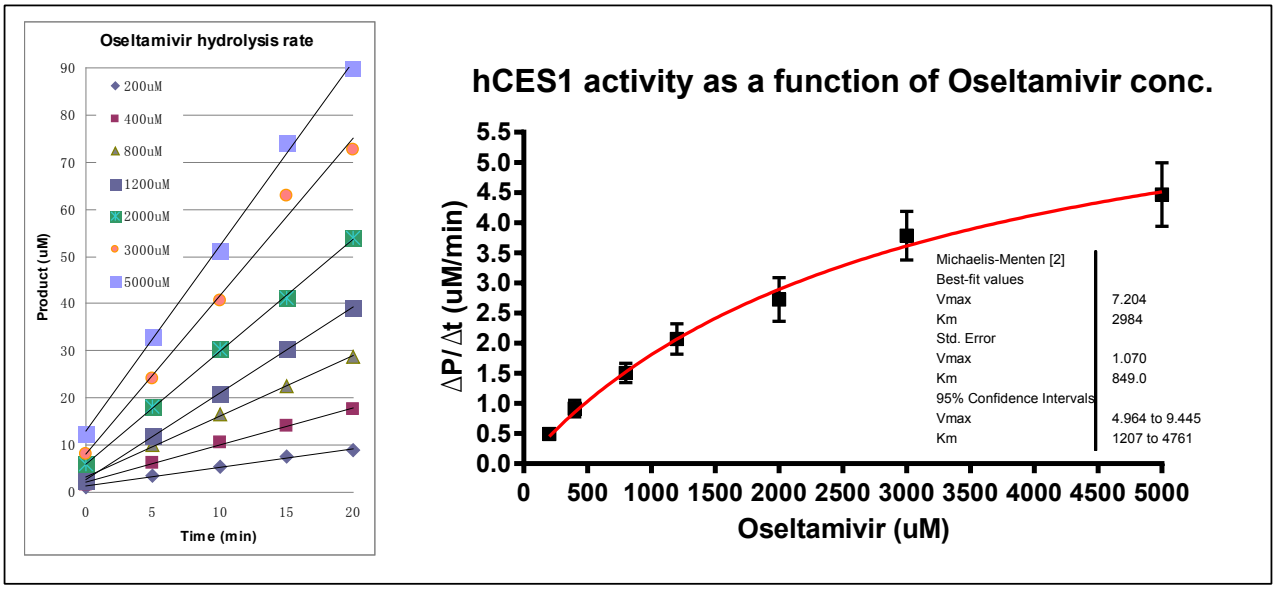

Figure 3.4. The hydrolysis of oseltamivir by recombinant hCES1 (a) and the determination of Vmax and KM by Michaelis-Menten curve (b). Oseltamivir (concentrations as noted in figure) was hydrolyzed in CES1 (160 nM) in Tris buffer with 1 mg/mL BSA (50 mM, pH 7.6). Sample was collected at each time point and analyzed by HPLC. Hydrolysis rate was calculated basing on the relative areas under the oseltamivir and prodruct curves. Oseltamivir hydrolysis rate versus oseltamivir concentration was plotted and non-linearly fitted into Michaelis - Menten equation by GraphPad Prism 6. Error bars represent the standard deviation of 3 individual experiments.

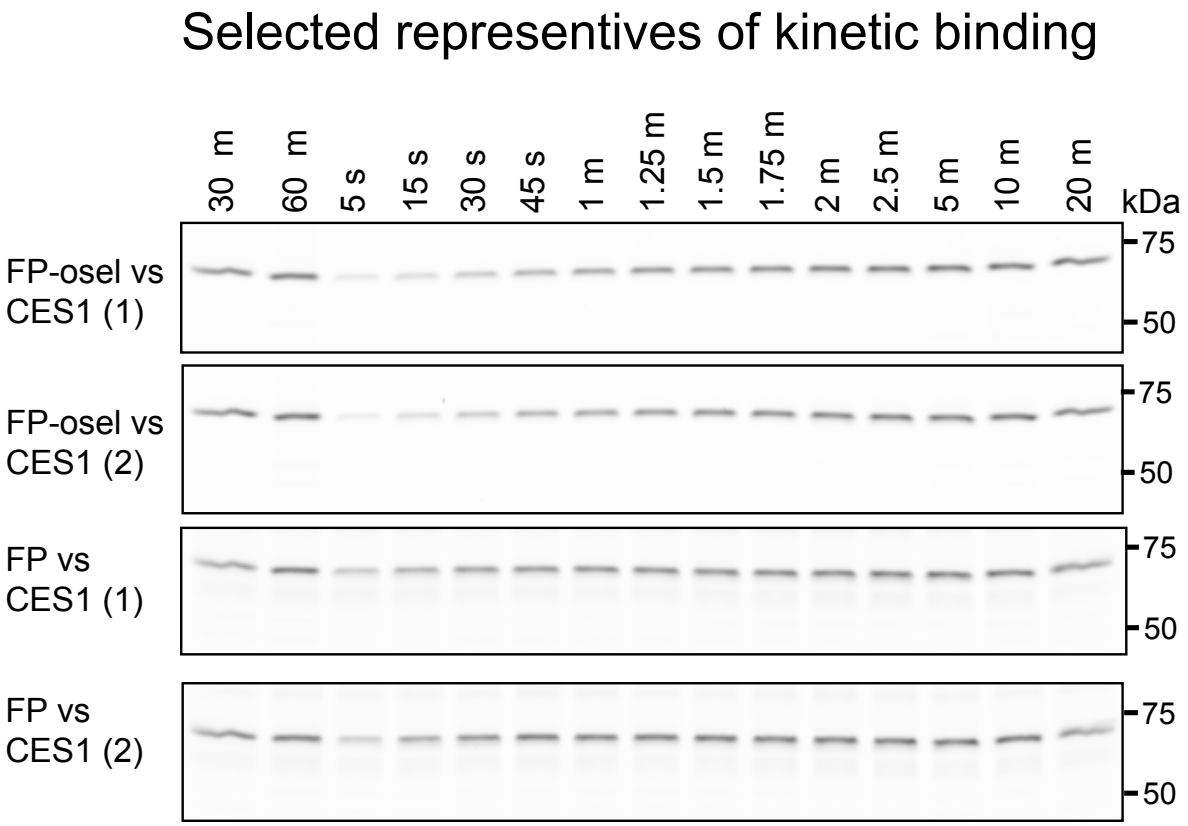

Figure 3.5. An on-gel comparison of CES1 binding kinetics on FP-PEG-rh alone and FP-PEG-rh vs oseltamivir competition. rhCES1 (6.25 mg/L, 100 nM) was incubated with vehicle (a) or oseltamivir (b) for 8 min at room temperature in TBS-F127 buffer (50mM Tris, 150mM NaCl, 0.5g/L Pluronic F127, pH 7.4), followed by the addition of FP-PEG-rh (1 μM) with vortex. Reactions were quenched at noted time points with sample loading buffer, heated at 95 ºC for 5 min, and through SDS-PAGE gel (1,1ug protein/lane,15% of 1:29 bis:mono acrylamide. 2, 1.5ug protein/lane, 4%-20% precasted Tris-Glycine gel, Invitrogen). Experiments were repeated as two individual SDS-PAGE gels as shown.

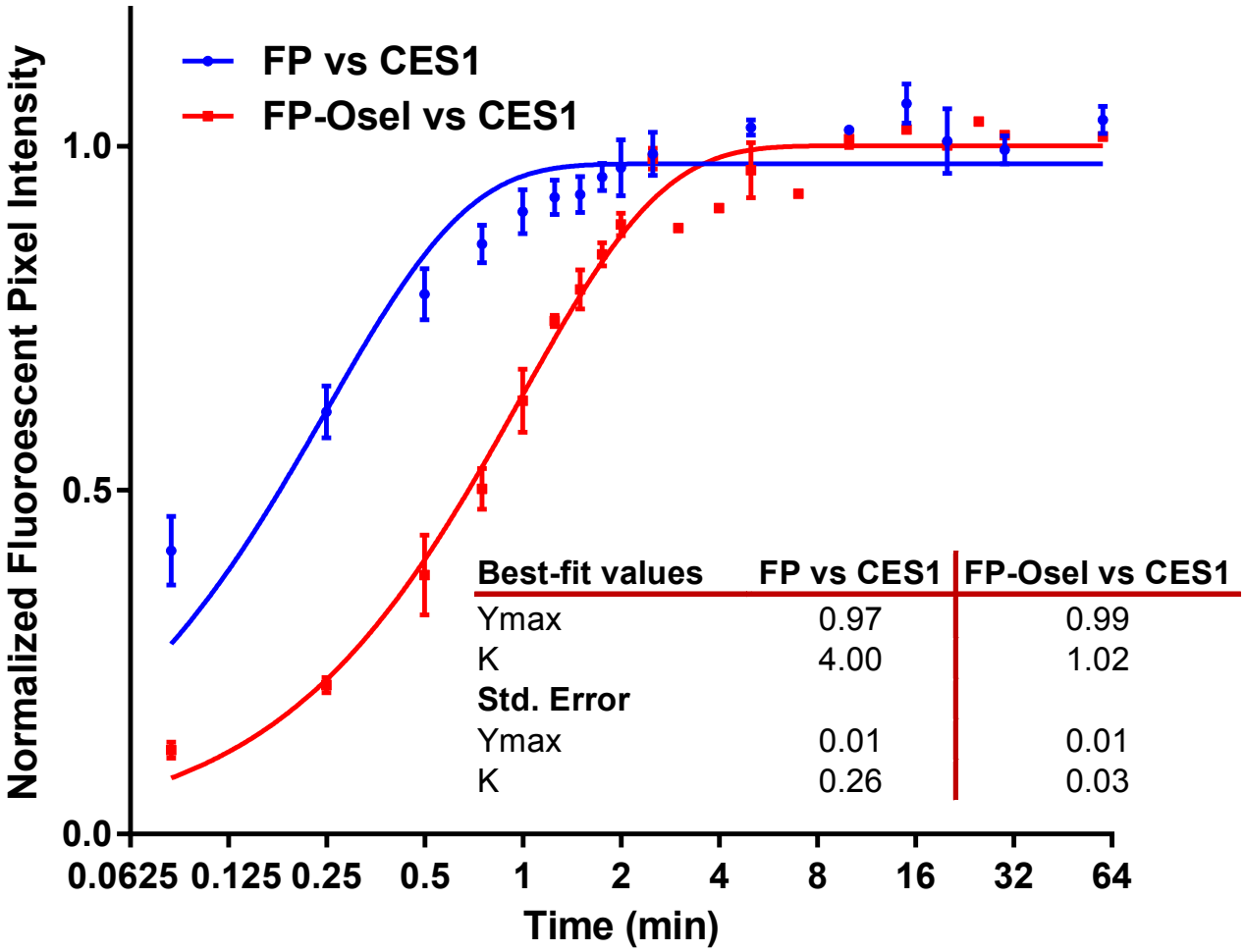

Figure 3.6. Pseudo-first-order curves for CES1binding by FP alone and oseltamivir-FP competition. Rate constant (*k*obs and *k'*obs) are represented as K in the figure.

Table 3.1. List of Possible Serine Hydrolases Identified in Caco-1 Cytosol Fraction Proteome by LC/MS-MS						
Protein ID	Gene Name	Discription	Confidence	Coverage	number of unique peptides	total independent spectral counts
Band A:						
sp|P23141|EST1_HUMAN	CES1	Liver Carboxylesterase 1	1.00	69.0%	56	232
sp|O00748|EST2_HUMAN	CES2	Carboxylesterase 2	1.00	24.5%	10	16
Band B:						
sp|P27348|1433T_HUMAN	YWHAQ	14-3-3 protein theta	1.00	48.2%	11	17
sp|P18669|PGAM1_HUMAN	PGAM1	Phosphoglycerate mutase 1	1.00	47.2%	11	16
sp|P78417|GSTO1_HUMAN	GSTO1	Glutathione S-transferase omega-1	1.00	24.5%	5	14
Band C:						
sp|P60174|TPIS_HUMAN	TPI1	Triosephosphate isomerase isoform 2	1.00	75.5%	24	98
sp|P30041|PRDX6_HUMAN	PRDX6	Peroxiredoxin-6	1.00	53.6%	19	47
sp|O43399|TPD54_HUMAN	TPD52L2	Tumor protein D54	1.00	41.3%	7	10

3.6 References

1. Berger, A. B.; Vitorino, P. M.; Bogyo, M. Activity-based protein profiling: applications to biomarker discovery, in vivo imaging and drug discovery. *Am J Pharmacogenomics* **2004,** *4*, (6), 371-81.
2. Saghatelian, A.; Cravatt, B. F. Assignment of protein function in the postgenomic era. *Nature chemical biology* **2005,** *1*, (3), 130-42.
3. Cravatt, B. F.; Wright, A. T.; Kozarich, J. W. Activity-based protein profiling: from enzyme chemistry to proteomic chemistry. *Annu Rev Biochem* **2008,** *77*, 383-414.
4. Ahn, K.; Johnson, D. S.; Mileni, M.; Beidler, D.; Long, J. Z.; McKinney, M. K.; Weerapana, E.; Sadagopan, N.; Liimatta, M.; Smith, S. E.; Lazerwith, S.; Stiff, C.; Kamtekar, S.; Bhattacharya, K.; Zhang, Y.; Swaney, S.; Van Becelaere, K.; Stevens, R. C.; Cravatt, B. F. Discovery and characterization of a highly selective FAAH inhibitor that reduces inflammatory pain. *Chemistry & biology* **2009,** *16*, (4), 411-20.
5. Long, J. Z.; Li, W.; Booker, L.; Burston, J. J.; Kinsey, S. G.; Schlosburg, J. E.; Pavon, F. J.; Serrano, A. M.; Selley, D. E.; Parsons, L. H.; Lichtman, A. H.; Cravatt, B. F. Selective blockade of 2-arachidonoylglycerol hydrolysis produces cannabinoid behavioral effects. *Nature chemical biology* **2009,** *5*, (1), 37-44.
6. Lone, A. M.; Bachovchin, D. A.; Westwood, D. B.; Speers, A. E.; Spicer, T. P.; Fernandez-Vega, V.; Chase, P.; Hodder, P. S.; Rosen, H.; Cravatt, B. F.; Saghatelian, A. A substrate-free activity-based protein profiling screen for the discovery of selective PREPL inhibitors. *Journal of the American Chemical Society* **2011,** *133*, (30), 11665-74.
7. Bachovchin, D. A.; Zuhl, A. M.; Speers, A. E.; Wolfe, M. R.; Weerapana, E.; Brown, S. J.; Rosen, H.; Cravatt, B. F. Discovery and optimization of sulfonyl acrylonitriles as selective, covalent inhibitors of protein phosphatase methylesterase-1. *J Med Chem* **2011,** *54*, (14), 5229-36.
8. Martin, B. R.; Wang, C.; Adibekian, A.; Tully, S. E.; Cravatt, B. F. Global profiling of dynamic protein palmitoylation. *Nat Methods* **2012,** *9*, (1), 84-9.
9. Barglow, K. T.; Cravatt, B. F. Activity-based protein profiling for the functional annotation of enzymes. *Nat Methods* **2007,** *4*, (10), 822-7.
10. Blankman, J. L.; Simon, G. M.; Cravatt, B. F. A comprehensive profile of brain enzymes that hydrolyze the endocannabinoid 2-arachidonoylglycerol. *Chemistry & biology* **2007,** *14*, (12), 1347-56.
11. Tully, S. E.; Cravatt, B. F. Activity-based probes that target functional subclasses of phospholipases in proteomes. *Journal of the American Chemical Society* **2010,** *132*, (10), 3264-5.
12. Kidd, D.; Liu, Y.; Cravatt, B. F. Profiling serine hydrolase activities in complex proteomes. *Biochemistry* **2001,** *40*, (13), 4005-15.
13. Xu, H.; Sabit, H.; Amidon, G. L.; Showalter, H. D. An improved synthesis of a fluorophosphonate-polyethylene glycol-biotin probe and its use against competitive substrates. *Beilstein J Org Chem* **2013,** *9*, 89-96.
14. Bachovchin, D. A.; Cravatt, B. F. The pharmacological landscape and therapeutic potential of serine hydrolases. *Nat Rev Drug Discov* **2012,** *11*, (1), 52-68.
15. Holmes, R. S.; Wright, M. W.; Laulederkind, S. J.; Cox, L. A.; Hosokawa, M.; Imai, T.; Ishibashi, S.; Lehner, R.; Miyazaki, M.; Perkins, E. J.; Potter, P. M.; Redinbo, M. R.; Robert, J.; Satoh, T.; Yamashita, T.; Yan, B.; Yokoi, T.; Zechner, R.; Maltais, L. J. Recommended nomenclature for five mammalian carboxylesterase gene families: human, mouse, and rat genes and proteins. *Mamm Genome* **2010,** *21*, (9-10), 427-41.
16. McClellan, K.; Perry, C. M. Oseltamivir: a review of its use in influenza. *Drugs* **2001,** *61*, (2), 263-83.

17. Shi, D.; Yang, J.; Yang, D.; LeCluyse, E. L.; Black, C.; You, L.; Akhlaghi, F.; Yan, B. Anti-influenza prodrug oseltamivir is activated by carboxylesterase human carboxylesterase 1, and the activation is inhibited by antiplatelet agent clopidogrel. *J Pharmacol Exp Ther* **2006,** *319*, (3), 1477-84.

Chapter 4

CHARACTERIZATION OF WWL50 AS A SELECTIVE HUMAN CARBOXYLESTERASE 1 INHIBITOR AND ITS UTILIZATION AGAINST GENERAL ESTER PRODRUGS

4.1 Introduction

Human carboxylesterase 1 (hCES1) is a broad-spectrum esterase with the function of xenobiotics detoxification, prodrugs activation as well as involvement in additional biological processes.[1] Analysis of the hCES1crystal structure with different therapeutic agents has provided mechanism information on its catalytic capability toward various substrates.[2] This enzyme exits as a trimer and its active site possesses a catalytic triad of Ser221-His468-Glu354 on a monomer in a hydrophobic pocket at the interface of three domains, which are the catalytic regulatory and α/β domains. As a serine hydrolase, a two-step hydrolysis mechanism has been proposed involving the formation of a covalent acyl intermediate at the active serine residue, followed by subsequent hydrolysis and release.

CES1 is widely distributed among different tissues such as intestine, kidney, lung, and testes but is mainly expressed in liver. The hydrolysis of esters with small alcohol groups and large acyl groups is preferred, which differs from hCES2. Due to its important role in metabolism and its broad-spectrum substrate properties, multiple drug-drug interactions have been observed among the prodrug activation, drug metabolism and in vivo hydrolysis coupled with endogenous

biological processes.[3] CES1 is known to be an endogenous detoxifying enzyme, and there's increasing evidence pointing to its activity contributing to obesity and diabetes.[5, 6] Thus, the development of selective inhibitors or chemical probes will significantly aid in the understanding of drug metabolizing and disease-related functions of CES1.

CES1 can be efficiently inhibited non-specifically by many compounds such as bis-(4-nitrophenyl) phosphate (BNPP), phenylmethanesulfonyl fluoride (PMSF), and 4-(2-aminoethyl) benzenesulfonyl fluoride hydrochloride (ABESF).[4, 7] High-throughput screening and structure-activity relationships have been performed to discover specific inhibitors of CES1.[8, 9] A selective CES1 inhibitor derived from a natural product, FR182877, has also been characterized by the competitive ABPP approach.[10] In this chapter, a carbamate compound inhibiting mouse carboxylesterases, WWL50, was profiled against hCES1 utilizing competitive ABPP and ABPP-SILAC approaches toward the determining CES1's contribution to the hydrolysis of ester prodrugs.

Carbamates have been reported as privileged scaffolds that covalently inhibit SHs.[11] Their reactivity is associated with a tempered electrophilicity and hydrolytic stability. Several carbamates targeting different SHs have been developed as inhibitors, for example, UBR597 for FAAH[12] and JZL184 for MAGL[13]. A carbamate library (>140) was developed by the Cravatt group and screened individually against a library of mouse SHs[11]. From these results, we selected two compounds, 4-fluoro-3-methylphenyl cyclohexylcarbamate (WWL50) and phenyl (3-morpholinopropyl)carbamate (WWL79) (Figure 1) for our studies based on the fact that they show the fewest off-target effects amongst the mouse Ces1 inhibitors. In the screening against

more than 200 serine hydrolases in Caco-2 cell homogenates, facilitated by ABPP-SILAC, WWL50 was shown to be a selective inhibitor of CES1.

Competitive ABPP with stable isotope labeling of amino acids in cell culture (ABPP-SILAC) is a recently developed quantitative MS-based platform for identification of activity-based probe targeted enzymes[14, 15] and selectivity profiling of small-molecule inhibitors.[16, 17] This technology utilizes proteome samples from the same cell line which are treated separately with normal amino acid "LIGHT samples" and isotopically labeled amino acid "HEAVY samples". Samples are then mixed and detected together with LC-LC/MS, which minimizes the signal intensity differences caused by the environmental variations. By comparison of the same protein from LIGHT and HEAVY samples, qualification and quantification results with greater accuracy can be obtained. The advantage of this approach is the application of mass spectrometry, enabling the profiling of a large number of enzymes (even with very low expression levels). Here we successfully confirm that CES1 is the primary activating enzyme of ethyl esters and that it contributes >95% to oseltamivir hydrolysis. This was corroborated by studies with the selective CES1 inhibitor, WWL50, which allows us to conclude that human CES1 is the primary activating enzyme for ethyl ester prodrugs.

4.2 Results

Selectivity Characterization of CES1 Inhibitors

Potency and selectivity of WWL50 and WWL79 (Figure 4.1) against CES1 was demonstrated by competitive ABPP on SDS-PAGE. The Caco-2 cytosolic and membrane fractions were pretreated with the carbamates at room temperature, followed by the incubation with FP-PEG-rh and FP-rh. Enzymes inhibited by the inhibitors gave reduced fluorescence signals. We

determined that WWL50 very selectively inhibited CES1 in Caco-2 lysates, competing either with FP-PEG-rh (Figure 4.2A) or FP-rh (Figure 4.2B), while no other SHs showed any inhibition effects. On the other hand, WWL79 displayed no inhibition toward any observable SHs in competitive ABPP. Due to the fact that the CES2 expression level in Caco-2 cells is small and its on-gel fluorescence signal could overlap with CES1, we then characterized the WWL50 selectivity with pure human recombinant CES1 and CES2. An ethyl ester prodrug, benazepril, was used as CES1 substrate with 4-nitrophenol acetate as a CES2 substrate. The hydrolyzed products were monitored by HPLC with or without inhibitor. As shown in figure 4.3, the IC_{50}s of WWL50 against recombinant hCES1 and hCES2 have about a 100 fold difference. Thus, we can conclude that WWL50 is selective for human CES1 inhibitor amongst SHs.

Inspired by the selectivity of WWL50, we further explored its potency against CES1. WWL50 with different concentrations was reacted with Caco-2 cytosolic fraction and then competed with the FP-PEG-rh probe in a competitive ABPP assay. As demonstrated on-gel, the IC_{50} of WWL50 against CES1 (~64 kD) in total cell homogenate is 2-4 μM without inhibiting any other observable SHs (Figure 4.4).

ABPP-SILAC

To identify other low level enzymes that are unobservable on-gel, we used an advanced quantitative MS-based platform termed 'competitive ABPP with stable isotope labeling by amino acids in cell culture (ABPP-SILAC)'.[14] This has been used to accurately identify and quantify the profile of small molecule inhibited enzymes.

Briefly, Caco-2 cell was cultured with isotopically labeled amino acids (HEAVY cells) and normal amino acids (LIGHT cells). The HEAVY and LIGHT cells were separated into membrane and cytosolic fractions. Light and heavy fractions were treated with WWL50 or vehicle, respectively, and then treated with FP-PEG-biotin. Samples were then mixed in a 1:1 ratio, enriched with streptavidin, digested on-bead with trypsin and analyzed by NanoAcquity UPLC system using Synapt G2-S mass-spectrometer enabled with ion-mobility. Heavey and light peptide data was compiled and analyzed by the ProteinLynx Global Server 3.0. Amongst approximately 200 quantified serine hydrolases of the ABPP-SILAC study, of which 45 were represented, only CES1 and CES1P were significantly inhibited by WWL50 in Caco-2 cell (Figure 4.5).

The carboxylesterase 1 pseudogene 1 (CES1P1, a.k.a CES4) is a pseudogene of CES1 with a premature stop codon in exon 6[18]. CES1 and CES1P1 genes are located inversely on chromosome 16q13-q22.1 and 28 kb apart. CES1P1 has a very high sequence similarity to CES1 (87.7% as shown on figure 4.6) and is believed to be its inverted duplication[19, 20]. Currently CES1P1 has only been characterized by DNA and mRNA sequences, and its mRNA has been usually detected in multiple tissues together with CES1[21-23]. However there are no published reports of its recombinant over-expression to address its functional enzyme activity. Inferred amino acid sequence of CES1P1 (30.7 kDa) indicates that it is a truncated protein that resembles the *N*-terminal half of CES1. This (half) of the CES1 sequence possesses only one of the three catalytic triad amino acids. No inhibition by WWL50 could be observed from the on-gel competition studies, indicating its overlap with other protein bands and its low expression in Caco-2 cell (Figure 4.2, 4.4). No clear evidence from our LC-LC/MS study was able to exclude the possibility that the specific CES1P1 peptides our quantification relied on are from the variant

of a corresponding CES1mutation. Although our results indicate that CES1P1 binds to and potentially is reactive with the inhibitor WWL50, the functional expression and activity of CES1P1 need to be further investigated. Its activity, if any, against the hydrolysis of oseltamivir in this case could be negligible considering its low expression. For this report we conclude that WWL50 is a very selective human CES1 inhibitor.

Oseltamivir Hydrolysis Inhibition by WWL50 and 79

WWL50 and WWL79 were then applied to the hydrolysis of oseltamivir in Caco-2 lysates. As illustrated in figure 4.7, both FP-PEG-rh and WWL50 inhibited oseltamivir hydrolysis >95%, with WWL79 showing partial inhibition, approximately 20% in cytosolic and 25% in membrane fractions. Collectively, these data lead to the conclusion that CES1 is the primary oseltamivir activating enzyme, contributing >95% in the Caco-2 cell line, and that WWL50 is a selective inhibitor of human CES1 in Caco-2 lysates.

Hydrolysis of Oseltamivir in Hep G2 Cell Lysates

We extended our study from Caco-2 to the human liver carcinoma cell line (Hep G2) in an attempt to broaden the range of substrate hydrolases. Again we started with the hydrolysis assay of oseltamivir, either in the presence or absence of the FP probe and WWL50 (Figure 4.8A). Similar results were generated for Hep G2 as for the Caco-2 cell line with >95% of oseltamivir hydrolysis inhibited by WWL50 and FP-PEG-rh. Competitive ABPP was then performed between WWL50 and FP-PEG-rh or FP-rh to determine the selectivity of WWL50 in Hep G2 lysates (Figure 4.8B). The results showed that WWL50 was selective against CES1 to an

observable extent in Hep G2 lysates. Oseltamivir was competed with FP-PEG-rh, which showed a reduced fluorescent signal in the CES1 band on SDS-PAGE (Figure 4.9).

Hydrolysis Studies on Other Ethyl Ester Prodrugs

Enalapril, benazepril, and tazarotene were chosen as examples of other ethyl ester prodrugs to evaluate. Valacyclovir with a valine ester pro-moiety was used as a negative control. The hydrolysis of these prodrugs in Hep G2 lysates, either in the presence or absence of WWL50, is shown in Figures 4.10A and 4.10B. The hydrolysis of all tested prodrugs was inhibited by WWL50, indicating that CES1 is the primary activating enzyme, although its catalyzing capability varies amongst substrate drugs.

4.3 Discussion

In this chapter, we characterized a selective CES1 inhibitor, WWL50, with which the hydrolysis contribution of CES1 against several ethyl ester prodrugs was determined. Theoretically, we could have recombinantly over-expressed all targeted oseltamivir binding enzymes in competitive ABPP, and tested them against oseltamivir individually to confirm their activation. However the discovery of WWL50 as a selective CES1 inhibitor significantly accelerates this process. After determining that CES1 accounts for >95% of the total hydrolysis activity, the activities of other non-specific binding enzymes can mostly be excluded from the activation of oseltamivir. The reason we did not assign 100% of hydrolysis activity to CES1 is that the hydrolysis of a prodrug is always a combination of chemical and enzymatic effects. We could always observe 1-2% more hydrolysis in cell lysates than in Tris buffer based on a previous

study, which may result from general acid-base catalysis by amino acid residues in the proteome sample.

CES1 is an important metabolizing enzyme with various substrates. CES1 was found to be more active in adipose tissue from humans with obesity and diabetes.[23] Inhibition of mouse Ces3, the ortholog of human CES1, can significantly increase insulin sensitivity and glucose tolerance, and alleviate the disease-related syndromes in the mouse model.[6] WWL50, easily synthesized, is useful in the study of CES1 related catalyzing pathways in human cells. With regard to the characterization of the CES1 inhibitor WWL50, it is selective towards CES1 in Caco-2 and Hep G2 cell lines according to on-gel and competitive ABPP-SILAC study. For many of the oral ethyl ester prodrugs (except for those selectively activated), activation occurs mainly in the intestine and liver. We believe that our studies on WWL50 will facilitate mechanistic studies on ethyl ester prodrugs and any other ester prodrugs that are likely to be hydrolyzed by CES1 due to WWL50's potency and selectivity for CES1 in Caco-2 and Hep G2 cell lines.

In summary, using advanced ABPP-SILAC technology, we have characterized WWL50 as a selective inhibitor of carboxylesterase 1 among the serine hydrolases in Caco-2 and Hep G2 human cell lines. Carboxylesterase 1 at the same time was determined as the principal activating enzyme, accounting for >95% of the ethyl ester prodrug hydrolase activity. We believe that WWL50 will facilitate the determination of CES1 related catalysis and have general utility in the study of other prodrug activating enzymes.

4.4 Experimental Methods

Materials.

Oseltamivir phosphate (Allichem LLC), enalapril maleate salt (Sigma-Aldrich), tazarotene (Selleckchem), benazepril HCl (Selleckchem), human carboxylesterase 1b (Sigma), and carboxylesterase 2 (Sigma) were purchased from commercial sources. FP-PEG-rhodamine, FP-PEG-biotin and FP-rhodamine were prepared as previously described[24, 25]

Competition assays

Inhibitor selectivity was examined using the same method above with different concentrations and incubation times. Briefly, proteome samples was diluted with 50 mM Tris buffer to 1 mg/mL and incubated with WWL79 and WWL50 at varying concentrations (as noted in figures) for 30 min at room temperature before the addition of FP-PEG-rhodamine (4 μM) in a 50-μL volume reaction. After 30 min at room temperature, the reaction was terminated by adding 5x sample loading buffer, heated, separated in SDS-PAGE and visualized on a Typhoon imager.

Competitive ABPP-SILAC study

Caco-2 was grown in SILAC-DMEM containing 100 μg/ml of $^{12}C_6$ $^{14}N_2$-lysine and $^{12}C_6$ $^{14}N_4$-arginine (light condition) and $^{13}C_6$ $^{15}N_2$-lysine and $^{13}C_6$ $^{15}N_4$-arginine (heavy condition), 10% dialyzed FBS, and 1x penicillin/streptomycin in 100 mm tissue culture dishes in an atmosphere of 5% CO_2 at 37 °C. The cells were grown until 13-14 days post-confluence before harvest. Preparation of proteome sample follows the procedure described previously.

Proteome samples were adjusted to final protein concentration of 1.5 mg/mL. Light and heavy fractions (1.5 mL each) were incubated with WWL50 (15 μM) and vehicle respectively for 30 min at room temperature. Then FP-PEG-biotin (7.5 μM) was added and reacted with rotation at room temperature for 1 h. After incubation, light and heavy proteomes were mixed in a 1:1 ratio.

Methanol (6 mL, 4 volumes) was added and vortexing, followed by the addition of chloroform (2.25 mL, 1.5 volumes) and vortexing, and then the addition of water (4.5 mL, 3 volumes) and vortexing to homogeneity. The mixture was centrifuged (10,000 x g) at room temperature for 10 min in a swinging bucket rotor to separate the aqueous and organic phases. The top aqueous phase was carefully removed and discarded and then 3 volumes of methanol (4.5 mL) were added and mixed gently, trying not to completely disrupt the pancake-like protein interface. The protein precipitate was centrifuged (10,000 x g, 10 min) and the liquid was removed. The resulting protein precipitate was mixed with 4 volumes of methanol (6 mL) and sonicated at 4 °C until homogenous. The protein precipitate was centrifuged (10,000 x g, 10 min) and air dried for 2-3 min after removing the methanol. The resulting protein was re-solubilized in 500 μL of 6M urea / 50 mM ammonium bicarbonate buffer, then reduced by DTT (10 mM, 65 °C , 15 min) and alkyated by iodoacetamide (40 mM, room temperature, 30 min, in dark) with rotation. Then with the addition of 140 μL of 10% SDS, the proteome mixture was incubated at 65 °C for 10 min. The protein solution was diluted with 5.5 mL of PBS buffer and cooled to room temperature. Strepavidin agarose resin (Thermo Scientific, 50% slurry, 200 μL) was added and the mixture incubated at room temperature for 1.5 h with rotation. The resin was centrifuged (3,000 x g, 2 min) to a pellet and the supernatant was removed. The resin was then washed three times each by 1% SDS in PBS buffer (200 μL) and PBS buffer (200 μL), respectively. On-bead digestion was performed for 12 h at 37 °C with trypsin (Promega) in the presence of $CaCl_2$ (2 mM). Peptide samples were acidified to a final concentration of 5% (v/v) formic acid and run in triplicate on the Waters® NanoAcquity UPLC system in 1D mode. The samples were further analyzed on the Waters ® Synapt G2-S mass-spectrometer enabled with ion-mobility (HDMSE).

General synthetic methods.

^{1}H and ^{13}C NMR spectra were obtained on Bruker 300 or Bruker 500 MHz spectrometers with $CDCl_3$ as solvent, and chemical shifts are reported relative to the residual solvent peak in δ (ppm). Mass spectrometry analysis was performed by using a Waters LCT time-of-flight mass spectrometry instrument. Flash column chromatography was performed with silica gel (220–240 mesh). Thin-layer chromatography (TLC) was performed on silica gel GHLF plates (250 microns) purchased from Analtech. Developed TLC plates were visualized with a UV lamp at 254 nm or by iodine staining. Extraction solutions were dried over MgSO4 prior to concentration.WWL79 and WWL50 were synthesized as previously described[11].

WWL79. A mixture of phenol (94.11 mg, 1 mmol), *N,N'*-disuccinimidyl carbonate (256.17 mg, 1 mmol), triethylamine (140 μL, 10 mmol) and acetonitrile (4 mL) was stirred at room temperature for 4 h. The reaction mixture was diluted with ethyl acetate and washed sequentially with 0.5% aqueous HCl and brine. Following drying and concentration of the organic phase, compound **2** was isolated and used directly without further purification. A mixture of compound **2** (235.05 mg, 1 mmol), 3-morpholinopropylamine (146.1 μL, 1 mmol), triethylamine (140 μL, 10 mmol) and dichloromethane (2 mL) was stirred at room temperature for 8 h. The mixture was distributed between dichloromethane and water, and the organic phase dried over $MgSO_4$.Concentration provided a residue which was purified by flash silica gel chromatography, eluting with dichloromethane/methanol (98:2). Product fractions were pooled and concentrated to leave pure **WWL79** (211 mg) as a white powder: ^{1}H NMR (400 MHz, $CDCl_3$) δ 7.33 (m, 2 H), 7.16-7.09 (m, 3 H), 3.71 (t, J = 7 Hz, 4 H), 3.32 (dd, J = 7 Hz, J = 13 Hz, 2 H), 2.46-2.43 (m, 6 H), 1.74-1.68 (m, 2 H).

WWL50. A solution of cyclohexyl isocyanate (100 μL, 0.78 mmol), 4-fluoro-3-methylphenol (87.1 μL, 0.78 mmol), triethylamine (100 μL, 7.1 mmol) and toluene (5 mL) was refluxed overnight. Concentration of the reaction mixture gave a pale solid powder, which was purified by flash silica gel chromatography eluting with hexane/ethyl acetate (10:1). Product fractions were pooled and concentrated to leave pure **WWL50** (175.7 mg) as a white powder: ^{1}H NMR (400 MHz, $CDCl_3$) δ 6.98-6.6.82 (m, 3 H), 4.87 (b, 1 H), 3.51 (m, 1 H), 2.25 (s, 3 H), 2.00 (m, 2 H), 1.74 (m, 2 H), 1.62 (m, 1 H), 1.39-1.29 (m, 2 H), 1.21 (m, 3 H).

4.5 Figures

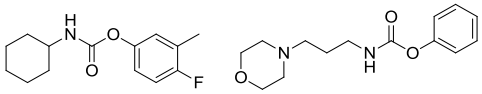

WWL50 WWL79

Figure 4.1. Structures of WWL50 and WWL79

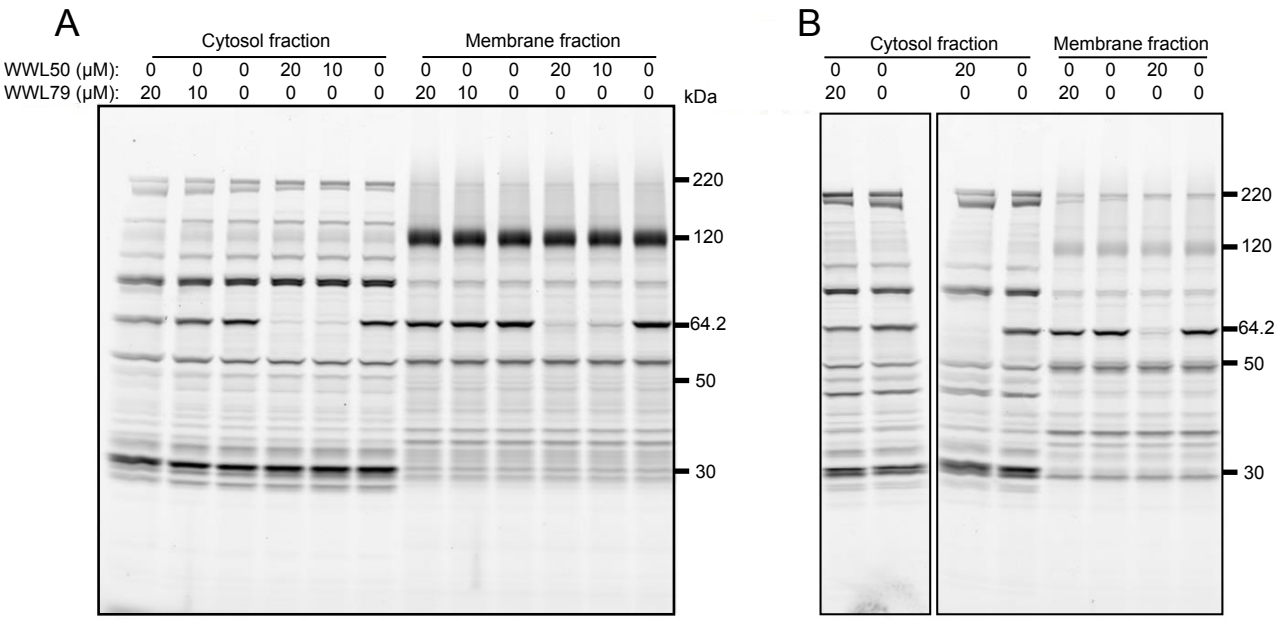

Figure 4.2. Competition of WWL50 and WWL79 against FP-PEG-rh and FP-rh. Proteome samples were treated with WWL50 or WWL79 (10 and 20 μM) for 30 min and then with FP-PEG-rh (4 μM) (A) or FP-rh (4 μM) (B) for 30 min. Proteome samples were then treated with sample loading buffer, heated at 85 °C for 5 min, and analyzed by SDS-PAGE. Results indicated that WWL50 is selective against CES1 in Caco-2 cytosolic and membrane fractions while WWL79 did not show any activity.

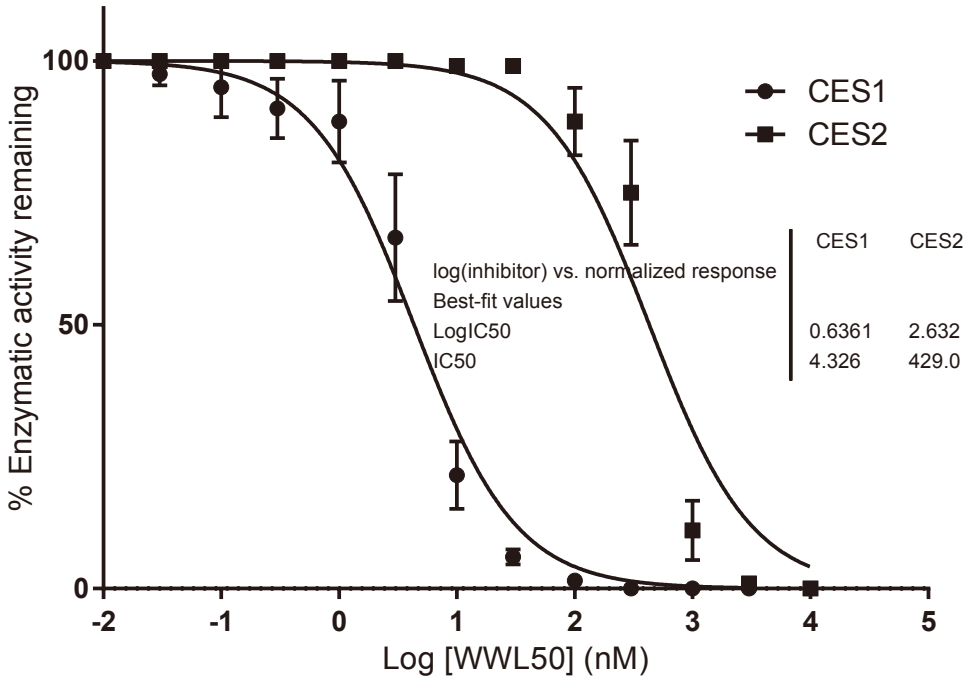

Figure 4.3. Selectivity study between pure human CES1 (isoform b) and human CES2. Pure human recombinant carboxylesterase 1b (500 ng/mL) and carboxylesterase 2 (500 ng/mL) in Tris buffer with 1 mg/mL BSA (50 mM, pH 7.4) were treated with WWL50 and DMSO (as control) for 20 min at room temperature, followed by the addition of benazepril for CES1 and *p*-nitrophenol acetate for CES2, respectively. Hydrolysis products were monitored by HPLC. Results are represented as the average inhibitor/vehicle ratios of 3-4 individual experiments.

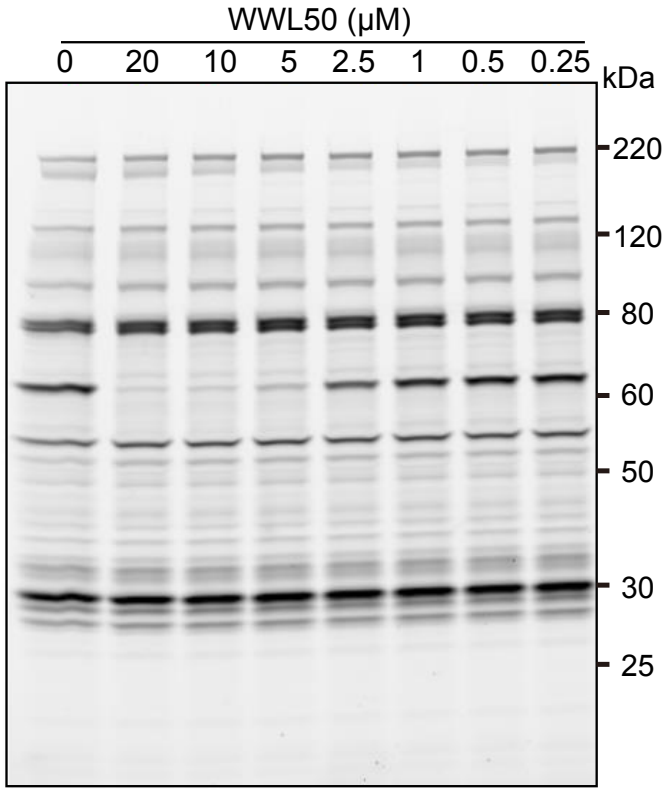

Figure 4.4. Inhibition potency determination of WWL50 on-gel in Caco-2 cell homogenate. Caco-2 homogenate (cytosol fraction, 1 mg/mL) was treated with WWL50 (concentration as noted in figure) for 30 min at room temperature, followed by the incubation of FP-PEG-rh (4 μM) for another 30 min at room temperature. Reactions were terminated by 5x sample loading buffer, heated at 85 °C for 5 min, separated by SDS-PAGE (4 - 20 % tris-glycine, Invitrogen), and visualized on fluorescence scanner.

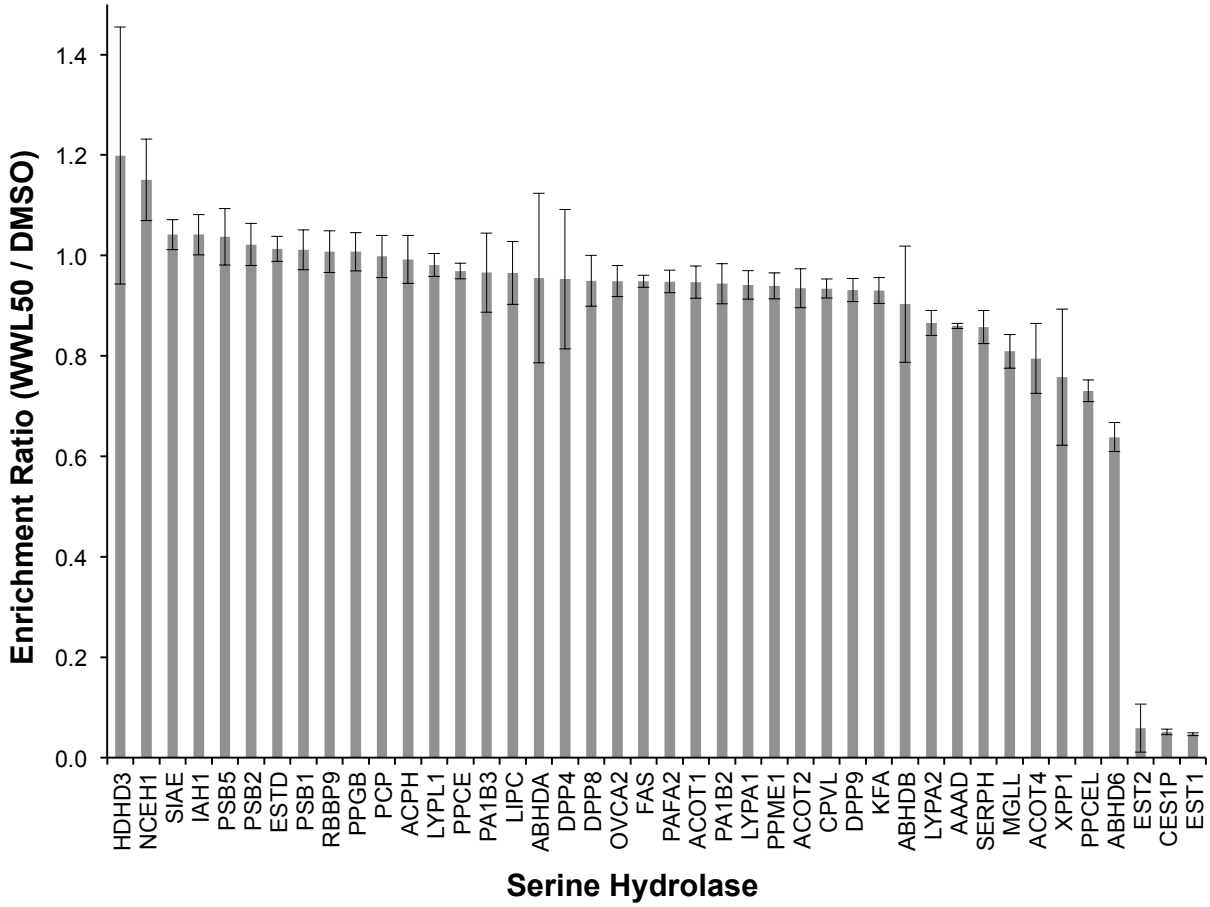

Figure 4.5. Selectivity characterization for WWL50 in human Caco-2 cells by ABPP-SILAC. Bars represent means ±s.e.m. of inhibitor/vehicle ratios of identified tryptic peptides in both soluble and membrane proteomes for two independent biological replicates. Analysis was performed in separate 90-min LC-MS gradients. 45 hydrolases were selected as representatives.

```
sp|P23141|EST1_HUMAN      MWLRAFILATLSASAAW-GHPSSPPVVDTVHGKVLGKFVSLEGFAQPVAIFLGIPFAKPP
sp|Q9UKY3|CES1P_HUMAN     MWLPALVLATLAASAAWAGHLSSPPLVDTLHGKVLGKFVSLEGFAQPVAVFLGIPFAKPP
                          *** *::****:***** ** ****:***:******************:**********

sp|P23141|EST1_HUMAN      LGPLRFTPPQPAEPWSFVKNATSYPPMCTQDPKAGQLLSELFTNRKENIPLKLSEDCLYL
sp|Q9UKY3|CES1P_HUMAN     LGPLRFTLPQPAEPWNFVKNATSYPPMFTQDPKAGQLISELFTNRKENIPLKLSEDCLYL
                          ******* *******.*********** *********:**********************

sp|P23141|EST1_HUMAN      NIYTPADLTKKNRLPVMVWIHGGGLMVGAASTYDGLALAAHENVVVVTIQYRLGIWGFFS
sp|Q9UKY3|CES1P_HUMAN     NIYTPADLTKKNRLPVMVWIHGGGLMVGAASTYDGLALAAHENVVVVTIQYRLGIWGFFS
                          ************************************************************

sp|P23141|EST1_HUMAN      TGDEHSRGNWGHLDQVAALRWVQDNIASFGGNPGSVTIFGESAGGESVSVLVLSPLAKNL
sp|Q9UKY3|CES1P_HUMAN     TGDEHSPGNWGHLDQLAALHWVQDNIASFGGNPGSVTIFGGSVGGESVSVLVLSPLAKNL
                          ****** ********:***:******************** *.*****************

sp|P23141|EST1_HUMAN      FHRAISESGVALTSVLVKKGDVKPLAEQIAITAGCKTTTSAVMVHCLRQKTEEELLETTL
sp|Q9UKY3|CES1P_HUMAN     FHRAISESGVALTSVLVKKGDVKPLAEVGLRLVRLRLDTPTSLALCS-------------
                          ***************************     .  :  * : :. *

sp|P23141|EST1_HUMAN      KMKFLSLDLQGDPRESQPLLGTVIDGMLLLKTPEELQAERNFHTVPYMVGINKQEFGWLI
sp|Q9UKY3|CES1P_HUMAN     ------------------------------------------------------------


sp|P23141|EST1_HUMAN      PMQLMSYPLSEGQLDQKTAMSLLWKSYPLVCIAKELIPEATEKYLGGTDDTVKKKDLFLD
sp|Q9UKY3|CES1P_HUMAN     ------------------------------------------------------------


sp|P23141|EST1_HUMAN      LIADVMFGVPSVIVARNHRDAGAPTYMYEFQYRPSFSSDMKPKTVIGDHGDELFSVFGAP
sp|Q9UKY3|CES1P_HUMAN     ------------------------------------------------------------


sp|P23141|EST1_HUMAN      FLKEGASEEEIRLSKMVMKFWANFARNGNPNGEGLPHWPEYNQKEGYLQIGANTQAAQKL
sp|Q9UKY3|CES1P_HUMAN     ------------------------------------------------------------


sp|P23141|EST1_HUMAN      KDKEVAFWTNLFAKKAVEKPPQTEHIEL
sp|Q9UKY3|CES1P_HUMAN     ----------------------------
```

Figure 4.6. Sequence alignment of CES1 and CES1P1. Protein sequence information was derived from Uniprot and aligned by Clustal Omega. Amino acid residues highlighted in yellow represent the catalytic triad of CES1.

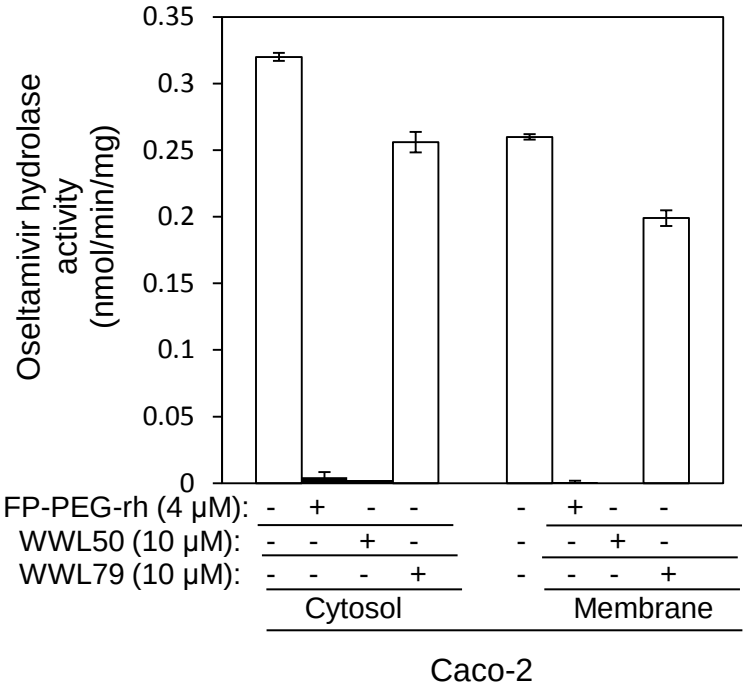

Figure 4.7. Inhibition of oseltamivir hydrolysis by probe and inhibitors. Caco-2 proteome samples (1 mg/mL) were incubated with DMSO (control), FP-PEG-rh (4 μM), WWL50 (10 μM) and WWL79 (10 μM), respectively, for 30 min at room temperature. Oseltamivir was then added followed by incubation at 37 °C. Reaction samples were collected at 20 min, 50 min, 80 min and 120 min, and analyzed by HPLC. Results are represented as the average ± SEM of 2-3 individual experiments.

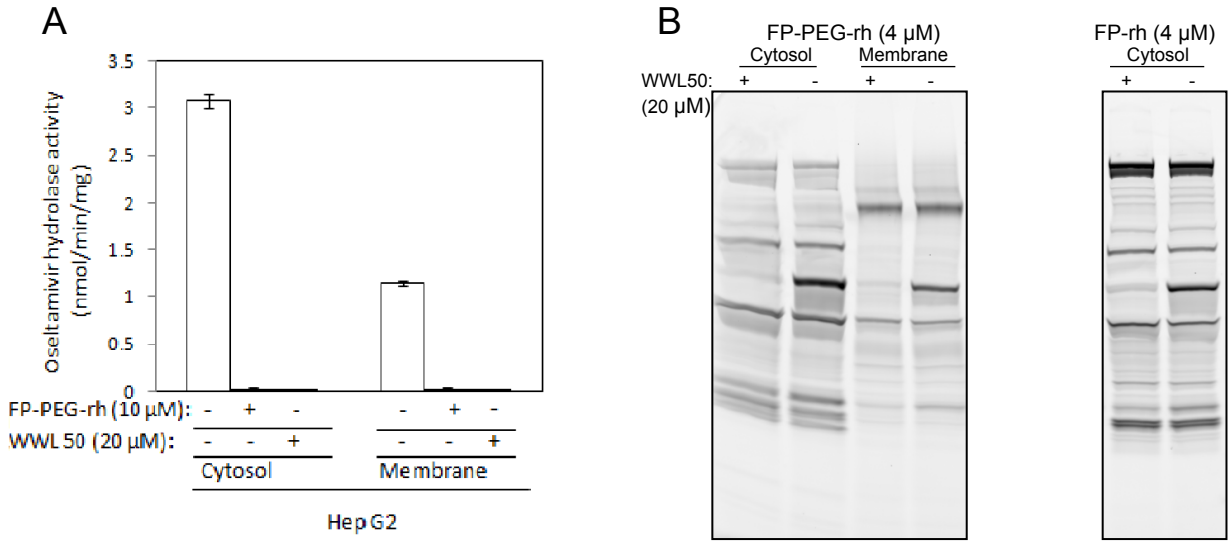

Figure 4.8. Oseltamivir hydrolysis study in Hep G2. (A) Hep G2 cytosolic (1 mg/mL) and membrane (1 mg/mL) fractions were treated with FP, WWL50, and oseltamivir as described above for Caco-2 lysates. Results are represented as the average ± SEM of 2-3 individual experiments. (B) Competitive ABPPs between FP-PEG-rh, FP-rh and WWL50 were performed as described for Caco-2 lysates.

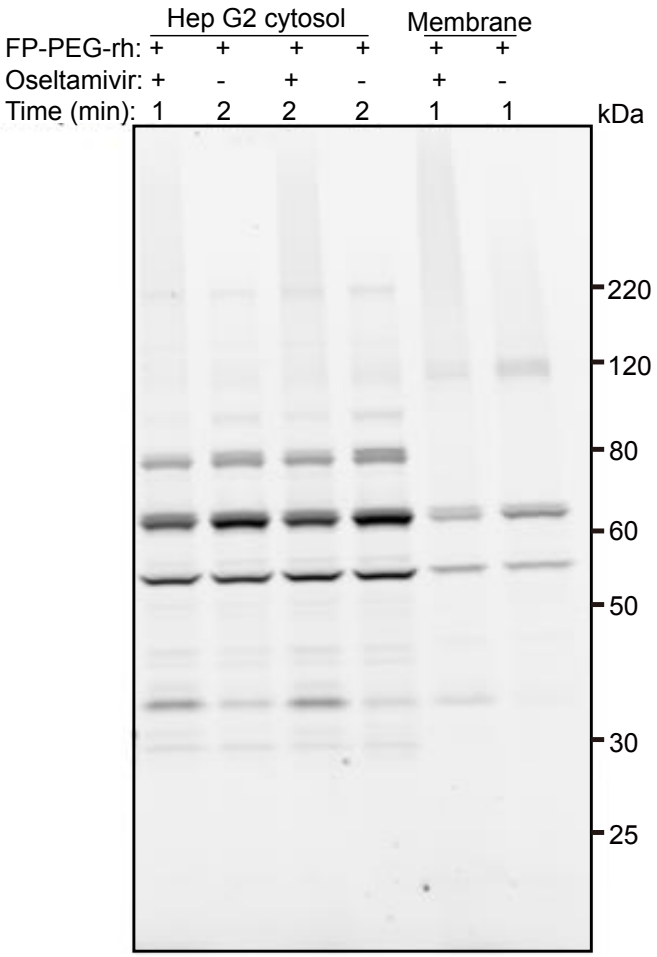

Figure 4.9. Competitive ABPPs between FP-PEG-rh, and oseltamivir. Experiments were performed the same as described previously for Caco-2 lysates.

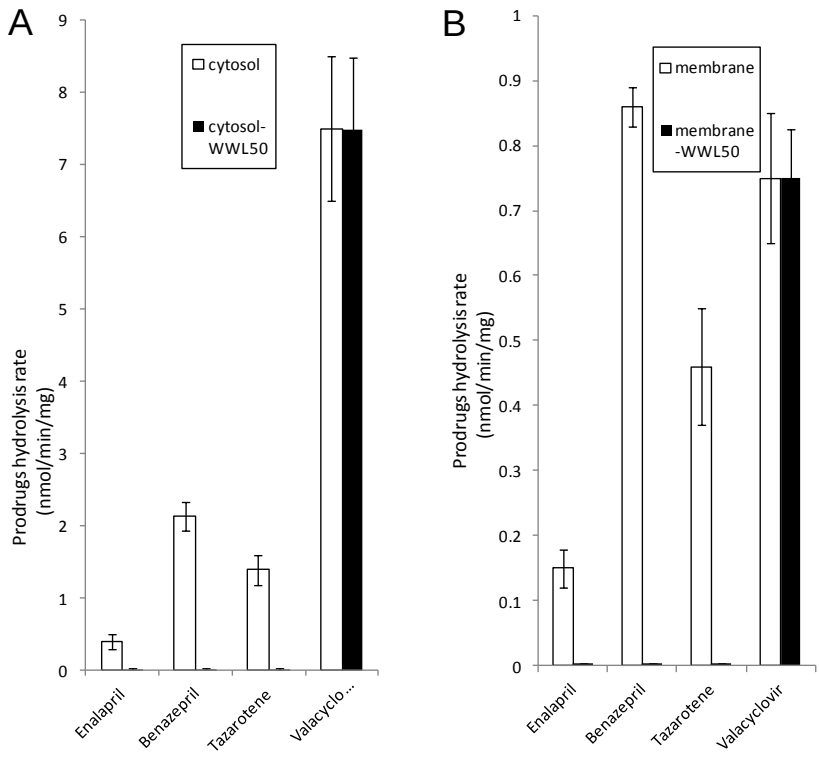

Figure 4.10. Hydrolysis of ethyl ester prodrugs in Hep G2 lysates. Enalapril (1 mM), benazapril (0.5 mM), tazarotene (0.25 mM) and valacyclovir (0.5 mM) were hydrolyzed at 37 °C in Hep G2 cytosolic (1 mg/ml) (A) and membrane (1 mg/ml) (B) proteome samples following preincubation with WWL50 (10 μM) and DMSO (control) for 30 min at room temperature. Reaction samples were collected at 10, 20, 30 and 60 min, and analyzed by HPLC. Results are represented as the average ± SEM of 2-3 individual experiments.

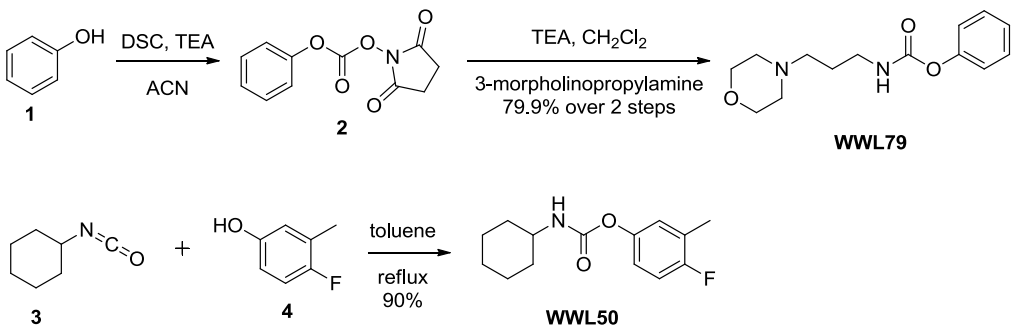

Scheme 4.1. Synthesis of WWL79 and WWL50.

4.6 References

1. Redinbo, M. R.; Bencharit, S.; Potter, P. M. Human carboxylesterase 1: from drug metabolism to drug discovery. *Biochemical Society transactions* **2003,** *31*, (Pt 3), 620-4.
2. Fleming, C. D.; Bencharit, S.; Edwards, C. C.; Hyatt, J. L.; Tsurkan, L.; Bai, F.; Fraga, C.; Morton, C. L.; Howard-Williams, E. L.; Potter, P. M.; Redinbo, M. R. Structural insights into drug processing by human carboxylesterase 1: tamoxifen, mevastatin, and inhibition by benzil. *J Mol Biol* **2005,** *352*, (1), 165-77.
3. Zhu, H. J.; Appel, D. I.; Peterson, Y. K.; Wang, Z.; Markowitz, J. S. Identification of selected therapeutic agents as inhibitors of carboxylesterase 1: potential sources of metabolic drug interactions. *Toxicology* **2010,** *270*, (2-3), 59-65.
4. Rhoades, J. A.; Peterson, Y. K.; Zhu, H. J.; Appel, D. I.; Peloquin, C. A.; Markowitz, J. S. Prediction and in vitro evaluation of selected protease inhibitor antiviral drugs as inhibitors of carboxylesterase 1: a potential source of drug-drug interactions. *Pharmaceutical research* **2012,** *29*, (4), 972-82.
5. Jernas, M.; Olsson, B.; Arner, P.; Jacobson, P.; Sjostrom, L.; Walley, A.; Froguel, P.; McTernan, P. G.; Hoffstedt, J.; Carlsson, L. M. Regulation of carboxylesterase 1 (CES1) in human adipose tissue. *Biochemical and biophysical research communications* **2009,** *383*, (1), 63-7.
6. Dominguez, E.; Galmozzi, A.; Chang, J. W.; Hsu, K. L.; Pawlak, J.; Li, W.; Godio, C.; Thomas, J.; Partida, D.; Niessen, S.; O'Brien, P. E.; Russell, A. P.; Watt, M. J.; Nomura, D. K.; Cravatt, B. F.; Saez, E. Integrated phenotypic and activity-based profiling links Ces3 to obesity and diabetes. *Nature chemical biology* **2014,** *10*, (2), 113-21.
7. Crow, J. A.; Bittles, V.; Borazjani, A.; Potter, P. M.; Ross, M. K. Covalent inhibition of recombinant human carboxylesterase 1 and 2 and monoacylglycerol lipase by the carbamates JZL184 and URB597. *Biochem Pharmacol* **2012,** *84*, (9), 1215-22.
8. Young, B. M.; Hyatt, J. L.; Bouck, D. C.; Chen, T.; Hanumesh, P.; Price, J.; Boyd, V. A.; Potter, P. M.; Webb, T. R. Structure-activity relationships of substituted 1-pyridyl-2-phenyl-1,2-ethanediones: potent, selective carboxylesterase inhibitors. *J Med Chem* **2010,** *53*, (24), 8709-15.
9. Shimizu, M.; Fukami, T.; Nakajima, M.; Yokoi, T. Screening of specific inhibitors for human carboxylesterases or arylacetamide deacetylase. *Drug metabolism and disposition: the biological fate of chemicals* **2014,** *42*, (7), 1103-9.
10. Adam, G. C.; Vanderwal, C. D.; Sorensen, E. J.; Cravatt, B. F. (-)-FR182877 is a potent and selective inhibitor of carboxylesterase-1. *Angew Chem Int Ed Engl* **2003,** *42*, (44), 5480-4.
11. Bachovchin, D. A.; Ji, T.; Li, W.; Simon, G. M.; Blankman, J. L.; Adibekian, A.; Hoover, H.; Niessen, S.; Cravatt, B. F. Superfamily-wide portrait of serine hydrolase inhibition achieved by library-versus-library screening. *Proceedings of the National Academy of Sciences of the United States of America* **2010,** *107*, (49), 20941-6.
12. Kathuria, S.; Gaetani, S.; Fegley, D.; Valino, F.; Duranti, A.; Tontini, A.; Mor, M.; Tarzia, G.; La Rana, G.; Calignano, A.; Giustino, A.; Tattoli, M.; Palmery, M.; Cuomo, V.; Piomelli, D. Modulation of anxiety through blockade of anandamide hydrolysis. *Nat Med* **2003,** *9*, (1), 76-81.
13. Long, J. Z.; Li, W.; Booker, L.; Burston, J. J.; Kinsey, S. G.; Schlosburg, J. E.; Pavon, F. J.; Serrano, A. M.; Selley, D. E.; Parsons, L. H.; Lichtman, A. H.; Cravatt, B. F. Selective blockade of 2-arachidonoylglycerol hydrolysis produces cannabinoid behavioral effects. *Nature chemical biology* **2009,** *5*, (1), 37-44.
14. Mann, M. Functional and quantitative proteomics using SILAC. *Nature reviews. Molecular cell biology* **2006,** *7*, (12), 952-8.

15. Everley, P. A.; Gartner, C. A.; Haas, W.; Saghatelian, A.; Elias, J. E.; Cravatt, B. F.; Zetter, B. R.; Gygi, S. P. Assessing enzyme activities using stable isotope labeling and mass spectrometry. *Molecular & cellular proteomics : MCP* **2007,** *6*, (10), 1771-7.
16. Ong, S. E.; Schenone, M.; Margolin, A. A.; Li, X.; Do, K.; Doud, M. K.; Mani, D. R.; Kuai, L.; Wang, X.; Wood, J. L.; Tolliday, N. J.; Koehler, A. N.; Marcaurelle, L. A.; Golub, T. R.; Gould, R. J.; Schreiber, S. L.; Carr, S. A. Identifying the proteins to which small-molecule probes and drugs bind in cells. *Proceedings of the National Academy of Sciences of the United States of America* **2009,** *106*, (12), 4617-22.
17. Adibekian, A.; Martin, B. R.; Wang, C.; Hsu, K. L.; Bachovchin, D. A.; Niessen, S.; Hoover, H.; Cravatt, B. F. Click-generated triazole ureas as ultrapotent in vivo-active serine hydrolase inhibitors. *Nature chemical biology* **2011,** *7*, (7), 469-78.
18. Balakirev, E. S.; Ayala, F. J. Pseudogenes: are they "junk" or functional DNA? *Annu Rev Genet* **2003,** *37*, 123-51.
19. The UCSC Genome Bioinformatics Genome Browser: http://genome.ucsc.edu/cgi-bin/hgGateway
20. NCBI browser: www.ncbi.nlm.nih.gov/.
21. Yan, B.; Matoney, L.; Yang, D. Human carboxylesterases in term placentae: enzymatic characterization, molecular cloning and evidence for the existence of multiple forms. *Placenta* **1999,** *20*, (7), 599-607.
22. Yamada, S.; Richardson, K.; Tang, M.; Halaschek-Wiener, J.; Cook, V. J.; Fitzgerald, J. M.; Elwood, K.; Marra, F.; Brooks-Wilson, A. Genetic variation in carboxylesterase genes and susceptibility to isoniazid-induced hepatotoxicity. *Pharmacogenomics J* **2010,** *10*, (6), 524-36.
23. Friedrichsen, M.; Poulsen, P.; Wojtaszewski, J.; Hansen, P. R.; Vaag, A.; Rasmussen, H. B. Carboxylesterase 1 gene duplication and mRNA expression in adipose tissue are linked to obesity and metabolic function. *PLoS One* **2013,** *8*, (2), e56861.
24. Kidd, D.; Liu, Y.; Cravatt, B. F. Profiling serine hydrolase activities in complex proteomes. *Biochemistry* **2001,** *40*, (13), 4005-15.
25. Xu, H.; Sabit, H.; Amidon, G. L.; Showalter, H. D. An improved synthesis of a fluorophosphonate-polyethylene glycol-biotin probe and its use against competitive substrates. *Beilstein J Org Chem* **2013,** *9*, 89-96.

Chapter 5

SUMMARY

Knowing the identity of select prodrug activating enzyme(s) is essential to understanding the mechanistic basis for enhanced cellular delivery, biodistribution, and prodrug stability. In addition, understanding species-specific pro-drug sensitivities is critical for evaluating pre-clinical animal models and evaluating drug-drug interactions. Competitive Activity Based Protein Profiling (ABPP) describes an emerging chemoproteomic approach to assay active site occupancy within a mechanistically similar enzyme class within native proteomes, and has proven to be a powerful approach for selectivity-guided medicinal chemistry. This approach uses enzyme class specific reporter-linked covalent probes, such as the serine hydrolase privileged fluorophosphonates, for mechanism-based covalent labeling of the more than 100 serine hydrolases in the human genome, including a broad profiling of serine proteases, lipases, and thioesterases.

In this regard, a synthetic route for a fluorophosphonate-polyethylene glycol-biotin probe was optimized and its capability of labeling serine hydrolases was verified in a human cell homogenate with an activity-based protein profiling competition between FP-PEG-rhodamine and oseltamivir established. Human carboxylesterase 1 was identified as an oseltamivir binding enzyme and WWL50 as a selective CES1 inhibitor. WWL50 selectivity was characterized and applied to the determination of CES1's contribution to ester prodrug hydrolysis.

Chapter 2 of this thesis describes a novel synthetic route to link the FP group to a biotin tag through a polyethylene glycol linker to improve the original synthesis. This route markedly increases the efficiency of the probe synthesis and overcomes problems from a prior literature synthesis. Special features of the synthesis include the use of a benzyl protecting group to provide a UV sensitive group for the purification steps that followed, and a facile incorporation of an iodide group resulting in high yield of key intermediate without any flash column purifications. Under novel reaction conditions, lithium azide was utilized in the monodealkylation of a phosphonate diester. The synthesis was completed by the clean incorporation of the reactive fluoride group in high yield with DAST. The purity of the final product was established by NMR, and the compound was then directly used in biological tests.

The Activity-Based Protein Profiling (ABPP) approach for the determination of functional enzymatic activity has been extensively developed for serine hydrolases by Cravatt et al. and cysteine hydrolases by Bogyo et al. A variety of probes have been designed for various other enzyme classes and have been used for the characterization of selective inhibitors and enzyme annotations. A few reports have focused on competitive ABPP between the enzyme probe and enzyme substrates. In chapter 3 we describe a modified ABPP approach using direct prodrug competition to FP probes to identify CES1 as the one of the prodrug hydrolyzing enzymes of oseltamivir. We utilize the fluorophosphonate probes developed by the Cravatt group with either a rhodamine or a biotin tag linked to the fluorophosphonate for either on-gel visualization or streptavidin bead purification, respectively. When present with time and concentration optimized, the prodrug will reduce the probe binding to the enzyme active site and thus detect potential activating enzymes. The hydrolysis of oseltamivir, an ethyl ester prodrug, in a Caco-2 cell homogenate was inhibited by FP-PEG-rh, demonstrating that all of the potential oseltamivir

hydrolyzing enzymes are effectively inhibited and bound by the FP probe. A subsequent on-gel competition between oseltamivir and FP-PEG-rhodamine was performed with kinetically controlled FP concentration and incubation time. By the direct comparison of different competition conditions, enzyme bands with the most significant fluorescent signal differences were targeted as potential oseltamivir binding enzymes.

In order to identify them, all the serine hydrolases in the Caco-2 cell homogenate were covalently linked by FP-PEG-biotin, and pulled down on streptavidin agarose beads by the strong interaction between biotin and streptavidin. The accumulated serine hydrolases were then separated on SDS-PAGE. A protein band observed at about 60 kDa was identified as human carboxylesterase 1 by LC-LC/MS. Two other protein bands at 30 kDa were excised from the gel and were identified as mixture of non-serine hydrolases. In this chapter, a new approach of identifying prodrug activating enzymes seldom discussed before was described and established with the hydrolysis of oseltamivir by carboxylesterase 1 as an example. The kinetic competition between a substrate with high enzymatic turnover rate (oseltamivir) and a covalent chemical probe (FP-PEG-rh) was demonstrated with different incubation times and concentrations.

Having identified CES1 as an activating hydrolase for oseltamivir, we next determined (Chapter 4) the level that it contributed to its hydrolysis, and which of the other binding enzymes identified above were also involved in the enzymatic hydrolysis. We selected two inhibitors, WWL50 and WWL79 as the most selective CES1 inhibitors for our studies. FP-PEG-rh was competed for by them to test their selectivity and potency. The on-gel competitive ABPP results showed no observable competition signals from WWL79 against any serine hydrolases while WWL50 exhibited strong inhibition activity against CES1 selectively in Caco-2 cell homogenate.

Determination of the IC_{50} of WWL50 against human CES1 and CES2 was further performed with the recombinantly over-expressed pure enzymes due to the low expression amount of hCES2 in Caco-2 cells. WWL50 is able to differentiate CES1 and CES2 by 100-fold in IC_{50} values. An even larger profiling of the selectivity of WWL50 among all serine hydrolases in Caco-2 cells was further pursued with the ABPP-SILAC based proteomic approach. Competition signals from FP-PEG-biotin versus WWL50 were observed from a mixture of isotopically labelled and native enzymes, pointing out that WWL50 is selective against CES1 amongst more than 200 profiled serine hydrolases in the Caco-2 cell. The results from the hydrolysis assay showed total inhibition of oseltamivir hydrolysis in a Caco-2 cell homogenate by WWL50, which led to the conclusion that CES1 is the primary activating enzyme of oseltamivir.

We then further tested the on-gel selectivity of WWL50 in Hep G2 cell homogenate (a cell line derived from human liver carcinoma) by competitive ABPP. The on-gel competition signal clearly indicated that WWL50 is also selective against CES1 in a Hep G2 homogenate. WWL50 was then applied to the hydrolysis assays of oseltamivir and several other ethyl ester prodrugs in a Hep G2 cell homogenate, with the conclusion that CES1 is the primary activating enzyme for ethyl ester prodrugs mediating more than 95% of the activation.

Overall, we present a modified substrate-competitive activity-based profiling approach for discovering specific prodrug hydrolyzing enzymes, which promises to be a useful methodology for ester prodrug design and preclinical development of ester prodrugs. The determination and characterization of prodrug activating enzymes and the corresponding inhibitors will significantly enhance our ability to unveil prodrug activation mechanisms.

APPENDICES

APPENDICES 1

SYNTHESIS OF NOVEL BENZOXAZINORIFAMYCINS ANALOGUES

A1.1 Introduction

Tuberculosis (TB) is a contagious and deadly disease that has reached pandemic proportions. According to the World Health Organization (WHO), 8−10 million new cases of TB are diagnosed each year, making Mycobacterium tuberculosis (MTB) a leading cause of death in adults (2−3 million/year) due to an infectious agent.[1] A high proportion of these new cases and deaths occur in HIV-positive people with a significant number of AIDS deaths in Africa being attributed to TB infections. Global population growth is increasing the disease burden, posing a continuing health and financial burden in various parts of the world, particularly Asia and Africa.

TB is caused predominantly by MTB, an obligate aerobic bacillus that divides at an extremely slow rate. The chemical composition of its cell wall includes peptidoglycans and complex lipids, in particular mycolic acids, which are a significant determinant of its virulence.[2] The unique structure of the cell wall of MTB allows it to lie dormant for many years as a latent infection, particularly as it can grow readily inside macrophages, hiding it from the host's immune system.

The continuing rise in multidrug-resistant strains of MTB (MDR-TB) has further contributed to the dire need for new TB antibiotics, as no new TB drugs have been introduced into clinical use

in the past 4 decades.[3, 4] Drugs that are active against resistant forms of TB are less potent, more toxic and need to be taken for an extended period of time (≥18 months). The recent emergence of virtually untreatable extensively drug-resistant TB (XDR-TB) poses a new threat to TB control worldwide. Furthermore, effective treatment of TB in persons co-infected with HIV is complicated because of drug−drug interactions. Shorter and simpler regimens that are safe, well tolerated, and effective against drug-susceptible and drug-resistant TB, which are appropriate for joint HIV-TB treatment and amenable to routine clinical settings, are needed urgently.[5, 6]

he rifamycins are the most commonly used drugs for TB, and semisynthetic derivatives have been reported that show improved antimycobacterial activities.[7] These include rifampin (**1a**, RMP, Figure A.1), which is the cornerstone of current short-term tuberculosis treatment. Among newer derivatives, rifalazil (**2a**, RLZ, Figure A.1) has proved most interesting not just because of its excellent potency but also because of its relative lack of toxicity in early rodent studies.[8] RLZ is an exceedingly potent rifamycin derivative, being 16−256 times more potent than RMP,[9-11] and is particularly effective against many of the RMP-resistant strains of MTB.[10, 12] Several studies involving strains with various *rpoB* mutations clearly indicated that the mutations identified with the RMP, rifapentine, and rifabutin resistant strains retained sensitivity to RLZ.[13, 14] RLZ and its benzoxazinorifamycin analogues also have showed excellent activity against other organisms with RMP-resistant mutations, including *Streptococcus pyogenes*, *Chlamydia trachomatis*, and *Chlamydia pneumonia*.[15, 16]

In mouse in vivo efficacy studies, RLZ has been shown to be clearly more potent than RMP including activity against some RMP-resistant strains,[9, 11, 17-19] and longer term MTB studies in combination with other agents indicated that the same level of cure could be achieved with

shorter (at least 2-fold) duration of treatment with RLZ compared to RMP.[20-22] In pharmacokinetic (PK) studies, RLZ has shown a high volume of distribution and produced tissue levels in rats up to 200 times those in plasma. It displayed a very long half-life (60−100 h) in human trials. One major downside to the rifamycins used to treat TB is their many drug−drug interactions. This effect appears to be diminished with RLZ, as shown in rat and the dog studies.[23] This study also showed RLZ not to be an inducer of hepatic cytochrome P450 (Cyp450). In a series of phase I[24, 25] and phase II[9, 24-26] clinical trials, RLZ proved to be quite toxic, with most adverse effects associated with a flulike syndrome and leucopenia even at lower dose levels. Hence, its development for TB indications has been suspended.[27]

In this section, we detail the structure-based design, and synthesis of representative compounds (**2b−d**, Figure A.1) of a novel subclass of RLZ (**2a**) in which ether tethers have been installed off the 3'-position of the "southeastern" part of the benzoxazinorifamycin template.

A1.2 Results and Discussion

The synthetic route utilized to make our target "one-armed" compounds **2b−d** is shown in scheme A.1. The RLZ literature[28] suggested a strategy of annulating the benzoxazino moiety onto rifamycin S (**12**) with a suitably protected monoether (e.g., TBS) of 2-aminoresorcinol, followed by ether deprotection and then side chain installation off the nascent phenol by any number of alkylation methodologies. This was investigated, but yields were very poor and the scope of alkylation possibilities was quite limited (data not shown). We opted instead to annulate a fully tethered 2-aminoresorcinol monoether onto the rifamycin S framework in a single step. This allowed us to consider a wide range of tethers off the "southeastern" part of the rifalazil-

type template and, more importantly, minimized difficult synthetic transformations and product purifications involving the complex rifamycin S core to a single last step. Thus, we set our sights initially on developing a robust procedure to intermediate **5**, which would serve as a key starting material for introduction of our chosen tethers. While there are two reports for the synthesis of this compound,[29, 30] neither was deemed practical for our needs. Instead, we pursued a two-step procedure. Accordingly, dialkylation of 2-nitroresorcinol (**3**), similar to the literature procedure,[31] gave a 95% yield of dibenzyl ether **4** which was then cleanly monodebenzylated to nitrophenol **5**[29] in 82% yield. With **5** now in hand, we were ready to install our target tethers. Phenolic alkylation with 2-(diethylaminoethyl)-ethyl chloride hydrochloride under standard conditions provided **6** in 87% yield. Hydrogenation of **6** utilizing Pearlman's catalyst simultaneously reduced the nitro function and hydrogenolyzed the benzyl protecting group to give the 2-aminoresorcinol ether **7** in 81% yield. A similar sequence of reactions was followed to provide ethers **11a, b**. Alkylation of **5** with 1,4-dibromobutane gave **8** in 93% yield, which was subsequently aminated with two monosubstituted piperazines to afford compounds **9a** and **9b** in 68% and 99% yields, respectively. *t*-Boc deprotection of **9b** followed by acylation of **9c** with 2-(1H-imidazol-1-yl)acetic acid provided **10**, the amide congener of **9a**, in 72% yield. Hydrogenation of **9a** and **10** was conducted as described for **6** to provide the remaining 2-aminoresorcinol ethers **11a** and **11b**, respectively, in nearly quantitative yields.

The structure of each 2-aminoresorcinol ether (**7, 11a, 11b**) is supported by mass spectrometry along with ^{1}H and ^{13}C NMR spectra. Each was then annulated onto rifamycin S (**12**) to provide target compounds **2b−d** in 35−74% yields following a two-stage purification utilizing medium pressure and then preparative plate silica gel chromatography. No effort was made to optimize

the condensation reaction with rifamycin S, but we feel that this has the potential to be an efficient transformation.

A1.3 Experimental Methods

All the reagents and solvents were purchased commercial chemical companies and used without further purification unless otherwise noted. Melting points were determined in open capillary tubes on a Laboratory Devices Mel-Temp apparatus and are uncorrected. ^{1}H and ^{13}C NMR spectra were obtained on Bruker 500 MHz spectrometers with $CDCl_3$ or d_6-DMSO as solvent and chemical shifts are reported relative to the residual solvent peak in δ (ppm). Mass spectrometry analysis was performed using a Waters LCT time-of-flight mass spectrometry instrument. High resolution mass spectrometry (HRMS) analysis was performed on an Agilent Q-TOF system. Perkin Elmer Series 200 HPLC system with Agilent Eclipse plus C18 (4.6 x 7.5 mm, 3.5 mm particle size) was used for analytical HPLC analysis. The mobile phase was a 11 min binary gradient of acetonitrile (containing 0.1 % TFA) and water (20–90%). Extraction solutions were dried over $MgSO_4$ prior to concentration. Silica Gel GHLF (250 microns), purchased from Analtech, was used as thin layer chromatography.

(((2-Nitro-1,3-phenylene)bis(oxy))bis(methylene))dibenzene (4). A mixture of 2-nitroresorcinol (**3**; 2.0 g, 12.9 mmol), Cs_2CO_3 (10.5 g, 32.2 mmol), benzyl bromide (3.39 ml, 28.4 mmol) and DMF (35 mL) was stirred at room temperature for 12 h. The mixture was diluted with ethyl acetate and washed sequentially with 1% aq HCl and brine. The organic phase was dried and concentrated to leave a yellow oil, which was diluted with 2-propanol to precipitate pure product. The solids were collected to leave **4** (4.11 g, 95%) as light yellow crystals: mp 87.5 - 88ºC (lit[31] 80ºC); R_f 0.26 (hexanes : ethyl acetate, 5 : 1); ^{1}H NMR ($CDCl_3$) δ 7.3 (m, 10 H),

7.23 (t, *J* = 8.5 Hz, 1 H), 6.64 (d, *J* = 8.5, 2 H), 5.16 (s, 4 H); ^{13}C NMR ($CDCl_3$) δ 150.9, 135.6, 130.9, 128.7, 128.2, 127.0, 106.2, 71.0; MS (ES^+) *m/z* 358.1 $(M+Na)^+$.

3-(Benzyloxy)-2-nitrophenol (5). A solution of dibenzyl ether **4** (3.0 g, 8.95 mmol) in dichloromethane (80 mL) at -78ºC was treated drop-wise with boron trichloride (13 mL, 1M in heptane) during which the color changed to dark purple. The reaction was monitored by TLC and stirred at -78ºC until all starting material was consumed (1 h). Methanol (5 mL) was added drop-wise and the mixture was brought to room temperature, cautiously diluted with 5% aq sodium bicarbonate, and then extracted with dichloromethane (2x). The combined extracts were dried and concentrated to an orange oil that was purified by flash silica gel chromatography eluting with hexanes : ethyl acetate (5 : 1). Product fractions were combined and concentrated to give **5** (1.79 g, 82%) as a bright yellow solid: mp 67 - 67.5 ºC; R_f 0.24 (hexanes : ethyl acetate, 5 : 1); ^{1}H NMR ($CDCl_3$) δ 10.18 (brs, 1 H), 7.4 (m, 2 H), 7.3 (m, 4 H), 6.72 (d, *J* = 8.5 Hz, 2 H), 6.6 (d, *J* = 8.5 Hz, 2 H), 5.21 (s, 2 H); ^{13}C NMR ($CDCl_3$) δ 155.7, 154.7, 135.6, 135.4, 128.7, 128.2, 126.9, 111.0, 105.1, 71.4; MS (ES^+) *m/z* 268.0 $(M+Na)^+$.

2-(3-(Benzyloxy)-2-nitrophenoxy)-*N*,*N*-diethylethanamine (6). A mixture of nitrophenol **5** (1.31 g, 5.4 mmol), 2-(diethylaminoethyl)ethyl chloride hydrochloride (1.2 g, 7 mmol), Cs_2CO_3 (4.37 g, 13.4 mmol) and acetone (20 mL) was stirred at 50ºC for 3 h. The mixture was filtered and the filtrate was concentrated to a residue that purified by flash silica gel chromatography eluting with hexanes : ethyl acetate (5 : 1). Product fractions were combined and concentrated to leave **6** (1.71 g, 93%) as a light yellow oil: R_f = 0.22 (CH_2Cl_2 : methanol, 95 : 5); ^{1}H NMR ($CDCl_3$) δ 7.3 (m, 6 H), 6.62, (dd, J_1 = 3.6 Hz, J_2 = 14.1 Hz, 2 H), 5.16 (s, 2 H), 4.1 (t, *J* = 10.5 Hz, 2 H), 2.8 (t, *J* = 10.5 Hz, 2 H), 2.6 (q, *J* = 11.9 Hz, 4 H), 1.0 (t, *J* = 11.9 Hz, 6 H); ^{13}C NMR

($CDCl_3$) δ 151.2, 150.8, 135.6, 130.9, 128.6, 128.2, 127.0, 105.9, 105.6, 70.9, 68.5, 51.2, 47.9, 11.9; MS (ES^+) *m/z* 245.1 $(M+H)^+$.

2-Amino-3-(2-(diethylamino)ethoxy)phenol (7). 2-(Diethylamino)ethyl ether **6** (1.8 g, 5.2 mmol) was dissolved in 10% acetic acid in methanol (50 mL) in a 250 mL Parr hydrogenation bottle. Catalyst (20% $Pd(OH)_2/C$, 0.1 g) was added and the mixture was hydrogenated at 40 psi H_2 for ~20 h. The reaction mixture was rapidly filtered over Celite®, and the filtrate was concentrated and diluted with ethyl acetate. The solution was washed with 5% aq sodium carbonate, dried, and concentrated to a brown solid that was triturated in hot hexanes. The solids were collected and dried to leave **7** (0.95 g, 81%): mp 91 - 91.5ºC; R_f 0.21 (CH_2Cl_2 : methanol, 85 : 15); ^1H NMR ($CDCl_3$) δ 6.55 (t, *J* = 7.7 Hz, 1 H), 6.4 (m, 2 H), 4.07 (t, *J* = 5.8 Hz, 2 H), 2.91 (t, *J* = 5.8 Hz, 2 H), 2.7 (m, 4 H), 1.1 (t, *J* = 7.1 Hz, 6 H); ^{13}C NMR ($CDCl_3$) δ 148.0, 145.3, 124.9, 117.8, 109.0, 104.4, 66.5, 51.9, 47.4, 11.1; MS (ES^+) *m/z* 225.1 $(M+H)^+$.

1-(Benzyloxy)-3-(4-bromobutoxy)-2-nitrobenzene (8). To a mixture of DMF (5 mL), 1,4-dibromobutane (5 mL) and Cs_2CO_3 (1.66 g, 5.1 mmol) was added slowly a solution of nitrophenol **5** (0.5 g, 2.0 mmol) in DMF (5 mL). The mixture was stirred at room temperature for 16 h, and then DMF was removed *in vacuo* to leave an oil that was distributed between 1% aq HCl and ethyl acetate. The organic phase was dried and concentrated to a light yellow oil that was purified by flash silica gel chromatography eluting with hexanes : ethyl acetate (6 : 1). Product fractions were combined and concentrated to give **8** (0.702 g, 93%) as a light yellow oil: R_f 0.45 (hexanes : ethyl acetate, 2 : 1); ^1H NMR ($CDCl_3$) δ 7.36 (m, 5 H), 7.26 (m, 1 H), 6.61 (m, 2 H), 5.16 (s, 2 H), 4.08 (t, *J* = 5.8 Hz, 2 H), 3.46 (t, *J* = 6.3 Hz, 2 H), 2.02 (m, 2 H), 1.92 (m, 2

H); ^{13}C NMR ($CDCl_3$) δ 151.1, 150.9, 135.6, 131.0, 128.7, 128.2, 127.0, 106.1, 105.6, 70.9, 68.4, 33.4, 28.9, 27.5; MS (ES^+) *m/z* 401.9, 403.9 $(M+Na)^+$.

1-(2-(1*H*-Imidazol-1-yl)ethyl)-4-(4-(3-(benzyloxy)-2-nitrophenoxy)butyl)piperazine (9a). A solution of bromobutyl ether **8** (1.0 g, 2.6 mmol), 1-[2-(1*H*-imidazol-1-yl)ethyl]piperazine (0.52 g, 2.9 mmol, purchased from Oakwood Products Inc.), *N*,*N*-diisopropylethylamine (5 mL) and acetonitrile (18 mL) was heated at reflux overnight. The solution was concentrated and the residue was distributed between dichloromethane and 5% aq sodium carbonate. The organic phase was dried and concentrated to an orange oil that was purified by flash silica gel chromatography eluting with dichloromethane : methanol : NH_4OH (90 : 10 : 0.5). Product fractions was combined and concentrated to leave **9a** (0.86 g, 68%) as an oil: ^{1}H NMR ($CDCl_3$) δ 7.53 (s, 1 H), 7.36-7.22 (m, 6 H), 7.03 (s, 1 H), 6.97 (d, *J* = 1.1 Hz, 1 H), 6.61 (m, 1 H), 5.15 (s, 1 H), 4.05 (t, *J* = 6.3 Hz, 2 H), 4.01 (t, *J* = 6.5 Hz, 2 H), 2.67 (t, *J* = 6.5 Hz, 2 H), 2.48 (bs, 8 H), 2.36 (t, *J* = 6.5 Hz, 2 H), 1.79 (m, 2 H), 1.61 (m, 2 H); ^{13}C NMR ($CDCl_3$) δ 151.3, 150.8, 137.4, 135.6, 132.8, 130.9, 129.2, 128.7, 128.2, 127.0, 119.3, 105.8, 105.6, 70.9, 69.3, 58.6, 57.8, 53.3, 53.0, 44.7, 26.9, 23.1; MS (ES^+) *m/z* 480.1 $(M+H)^+$.

***tert*-Butyl 4-(4-(3-(benzyloxy)-2-nitrophenoxy)butyl)piperazine-1-carboxylate (9b).** A solution of bromobutyl ether **8** (0.4 g, 1.05 mmol), 1-Boc-piperazine (0.282 g, 1.514 mmol) *N*,*N*-diisopropylethylamine (4 mL) and acetonitrile (10 mL) was heated at 80ºC for 12 h. The solution was concentrated and distributed between ethyl acetate and brine. The organic phase was dried and concentrated to residue that was purified by flash silica gel chromatography eluting with ethyl acetate. Product fractions were combined and concentrated to leave **9b** (0.505 g, 99%): ^{1}H NMR ($CDCl_3$) δ 7.36 (m, 4H), 7.31 (m, 1 H), 7.24 (m, 1 H), 6.61 (m, 2 H), 5.16 (s, 2 H), 4.06 (t,

J = 6.2 Hz, 2 H), 3.41 (t, *J* = 7.0 Hz, 4 H), 2.36 (t, *J* = 7.0 Hz, 4 H), 1.80 (m, 2 H), 1.62 (m, 2 H), 1.46 (s, 9 H), 1.26 (t, *J* = 7.2 Hz, 2 H); ^{13}C NMR ($CDCl_3$) δ 154.9, 151.5, 150.9, 135.8, 131.0, 128.8, 128.3, 127.1, 106.0, 105.7, 79.7, 71.1, 69.4, 60.5, 58.1, 53.1, 28.6, 27.0, 23.2, 21.2, 14.3; MS (ES^+) *m/z* 486.1 $(M+H)^+$.

1-(4-(4-(3-(Benzyloxy)-2-nitrophenoxy)butyl)piperazin-1-yl)-2-(1*H*-imidazol-1-yl)ethanone (10). Trifluoroacetic acid (2 mL) was added dropwise to a solution of **9b** (0.505 g, 1.04 mmol) in dichloromethane (8 mL), and the resultant mixture was stirred at room temperature for 3 h. The solution was concentrated to leave **9c** (0.52 g, quantitative) as the crystalline trifluoroacetate salt. This was then dissolved into DMF (10 mL) and *N*,*N*-diisopropylethylamine (3 mL) and the mixture was stirred at room temperature for 10 min followed by treatment with 1-ethyl-3-[3-dimethylaminopropyl]carbodiimide hydrochloride (EDC·HCl; 0.22 g, 1.14 mmol), *N*-hydroxybenzotriazole (HOBt; 0.175 g, 1.14 mmol) and imidazoacetic acid (0.197 g, 1.56 mmol, purchased from Tokyo Chemical Industry Co. Ltd.) After stirring under N_2 at room temperature for 16 h, DMF was removed *in vacuo* and the residue was distributed between dichloromethane and 5% aq sodium carbonate. The organic phase was dried and concentrated to an oil that was purified by flask silica gel chromatography eluting with methanol : CH_2Cl_2 : NH_4OH (5 : 95 : 0.5). Product fractions were pooled and concentrated to give **10** (0.37 g, 72%) as a yellow oil: ^{1}H NMR ($CDCl_3$) δ 7.49 (s, 1 H), 7.36 (m, 5 H), 7.26 (m, 1 H), 7.09 (s, 1 H), 6.95 (s, 1 H), 6.61 (m, 1H), 5.16 (s, 2 H), 4.75 (s, 2 H), 4.07 (t, *J* = 5.9 Hz, 2 H), 3.62 (m, 2 H), 3.44 (m, 2 H), 2.42 (t, *J* = 4.9 Hz, 4 H), 2.39 (t, *J* = 7.2 Hz, 2 H), 1.81 (m, 2 H), 1.62 (m, 2 H); ^{13}C NMR ($CDCl_3$) δ 164.4, 151.3, 150.8, 138.0, 135.6, 131.0, 129.5, 128.7, 128.2, 127.0, 120.1, 105.9, 105.5, 70.9, 69.1, 57.6, 52.6, 47.9, 45.1, 42.3, 26.7, 22.9; MS (ES^+) *m/z* 494.1 $(M+H)^+$.

3-(4-(4-(2-(1*H*-Imidazol-1-yl)ethyl)piperazin-1-yl)butoxy)-2-aminophenol (11a). Compound **9a** (0.86 g, 1.8 mmol) was dissolved in a mixture of 10% aq HCl (10 mL) and methanol (90 mL) in a Parr hydrogenation bottle. Catalyst (20% $Pd(OH)_2/C$, 0.05 g) was added and the mixture was hydrogenated at 40 psi H_2 for ~40 h. The reaction mixture was rapidly filtered over Celite®, and the filtrate was concentrated and diluted with ethyl acetate. The solution was washed with 5% aq sodium carbonate, dried, and concentrated to give **11a** (0.61 g, 95%) as a brown solid: ^{1}H NMR ($CDCl_3$) δ 7.56 (s, 1 H), 7.05 (s, 1 H), 6.96 (s, 1 H), 6.52 (t, *J* = 7.2 Hz, 1 H), 6.44 (s, 1 H), 6.37 (d, *J* = 8.0 Hz, 1 H), 3.98 (m, 4 H), 2.66 (t, *J* = 6.2 Hz, 2 H), 2.49 (bs, 8 H), 2.41 (t, *J* = 6.5 Hz, 2 H), 1.78 1.68 (m, 2 H); ^{13}C NMR ($CDCl_3$) δ 147.6, 145.5, 128.6, 124.9, 119.4, 117.3, 108.7, 103.7, 68.1, 58.4, 58.2, 53.0, 50.4, 44.7, 27.5, 23.3; MS (ES^+) *m/z* 360.1 $(M+H)^+$.

1-(4-(4-(2-Amino-3-hydroxyphenoxy)butyl)piperazin-1-yl)-2-(1*H*-imidazol-1-yl)ethanone (11b). Compound **10** (0.37 g, 0.75 mmol) was dissolved in a mixture of 10% aq HCl (5 mL) and methanol (45 mL) in a Parr hydrogenation bottle. Catalyst (20% $Pd(OH)_2/C$, 0.02 g) was added and the mixture was hydrogenated at 40 psi H_2 for ~40 h. Workup as described above for the synthesis of **11a** gave **11b** (0.27 g, 98%) as a brown solid: ^{1}H NMR (CD_3OD) δ 7.78 (s, 1 H), 7.13 (s, 1 H), 7.06 (s, 1 H), 6.58 (m, 1 H), 6.43 (m, 2 H), 5.08 (s, 2 H), 4.03 (t, *J* = 5.9 Hz, 2 H), 3.66 (s, 2 H), 3.62 (s, 2 H), 2.75 (s, 2 H), 2.65 (m, 4 H), 1.82 (m, 4 H); ^{13}C NMR (CD_3OD) δ 174.8, 165.8, 148.0, 145.8, 138.1, 126.0, 123.0, 121.3, 118.2, 107.8, 103.5, 67.7, 57.3, 52.1, 51.8, 43.5, 40.9, 26.8, 22.2, 20.1; MS (ES^+) *m/z* 374.1 $(M+H)^+$.

Benzoxazinorifamycin (2b). A mixture of aminophenol **7** (0.336 g, 1.5 mmol), rifamycin S (**12**; 2.085 g, 3 mmol) and 1,4-dioxane (20 mL) was stirred at room temperature overnight. The mixture was then concentrated to a black solid and dissolved into 20 mL of methanol followed

by the addition of MnO_2 (0.3 g, 3.45 mmol). The mixture was stirred at room temperature for 30 min and MnO_2 was filtered over Celite®. Methanol was removed to give dark residue which was purified by flash silica gel chromatography eluting with dichloromethane : methanol (95 : 5 to 90 : 10). Product fractions were combined and concentrated to give partially purified **2b** as a deep purple solid. Further purification by preparative TLC was conducted on a 20 mg scale, eluting the plate with dichloromethane : methanol (90 : 10). The yield is ~55%. R_f = 0.58 (dichloromethane : methanol, 85 : 15); HPLC t_R 6.1 min (95.4% purity); ^{1}H NMR ($CDCl_3$) δ 7.48 (t, *J* = 8.4 Hz, 1 H), 6.92 (d, *J* = 8.2 Hz, 2 H), 5.98 (d, *J* = 15.4 Hz, 2 H), 5.14 (bs, 2 H), 4.97 (m, 1 H), 4.41 (t, *J* = 11.6, 2 H), 3.29 (s, 2 H), 3.13 (s, 1 H), 3.08 (s, 3 H), 3.01 (d, *J* = 9.3, 2 H), 2.65 (m, 4 H), 2.29 (s, 3 H), 2.09 (s, 3 H), 2.05 (s, 3 H), 1.79 (s, 3 H), 1.70 (m, 2 H), 1.60 (m, 2 H), 1.25 (s, 3 H), 1.15 (t, *J* = 7.1 Hz, 6 H), 0.94 (d, *J* = 7.1 Hz, 3 H), 0.76 (d, *J* = 6.9 Hz, 3 H), 0.63 (d, *J* = 7.1 Hz, 3 H); MS (ES^+) *m/z* 900.1 $(M+H)^+$; HRMS (MALDI) calcd for $C_{49}H_{61}N_3O_{13}$ $[(M + H)^+]$, 900.4277; found 900.4269.

Benzoxazinorifamycin (2c) A mixture of aminophenol **11a** (80 mg, 0.22 mmol), rifamycin S (**12**; 220 mg, 0.32 mmol) and 1,2-dichloroethane (10 mL) was stirred at room temperature for 16 h. . The reaction mixture was then concentrated to a black solid and dissolved into 10 mL of methanol followed by the addition of MnO_2 (80 mg, 0.92 mmol). The mixture was stirred at room temperature for 30 min and MnO_2 was filtered over Celite®. Methanol was removed to give dark residue which was loaded directly onto a flash silica gel column, and was eluted with dichloromethane/methanol/ NH_4OH (94 : 6 : 0.5). Product fractions were pooled and concentrated to give a solid that was further purification by preparative TLC, eluting the plate with dichloromethane/methanol (92 : 8). The product band was processed to give **2c** (170 mg,

74%) as a dark purple solid: HPLC t_R 5.15 min (91.7% purity); ^{1}H NMR ($CDCl_3$) δ 7.56 (s, 1 H), 7.48 (t, *J* = 8.4 Hz, 1 H), 7.04 (s, 1 H), 6.98 (s, 1 H), 6.92 (d, *J* = 8.3 Hz, 1 H), 6.80 (d, *J* = 8.2 Hz, 1 H), 5.97 (m, 2 H), 5.12 (bs, 2 H), 4.94 (m, 1 H), 4.24 (t, *J* = 5.6 Hz, 2 H), 4.03 (t, *J* = 6.5 Hz, 2 H), 3.09 (s, 3 H), 3.01 (d, *J* = 9.3 Hz, 1 H), 2.68 (m, 2 H), 2.52 (bs, 11 H), 2.29, (s, 3 H), 2.09 (s, 3 H), 2.05 (s, 6 H), 1.80 (s, 5 H), 1.69 (m, 2 H), 1.60 (m, 2 H), 1.25 (s, 3 H), 0.93 (s, 3 H), 0.75 (s, 3 H), 0.64 (s, 3 H); MS (ES^+) *m/z* 1035.1 $(M+H)^+$; HRMS (MALDI) calcd for $C_{49}H_{61}N_3O_{13}$ [$(M + H)^+$], 1035.5074; found 1035.5095.

Benzoxazinorifamycin (2d) Reaction of a mixture of aminophenol **11b** (30 mg, 0.08 mmol), rifamycin S (**12**; 102 mg, 0.15 mmol) and 1,2-dichloroethane (4 mL) and subsequent purification were carried out exactly as described above for the synthesis of **2c** to provide **2d** (29 mg, 34.5%) as a dark purple solid: HPLC t_R = 5.11 min (91.8% purity); ^{1}H NMR ($CDCl_3$) δ 7.50 (m, 2 H), 7.10 (s, 1 H), 6.95 (m, 2 H), 6.87 (d, *J* = 8.3 Hz, 1 H), 5.98 (s, 1 H), 5.96 (s, 1 H), 5.30 (s, 2 H), 4.95 (m, 1 H), 4.76 (m, 2 H), 4.25 (m, 2 H), 3.68 (s, 1 H), 3.63 (s, 1 H), 3.49 (s, 1 H), 3.44 (s, 1 H), 3.11 (s, 3 H), 3.03 (s, 1 H), 2.58 (m, 2 H), 2.51 (m, 4 H), 2.29 (s, 3 H), 2.09 (s, 3 H), 2.06 (s, 3 H), 1.86 (d, *J* = 8.5 Hz, 1 H), 1.80 (s, 3 H), 1.68 (s, 2 H), 1.61 (bs, 9 H), 1.25 (s, 3 H), 0.94 (s, 3 H), 0.75 (s, 3 H), 0.65 (s, 3 H). MS (ES^+) *m/z* 1049.2 $(M+H)^+$; HRMS (MALDI) calcd for $C_{49}H_{61}N_3O_{13}$ [$(M + H)^+$], 1049.4866; found 1049.4857.

A1.4 Figures

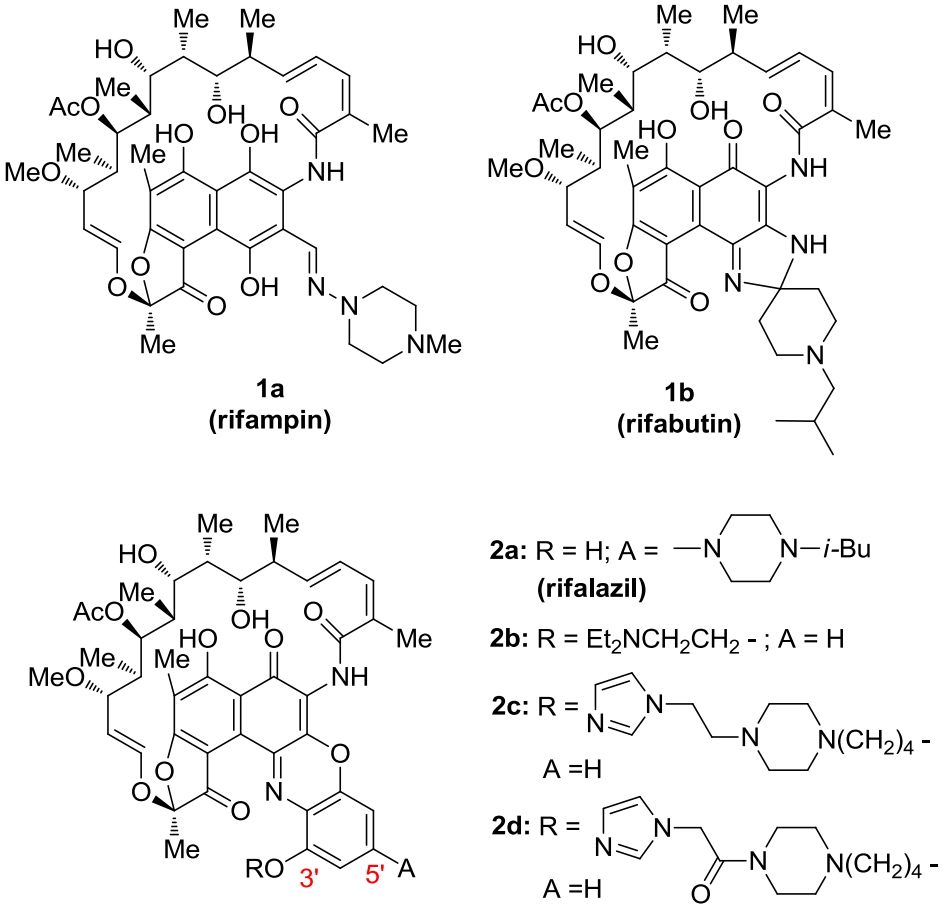

Figure A1.1. Structures of reference agents (1a, 1b, 2a) and novel benzoxazinorifamycins (2b−d).

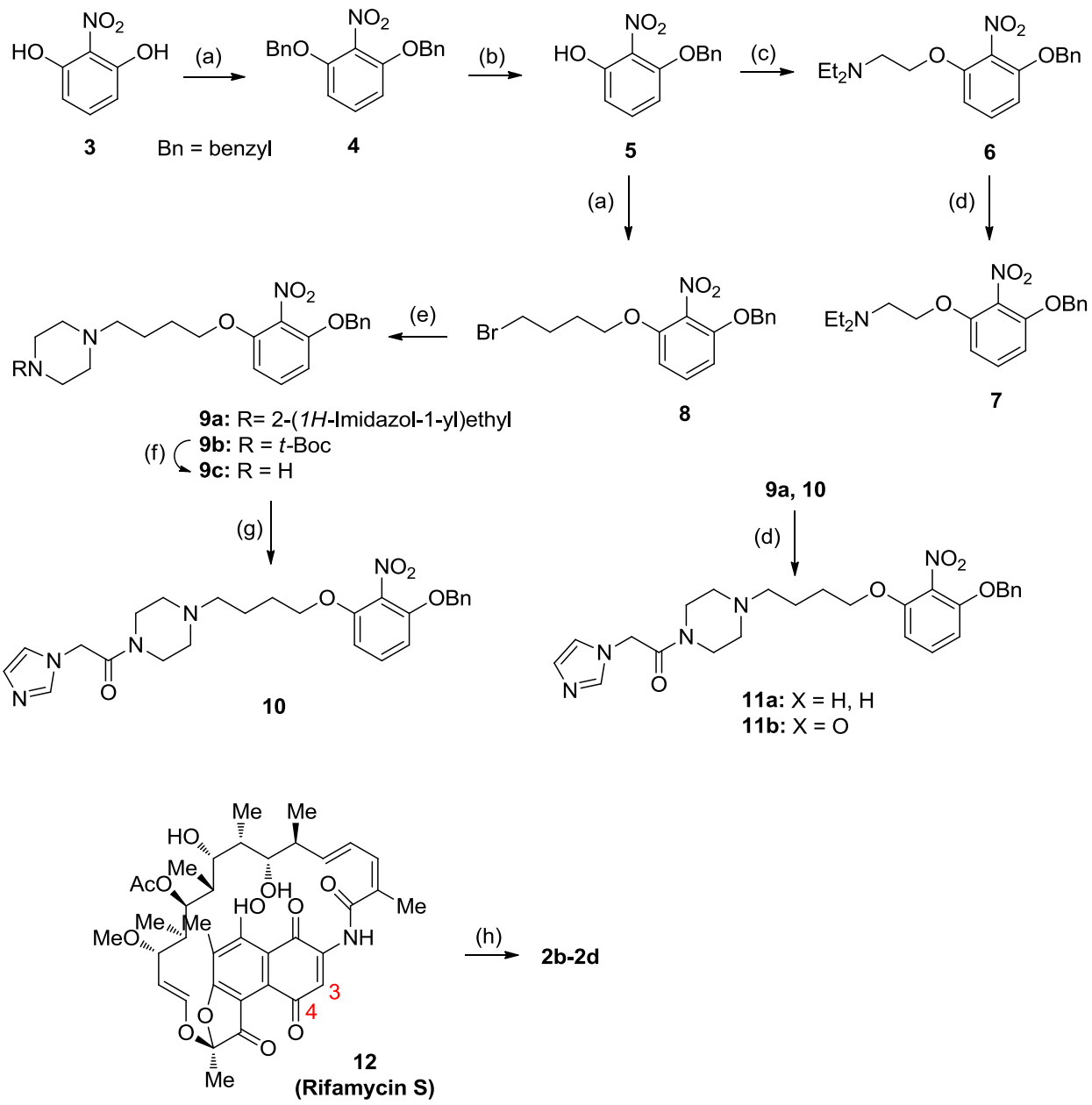

Scheme A1.1. Synthesis of 2b-2d. Reagents and conditions: (a) benzyl bromide (for **3**) and 1,4-dibromobutane (for **5**), Cs_2CO_3, DMF, 25 °C, 12−16 h, 93−95%; (b) BCl_3, DCM, −78 °C, 1 h, 82%; (c) $Et_2NCH_2CH_2Cl{\cdot}HCl$, Cs_2CO_3, acetone, 50 °C, 3 h, 93%; (d) 20% Pd/C, H_2 (40 psi), 25 °C, 20−40 h, MeOH/HOAc (9:1) for **6**; MeOH/10% aqueous HCl (9:1) for **9a**, **10**; 81 − 98%; (e) 1-[2-(1H-imidazol-1-yl)ethyl]piperazine or 1-Boc-piperazine, DIPEA, CH_3CN, reflux, 12−18 h, 68−99%; (f) TFA, DCM, 25 °C, 3 h; (g) 2-(1H-imidazol-1-yl)acetic acid, DIPEA, EDC·HCl, HOBT, DMF, 25 °C, 16 h, 72% from **9b**; (h) **7**, **11a**, or **11b**; p-dioxane or 1,2-DCE, MnO_2, 25 °C to reflux, 35−74%.

A1.5 References

1. WHO Report 2008 Global Tuberculosis Control: Surveillance, Planning, Financing. *World Health Organization: Geneva, Switzerland* **2008**.
2. Barrera, L., *The Basics of Clinical Bacteriology. In Tuberculosis 2007: From Basic Science to Patient Care*. Amedeo Challenge: 2007.
3. Garcia, A. B.; Palacios, J. J.; Ruiz, M. J.; Barluenga, J.; Aznar, F.; Cabal, M. P.; Garcia, J. M.; Diaz, N. Strong in vitro activities of two new rifabutin analogs against multidrug-resistant Mycobacterium tuberculosis. *Antimicrobial agents and chemotherapy* **2010,** *54*, (12), 5363-5.
4. Koul, A.; Arnoult, E.; Lounis, N.; Guillemont, J.; Andries, K. The challenge of new drug discovery for tuberculosis. *Nature* **2011,** *469*, (7331), 483-90.
5. Siddiqi, M. I.; Kumar, A. Review of knowledge for rational design and identification of anti-tubercular compounds. *Expert opinion on drug discovery* **2009,** *4*, (10), 1005-15.
6. Lienhardt, C.; Vernon, A.; Raviglione, M. C. New drugs and new regimens for the treatment of tuberculosis: review of the drug development pipeline and implications for national programmes. *Current opinion in pulmonary medicine* **2010,** *16*, (3), 186-93.
7. Aristoff, P. A.; Garcia, G. A.; Kirchhoff, P. D.; Showalter, H. D. Rifamycins--obstacles and opportunities. *Tuberculosis* **2010,** *90*, (2), 94-118.
8. Saito, H.; Tomioka, H.; Sato, K.; Emori, M.; Yamane, T.; Yamashita, K.; Hosoe, K.; Hidaka, T. In vitro antimycobacterial activities of newly synthesized benzoxazinorifamycins. *Antimicrobial agents and chemotherapy* **1991,** *35*, (3), 542-7.
9. Lounis, N.; Roscigno, G. In vitro and in vivo activities of new rifamycin derivatives against mycobacterial infections. *Current pharmaceutical design* **2004,** *10*, (26), 3229-38.
10. Luna-Herrera, J.; Reddy, M. V.; Gangadharam, P. R. In vitro activity of the benzoxazinorifamycin KRM-1648 against drug-susceptible and multidrug-resistant tubercle bacilli. *Antimicrobial agents and chemotherapy* **1995,** *39*, (2), 440-4.
11. Tomioka, H. Current status of some antituberculosis drugs and the development of new antituberculous agents with special reference to their in vitro and in vivo antimicrobial activities. *Current pharmaceutical design* **2006,** *12*, (31), 4047-70.
12. Yamamoto, T.; Amitani, R.; Suzuki, K.; Tanaka, E.; Murayama, T.; Kuze, F. In vitro bactericidal and in vivo therapeutic activities of a new rifamycin derivative, KRM-1648, against Mycobacterium tuberculosis. *Antimicrobial agents and chemotherapy* **1996,** *40*, (2), 426-8.
13. Moghazeh, S. L.; Pan, X.; Arain, T.; Stover, C. K.; Musser, J. M.; Kreiswirth, B. N. Comparative antimycobacterial activities of rifampin, rifapentine, and KRM-1648 against a collection of rifampin-resistant Mycobacterium tuberculosis isolates with known rpoB mutations. *Antimicrobial agents and chemotherapy* **1996,** *40*, (11), 2655-7.
14. Yang, B.; Koga, H.; Ohno, H.; Ogawa, K.; Fukuda, M.; Hirakata, Y.; Maesaki, S.; Tomono, K.; Tashiro, T.; Kohno, S. Relationship between antimycobacterial activities of rifampicin, rifabutin and KRM-1648 and rpoB mutations of Mycobacterium tuberculosis. *The Journal of antimicrobial chemotherapy* **1998,** *42*, (5), 621-8.
15. Mullin, S.; Rothstein, D. M.; Murphy, C. K. Activity of novel benzoxazinorifamycins against rifamycin-resistant Streptococcus pyogenes. *Antimicrobial agents and chemotherapy* **2006,** *50*, (5), 1908-9.
16. Roblin, P. M.; Reznik, T.; Kutlin, A.; Hammerschlag, M. R. In vitro activities of rifamycin derivatives ABI-1648 (Rifalazil, KRM-1648), ABI-1657, and ABI-1131 against Chlamydia trachomatis and

recent clinical isolates of Chlamydia pneumoniae. *Antimicrobial agents and chemotherapy* **2003,** *47*, (3), 1135-6.
17. Brooks, J. V.; Orme, I. M. Evaluation of once-weekly therapy for tuberculosis using isoniazid plus rifamycins in the mouse aerosol infection model. *Antimicrobial agents and chemotherapy* **1998,** *42*, (11), 3047-8.
18. Klemens, S. P.; Grossi, M. A.; Cynamon, M. H. Activity of KRM-1648, a new benzoxazinorifamycin, against Mycobacterium tuberculosis in a murine model. *Antimicrobial agents and chemotherapy* **1994,** *38*, (10), 2245-8.
19. Kelly, B. P.; Furney, S. K.; Jessen, M. T.; Orme, I. M. Low-dose aerosol infection model for testing drugs for efficacy against Mycobacterium tuberculosis. *Antimicrobial agents and chemotherapy* **1996,** *40*, (12), 2809-12.
20. Klemens, S. P.; Cynamon, M. H. Activity of KRM-1648 in combination with isoniazid against Mycobacterium tuberculosis in a murine model. *Antimicrobial agents and chemotherapy* **1996,** *40*, (2), 298-301.
21. Lenaerts, A. M.; Chase, S. E.; Cynamon, M. H. Evaluation of rifalazil in a combination treatment regimen as an alternative to isoniazid-rifampin therapy in a mouse tuberculosis model. *Antimicrobial agents and chemotherapy* **2000,** *44*, (11), 3167-8.
22. Shoen, C. M.; Chase, S. E.; DeStefano, M. S.; Harpster, T. S.; Chmielewski, A. J.; Cynamon, M. H. Evaluation of rifalazil in long-term treatment regimens for tuberculosis in mice. *Antimicrobial agents and chemotherapy* **2000,** *44*, (6), 1458-62.
23. Mae, T.; Hosoe, K.; Yamamoto, T.; Hidaka, T.; Ohashi, T.; Kleeman, J. M.; Adams, P. E. Effect of a new rifamycin derivative, rifalazil, on liver microsomal enzyme induction in rat and dog. *Xenobiotica; the fate of foreign compounds in biological systems* **1998,** *28*, (8), 759-66.
24. Rose, L. M. P., D. J.; Montgomery, A. B. Method for Treatment of Bacterial Infections with Once or Twice Weekly Administered Rifalazil. 2000.
25. Dietze, R.; Teixeira, L.; Rocha, L. M.; Palaci, M.; Johnson, J. L.; Wells, C.; Rose, L.; Eisenach, K.; Ellner, J. J. Safety and bactericidal activity of rifalazil in patients with pulmonary tuberculosis. *Antimicrobial agents and chemotherapy* **2001,** *45*, (7), 1972-6.
26. Barry, P. J.; O'Connor, T. M. Novel agents in the management of Mycobacterium tuberculosis disease. *Current medicinal chemistry* **2007,** *14*, (18), 2000-8.
27. Portero, J.-L. R., M. New anti-tuberculosis therapies. *Expert. Opin. Ther. Pat.* **2007,** *17*, 617−637.
28. Yamane, T.; Hashizume, T.; Yamashita, K.; Konishi, E.; Hosoe, K.; Hidaka, T.; Watanabe, K.; Kawaharada, H.; Yamamoto, T.; Kuze, F. Synthesis and biological activity of 3'-hydroxy-5'-aminobenzoxazinorifamycin derivatives. *Chemical & pharmaceutical bulletin* **1993,** *41*, (1), 148-55.
29. Dhingra, K.; Maier, M. E.; Beyerlein, M.; Angelovski, G.; Logothetis, N. K. Synthesis and characterization of a smart contrast agent sensitive to calcium. *Chemical communications* **2008**, (29), 3444-6.
30. Binggeli, A. C., A. D.; Green, L.; Guba, W.; Maerki, H. P.; Martin, R. E.; Mohr, P. Preparation of Benzoxazole, Oxazolopyridine, Benzothiazole and Thiazolopyridine Derivatives as Somatostatin Receptor Modul a tors and Antidi abet i c Compounds. 2007.
31. Havera, H. J. S., W. G. 3-Substituted-5-phenyl-5-pyridylhydantoins. US3994904A, 1976.

APPENDICES 2

STUDY ON THE FACTORS RESPONSIBLE FOR THE LOW BIOAVAILABILITY OF DABIGATRAN ETEXILATE

A2.1 Introduction:

Dabigatran etexilate (DE; Pradaxa®, Boehringer Ingelheim Pharma GmbH & Co.) is approved as an oral anticoagulant for the prevention of stroke and thromboembolism in the form of a prodrug of the active ingredient, dabigatran.[1-4] DE is a weak base with its pKa values of 4.0 and 6.7. Its solubility is low at neutral pH (3 µg/mL at pH 7.4) and it increases with decreasing pH.[5] An intrinsic permeability of 2.9 x 10^{-5} cm/s was determined in Caco-2 cell monolayer (log P = 3.8) which is comparable to that of metoprolol.[6-7] DE with high permeability and low solubility is classified as BCS IIb compound based on Biopharmaceutical Classification System (BCS).[8] DE has only 6-7% bioavailability when administrated as capsules.[9] The low solubility can be one of the potential reasons, other factors also have to be investigated for the poor oral bioavailability.

The disintegration and dissolution are the first steps for the oral absorption of drug products as well as the rate determining step for BCS II compounds (low solubility and high permeability). This process is significantly influenced by the formulation content, dosage form, and biopharmaceutical properties of specific drug substance. Therefore the in vitro dissolution of DE was interrogated here as the first factor to understand the absorption mechanism. The most commonly used USP dissolution apparatuses for dissolution tests are unable to accurately reflect

the dissolution of DE in the gastrointestinal (GI) tract with dynamic fluid volumes and pH changes. In this report we utilized a recently developed three compartments GastroIntestinal Simulator (GIS) apparatus to evaluate the in vitro dissolution profiles of DE capsules under dynamic pH conditions.[10] GIS system with separate gastric, duodenal and jejunal chambers could test in vitro dissolution of medications in fed/fasted condition by different gastric half-emptying time. The in vitro dissolution of metoprolol (BCS I) was tested with GIS system, and the observed dissolution profile was similar to the clinical studies under the gastric half-emptying time of 5-10 min.[10] In this report we adopted a gastric half-emptying time of 8 min to check the supersaturation and precipitation conditions of DE with capsule formulation under dynamic changes of pH in each chamber. Clinical study on DE 150 mg capsule showed that its bioavailability reduced to 70% in the patients concomitantly treated with pantoprazole (a proton pump inhibitor) relative to the ones without pantoprazole, indicating the impact of pH changes on the DE absorption.[11-12] Thus two sets of gastric buffers with pH of 2 and 6 were chosen to simulate the clinical studies with and without pantoprazole.

The prodrug dabigatran etexilate, but not dabigatran, is a substrate of P-glycoprotein (P-gp).[5-6] P-gp is one of the efflux transporters presenting along human intestinal tract and is another factor that could potentially affect the bioavailability of DE. As a P-gp substrate, DE is reported to have an efflux ratio of 13.8 in the Caco-2 monolayer transport study and the ratio was brought to 1 after P-gp activity was completely inhibited[6]. Clinically the bioavailability of DE capsule could be increased from 6.5 % to 15.6 % by pre-treatment with verapamil[13] and to 10.1% with clarithromycin.[14] When the patients were treated with rifampicin, a strong inducer of P-gp,[15] the DE absorptions were reduced more than half compared to those without rifampicin.[16] Transporter-mediated drug-drug interaction (DDI) studies were also conducted among DE and

many other known P-gp substrates and demonstrated significant interference of P-gp-mediated transport.[17]

Nevertheless, when examining the expression of P-gp transport within the small intestine, the upper segments of the GI tract where major absorption occur have low amounts of P-gp expressed while its amount increases along the GI tract.[18] Furthermore, some BCSII/IV drugs as P-gp substrates could have good oral bioavailability as summarized in table 1. All of the reported results suggest that P-gp is an important factor, but other factors, like solubility and stability, need to be taken into consideration to fully understand the absorption mechanism.

DE has two pro-moieties: an ethyl ester and a hexyl carbamate, and the hydrolysis of either of them will lower its permeability. Human carboxylesterase 1 and 2 (CES1 and CES2) have been reported accounting for the enzymatic hydrolysis of both pro-moieties,[15] and such hydrolysis was also inhibited by non-specific CES inhibitor in Caco-2 cell line.[6] In this report, the enzymatic degradation of DE was evaluated with human pancreatic tissue, human intestinal tissue and mouse intestinal fluid, to best mimic human digestive juices and the stability is compared with several ester prodrugs.

Solubility, in vitro dissolution rate, transporter mediated drug efflux, and chemical/enzymatic stability of DE are discussed here to address the potential factors affecting the bioavailability of dabigatran etexilate capsules. The results combined with previously reported clinical data suggest that the P-gp efflux effect and the enzymatic degradation of DE in GI tract are important factors for the low absorptions. Solubility of DE is increased significantly by the capsule components, thus plays a minor role in the absorption process.

A2.2 Results

Evaluation of solubility in DE absorption

The solubility of pure DE was tested at different pH values as illustrated in the solubility - pH curve (Figure 1). The lowest solubility is 2-3 µg/mL in buffer with pH > 5 while it increases by more than 1000-fold when the pH decreases. When only the solubility factor is considered in the DE absorption, the dissolution and absorption were postulated with a GastroPlus™ simulation by applying the measured solubility - pH curve as a parameter. P-gp and enzymatic effects were not applied in the virtual trials in this case. Results were plotted as a function of time for the first 24 h (Figure 2a, Table 2). DE was rapidly dissolved and precipitated in the first hour which was consistent with *in vivo* pH changes, and then more dissolved gradually with the absorption increased (Figure 2a dotted line). The total bioavailability (solid line) eventually reached about 80%. Discrepancy in the bioavailability from GastroPlus™ compared with clinical data (6-7 %) [9] could be observed when only evaluating solubility factor. This *in silico* postulation indicated the existence of other factors affecting DE absorption that are yet to be uncovered.

Dissolution profiles of DE capsules

In vitro dissolution profiles of dabigatran etexilate under dynamic pH changes were studied with GIS system. Gastric fluid and secretion buffers at two pH-value sets, 2.0 and 6.0, were adopted here to simulate clinical studies of orally administrated DE capsule with and without pantoprazole. Duodenal fluid buffer (50 mM PBS, pH 6.5) and duodenal secretion buffer (100 mM PBS, pH 6.5) were kept unchanged in both sets. Mixed buffers from gastric and duodenal chambers were transferred to a jejunal chamber after the experiment began. Crude samples were

collected every 3 minutes in a 2 - 47 min time frame from every chamber and centrifuged at 16,100 x g for 1.5 min. Supernatants were collected, mixed with 1 equivalent volume of methanol and analyzed as dissolution concentrations. Crude samples were then vortexed well, kept still at room temperature for 24 h, processed as above and analyzed as equilibrium concentrations.

As illustrated in figure 3, DE dissolved well in the gastric chamber at either pH 6.0 or 2.0, although the concentration didn't increase until 10 min after the experiment began caused by the disintegration rate (Figure 3a, 3d). After reaching a peak concentration at around 25 min, the concentration began to fall, indicating that all dosed drug was dissolved at this time point in the gastric chamber. The pumps for gastric transfer and secretion were set to stop at 48 min based on the gastric emptying time and the final amount of buffer remaining in gastric chamber. No significant concentration differences were observed in the samples after 24 hr, suggesting no supersaturation effect in the gastric chamber. This dissolution pattern was then confirmed by pH variations in gastric chamber, which were monitored by pH meters after each sample was drawn. The acidity of the gastric buffer at pH 6.0 was decreased by the components in the capsule, resulting in the increase of corresponding DE solubility (Figure 3g, dotted line).

In the duodenal chamber, the two sets of dissolutions were similar in the early stage but different later. Supersaturation was observed much sooner in experimental set of pH 6 than in the set of pH 2 (Figure 3e); however the dissolution concentration was not dramatically affected by the supersaturation effect. Similar to the gastric chamber, the buffer pH in duodenal chamber was also influenced by the acidic components in the DE capsule as illustrated in figure 3h.

Both the dissolution and equilibrium concentrations in the jejunal chamber with gastric pH of 6 were lower compared to those of gastric pH of 2, which suggests the impact from gastric pH on the dissolution of DE in the jejunal chamber (Figure 3c, f and h). Precipitations were observed in both sets, but were more pronounced in pH 6 experimental set. Generally, although both precipitation and supersaturation were observed in the jejunum chamber, the dissolved concentrations of DE could be increased by as much as 100-fold relative to pure DE, caused by the strong buffering ability of acidic components from the DE capsule.

Degradation of dabigatran etexilate

The chemical stability of DE was tested in buffers of pH 2.0 and 6.5, and found to be stable over 24 h (data not shown) as reported previously.[6] Besides chemical degradation, various hydrolases such as esterases, and peptidases exist in GI tract secretions, which could potentially hydrolyze DE. To best mimic degradation of DE in human pancreatic juice, DE was tested in human pancreatic tissue (HP) homogenate and mouse instestinal fluid (MIF). The degradation rate of DE was very fast in HP homogenate, showing a half-life of 24 ± 5 min, with the hydrolysis rate of the carbamate group 2-3 fold higher than the ester group (Figure 4)., The hydrolysis of both ester and carbamate groups was not inhibited by bis(4-nitrophenyl) phosphate (BNPP, known human carboxylesterases inhibitor[6, 9, 19]) in HP homogenate, but could be greatly inhibited by fluorophosphonate-PEG-rh (FP; a comprehensive serine hydrolase inhibitor[20]). The hydrolysis rates of DE and other ethyl ester prodrugs in MIF and human intestinal (HI) homogenate are listed in table 3 for comparison. In both HP homogenate and MIF, DE is hydrolyzed significantly faster than other prodrugs while rate differences are not significant in HI homogenate.

A2.3 Discussion

Solubility and dissolution issues are not significant contributors to the low bioavailability of DE capsules

Small-molecular therapeutic agents falling in the BCS II classification are characterized by high permeability and low solubility. Thus the solubility is always considered as their limitation during oral absorption process. The dissolution profiles for such drug products are required as important criteria to demonstrate bioequivalence. The solubility of dabigatran etexilate (DE), a weak base varies by more than 1000-fold under different pH conditions. To reflect the variation that dynamic pH condition poses on DE solubility, *in vitro* dissolution of DE capsules was tested in the gastrointestinal simulator (GIS) system.

In blank experiments without any tested drug products (Figure 3g-i), the pH value of duodenal buffer in GIS was lowered in the beginning by gastric buffer (pH 2.0). Duodenal buffer pH returned to neutral range when the buffer transfer rate decreased and more duodenal secretion buffer (100 mM PBS, pH 6.5) was added. On the other hand when DE capsule was added, duodenal buffer stayed acidic until most of the components in the capsule were transferred to the jejunal chamber after 40 min. When the gastric buffer was set to pH 6.0, it was acidified by the DE capsule. Such an acidic environment further extended to the duodenal and jejunal chambers.

The buffer system selected in our GIS study may not present *in vivo* due to the *in vivo* complexities and individual variations (fed or fasted). The goal in GIS *in vitro* dissolution studies outlined here is to demonstrate the impact of supersaturation effects and acidic components from the capsule formulation on the *in vitro* DE dissolution. The solubility of DE is improved

significantly by such effects in *in vitro* tests. The *in vivo* dissolution of DE capsule in the upper GI tract should provide equivalent or higher drug concentration in the case that the in vivo buffer system in fasted state is not stronger than that were used in our *in vitro* study.[21-22] In the human fed state, high-fat, high-calorie food does not affect the bioavailability of DE but only postpones its absorption,[12] and the *in vitro* test in such situation was not discussed in this report. Thus greatly increased concentrations of DE could be created by the supersaturation effect and acidic environment among dynamic pH environments, suggesting that solubility is not a significant contributor to the low bioavailability of DE in upper GI tract.

DE is rapidly degraded by digestive enzymes

Dabigatran, when dosed through i.v. infusion, was predominantly excreted via the urine (85.4%).[9] The prodrug dabigatran etexilate (DE) was predominantly excreted in feces (>80%) as dabigatran following p.o. administration of the DE capsule in a clinical radiolabeled pharmacokinetics study.[9] This can only be explained by hypothesizing that DE is degraded to dabigatran in the GI tract before absorption, considering dabigatran is not a P-gp substrate.[6, 17]

Degradation within the GI tract is a common phenomenon for drugs and prodrugs. The compounds with ester, amide, or even ether bond are vulnerable to chemical or enzymatic hydrolysis before absorption. When DE is transferred to duodenum and mixed with digestive juices, degradation starts. Based on the clinical studies, high concentrations of DE should be maintained in the duodenum and jejunum. DE was then rapidly hydrolyzed in lower parts of the GI tract with reduced concentration and eventually excreted as unabsorbed dabigatran. This assumption is also supported by a recent clinical study on the coadministration of clopidogrel and DE.[23] Clopidogrel is a prodrug that affects the hydrolysis of ethyl ester prodrugs through

drug-drug interactions[24]. When it is concomitantly administrated with DE, the bioavailability increased to 135% (AUC) relative to the studies without clopedogrel.

Interestingly, the hydrolysis of DE in HP homogenate could not be inhibited by BNPP, indicating that DE is hydrolyzed by other hydrolases besides CES1 and CES2. The hydrolysis results pointed out that other unknown activating enzyme with high efficacy against DE have yet to be uncovered in pancreatic tissue.

Collectively, the absorption mechanism of the DE capsule is depicted in figure 5. After DE is released from capsules and dissolved in the stomach, it enters the duodenum where it mixes with digesting juices. DE maintains a high concentration due to supersaturation effects, with less involvement of P-gp efflux and enzymatic degradation through duodenum to upper jejunum. While moving through the GI tract, DE precipitates out with the increasing pH and is effluxed by the P-gp transporter. Eventually, DE is hydrolyzed to dabigatran and then excreted. Its low oral bioavailability generally results from a combination of solubility, P-gp efflux and enzymatic degradation. Among these factors, DE solubility has the minor impact to the poor absorption of DE capsule.

A2.4 Experimental materials

Chemicals

Dabigatran etexilate mesylate 150 mg capsules (Pradaxa; Boehringer Ingelheim Pharma GmbH & Co), dabigatran etexilate free base (Shanghai Race Chemical Co., Ltd. Shanghai, China), Oseltamivir phosphate (Allichem LLC Baltimore, MD), Benazepril HCl (Selleck Chemicals, Houseton, TX) were purchased from commercial sources. Hydrochloric acid, sodium chloride,

sodium phosphate monobasic, acetonitril, trifluoroacetic acid, enalapril maleate, methanol and BNPP were purchased from Sigma-Aldrich Chemicals Co. (St. Louis, MO). FP-PEG-rhodamine were prepared as previously described[25]. Human small intestinal and human pancreatic tissues were obtained from the Tissue Core of the University of Michigan Comprehensive Cancer Center (UMCCC).

Dabigatran Etexilate Solubility Study

Phosphate buffers were prepared by sodium monobasic phosphate of 50 mM in DI water and pH values were adjusted to 2.0, 2.5, 3.0, 3.8, 4.0, 5.0, and 5.5 by hydrochloric acid or sodium hydroxide respectively. Extra amount of DE free base was added to the phosphate buffers and incubated at 37 °C with occasional vertex for 30 min. After centrifuged at 16,100 x g for 10 min at room temperature, supernatant was pipetted out and mix well with equal amount of methanol. Samples were then analyzed together with DE standard solution in methanol by an Agilent 1100 HPLC system. Briefly, chromatography was performed on a 4.6 x 150 mm 3.5 micron ZORBAX Eclipse XDB-C18 column (Agilent), and samples were eluted with an 9 min gradient of 20%- 90% buffer B (Buffer A: H_2O with 0.1% TFA; Buffer B: ACN with 0.1% TFA).

Dissolution Study

Dissolution studies by gastrointestinal simulator were performed as previously described[10]. Briefly, gastric, duodenal and jejunal chambers, are maintained at 37°C with stirring. Four pumps simulating gastric secretion, duodenal secretion, gastric emptying and duodenal emptying were calibrated before experiments started. Gastric-emptying time of 8 min was adopted in the experiments to simulate human fasted state. The gastric chamber was filled with 50 mL of 0.01

N HCl (pH 2.0) as gastric fluid and 250 mL of DI water as dose volume. Duodenal chamber was filled with 50 mL of 50 mM phosphate buffer (pH 6.5) and jejunal chamber was left empty. When the experiment started, the simulated gastric secretions (0.01 N HCl, pH 2.0) and duodenal secretion (100 mM phosphate buffer, pH 6.5) were pumped into gastric chamber and duodenal chamber at 1 mL/min, respectively. Gastric fluid were transferred into duodenal chamber following first-order rate ($t_{1/2}$ = 8 min). The fluid in duodenal chamber was transferred into jejunal chamber by duodenal - jejunal transferring pump which kept the duodenal fluid volume constant at 50 mL during the dissolution study. When simulating impact of pantoprazole, stomach fluid buffer and secretion buffer were replaced by 1 x 10^{-6} N HCl (pH 6.0) buffer, and other buffers and parameters were kept the same.

Crude solutions were sampled every 3 min from 2 min to 47 min from each chamber. After centrifuged at 16.100 x g for 1.5 min, supernatants were taken carefully, mixed with equal volume of methanol and analyzed as dissolution concentration by HPLC. Crude solution samples at each time point were vortexed, kept at room temperature for 24 h, then centrifuged and treated the same as above as equilibrium concentration. pH changes were monitored by pH meter every 3 min after crude samples were taken.

GastroPlus™ Simulation

The physicochemical and biopharmaceutical parameters of DE used in GastroPlus prediction are listed in Table 1. The solubility - pH curve from DE solubility study was used for the simulation. The variations in population physiology were defined as means with coefficients of variation and individual trials (n = 250) were randomly selected within those ranges. An initial dose of 150 mg with a dosing volume of 250 mL was selected in immediate release form (capsule). The gastric

emptying time of 15 min was adopted as a mean value. Other parameters were set based on previous report.[8]

Human tissue homogenates

The obtained human tissues were rinsed with phosphate buffer (50mM, pH7.4) for three times then grinded with a mortar and a pestle in liquid nitrogen. The yielded frozen powder was transferred to Dounce homogenizer, mixed with sterilized PBS buffer (50 mM, pH 7.4) and homogenized at 0 °C. Debris was pelleted by centrifugation for 5 min at 1,000 x g. Protein concentration was determined by the BCA assay and aliquots of the proteome were stored at -80 °C until use.

Collection of mouse intestinal fluid

All animal experiments were conducted using protocols approved by the University of Michigan Committee of Use and Care of Animals (UCUCA). The animals were housed and handled according to the University of Michigan Unit for Laboratory Animal Medicine guidelines. Mouse intestinal fluid (MIF) was collected from male BALB/c mice (Charles River, IN) weighing 20−25 g. Mice were sacrificed by CO_2 and intestines (~ 20 cm) were cut off from upper duodenum. PBS buffer of 400 µL (50 mM, pH 7.4) was flush into the intestinal tract. The liquid was squeezed out by hands gently, mixed and centrifuged at 16,100 x g for 5 min to remove feces. Protein concentration was determined by BCA assay and aliquots of the proteome were stored at -80 °C until use.

Enzymatic hydrolysis of dabigatran etexilate

Proteome samples (1 mg/mL) were treated with vehicle, BNPP (100 μM) or FP (5 μM) for 30 min at 37 °C in 50 mM Tris buffer (pH 7.4). DE was then added and incubated for 0, 15, 30, and 60 min or 2 h, 3 h (depended on different enzymatic activities). Reactions were terminated by equal volume of acetonitrile with 0.1% TFA and centrifuged at 16,100 x g for 5 min. Supernatants were filtered by with Microplate PVDF filter and analysed by an Agilent 1100 HPLC system. Briefly, chromatography was performed on a 4.6 x 150 mm 3.5 micron ZORBAX Eclipse XDB-C18 column (Agilent), and samples were eluted with an 11 min gradient of 2%-90% buffer B (Buffer A: H_2O with 0.1% TFA; Buffer B: ACN with 0.1% TFA). The hydrolysis rates of products generated were calculated based on the relative areas under the curve of the prodrugs and products.

A2.5 Figures

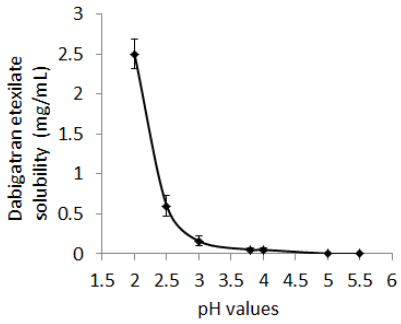

Figure A2.1. Solubility vs pH value curve of DE. DE was added to phosphate buffers with different acidity (as noted in figure) until saturated and incubated at 37 °C for 30 min with occasional vertex. Samples were centrifuged at 16,100 x g for 5min and supernatant was mixed well with equal volume of methanol as unknown samples. DE standard solution was prepared by dissolving DE in methanol. Unknown samples and standard solutions were analyzed together by HPCL. Results are represented as the average ± S.D. of 2-3 individual experiments.

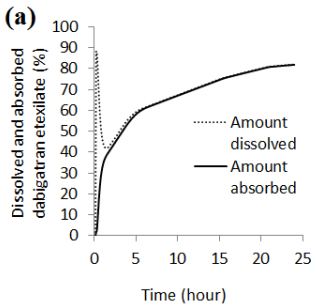

Figure A2.2. Amount of dissolved and absorbed dabigatran etexilate predicted by GastroPlus™: (a) percentage of DE relative to total dose in 24 h. (b) percentage of DE absorbed in each GI segment.

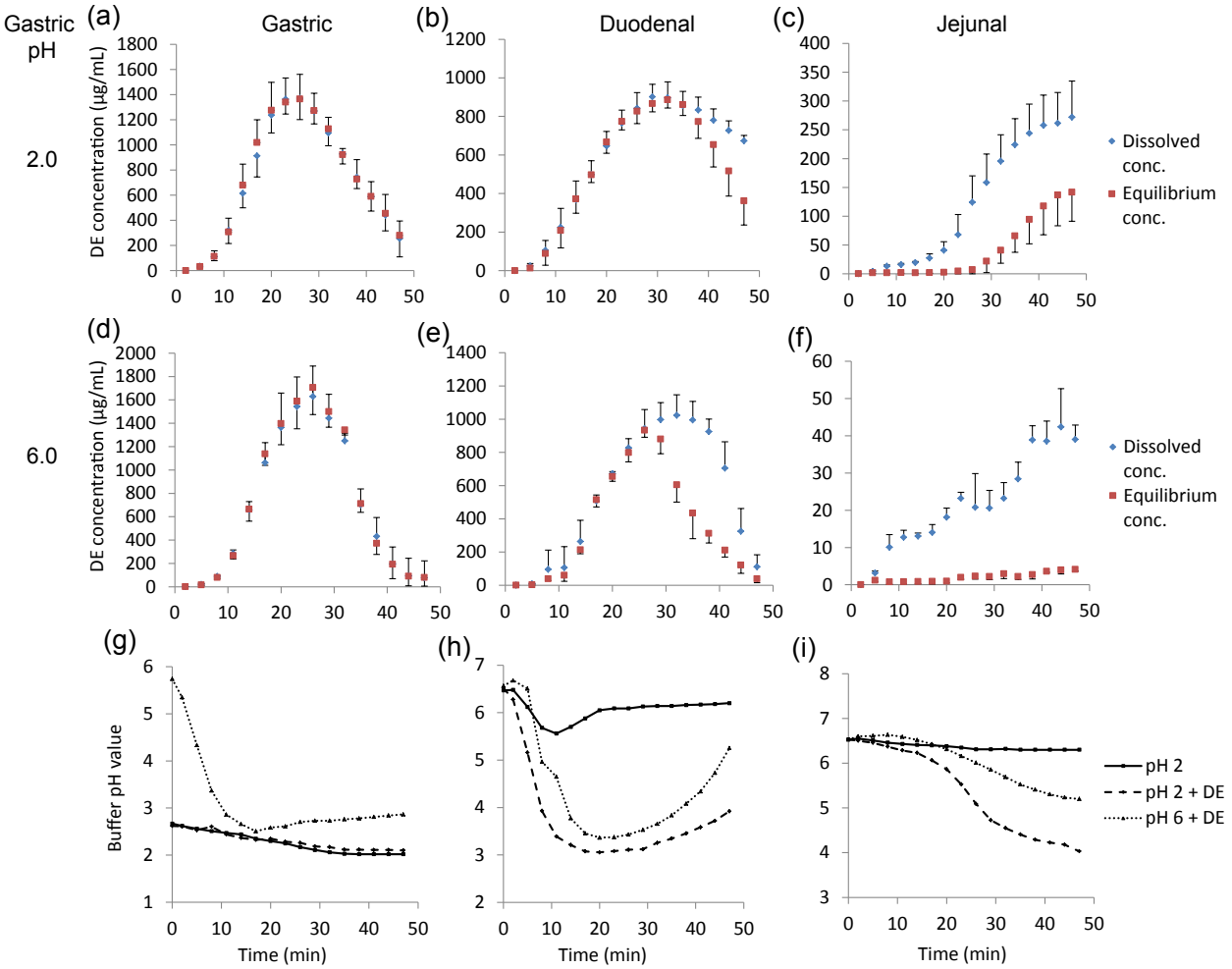

Figure A2.3. In vivo predictive dissolutions by gastrointestinal simulator. When pH value of stomach fluid and secretion buffers are at 2.0, the dissolution results of gastric chamber (a), duodenal chamber (b) and jejunal chamber (c); when pH value of stomach fluid and secretion buffers are at 6.0, the dissolution results of gastric chamber (d), duodenal chamber (e) and jejunal chamber (f); pH changes were monitored at each time point in gastric chamber (g), duodenal chamber (h) and jejunal chamber (i). Error bars represent S.D. of 3-4 independent experiments in dissolution study. pH values were presented as mean values of 2-3 independent experiments.

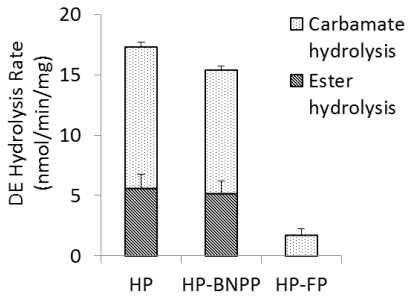

Figure A2.4. DE hydrolysis in human pancreatic tissue. Human pancreas homogenate (1 mg/mL) in Tris buffer (50 mM, pH 7.4) was treated with vehicle, BNPP and FP for 30 min, following the addition of DE at 37 °C. Samples were collected at 0, 15, 30 and 60 min, and then analyzed by HPCL. Results are represented as the average ± SEM of 2-3 individual experiments.

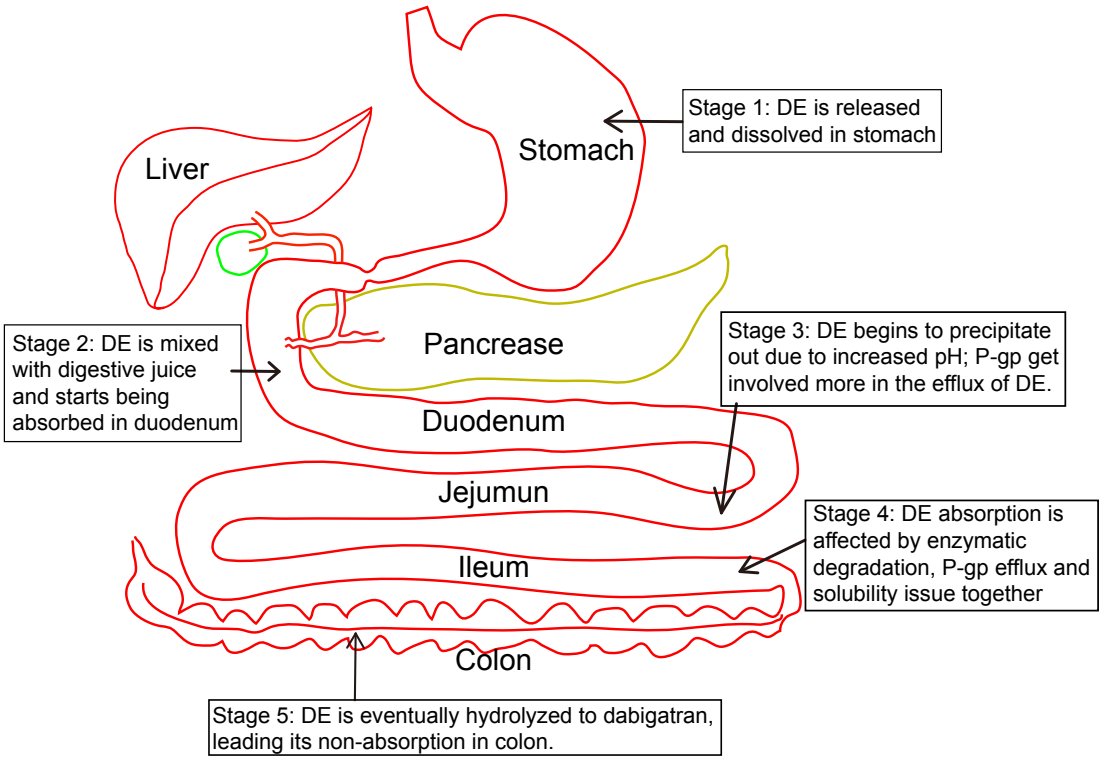

Figure A2.5. Absorption mechanism of dabigatran etexilate.

Table A2.1. List of BCSIIb drugs.

Compound	BCS class	LogP	pKa	Pgp substrate	bioavailability
dipyridamole	II	3.71	6.47	yes	27-59%[26]
itraconazole	II	6.2	3.7	yes	55%[27]
cefpodoxime	IV	0.05	3.2	yes	50%[28]
atazanavir	II	6.46	4.7	yes	60-68%[29]
indinavir	II / IV	5.62	3.8 / 6.2	yes	63%[30]
dasatinib	II	1.8	3.1 / 6.8	yes	well absorbed >50%[31]
erlotinib	II	2.87	5.4	yes	59%[32]

Table A2.2. Chemical/physiological/pharmacological parameters of dabigatran etexilate for GastoPlus™ simulation

Molecular weight	627.32 [5]	pKa	4.0 [5]
Dose	150 mg [4]	Mean precipitation time	900 s
Dose number	300 [A]	Human Peff	4.02×10^{-4} cm^2/s [6,B]
Dose volume	250 mL	Body weight	80.2 kg [9]
Solubility (pH 7.4)	0.003 mg/mL [5]	Vc	1.25 L/kg [9]
log P	3.8 [5]	CL	0.1162 L/h/kg [9]

Vc: Volume of Central Compartment.
[A] Calculated by GastroPlus™.
[B] Converted from Caco-2 perfusion coefficient by GastroPlus™.

Table A2.3. Hydrolysis rate (nmol/min/mg) of dabigatran etexilate in different protein homogenates.

	HP	MIF	HI
DE	17.2 ± 1.18	2.5 ± 0.5	0.63 ± 0.19
Benezapril	0.87 ± 0.2	0.83 ± 0.08	0.108 ± 0.02
Oseltamivir	<0.1	<0.1	<0.1
Enalapril	<0.1	<0.1	<0.1

A2.5 References

1. Wilson, J. A.; Goralski, K. B.; Soroka, S. D.; Morrison, M.; Mossop, P.; Sleno, L.; Wang, Y.; Anderson, D. R., An evaluation of oral dabigatran etexilate pharmacokinetics and pharmacodynamics in hemodialysis. *Journal of clinical pharmacology* **2014,** *54* (8), 901-9.
2. Greig, S. L.; McKeage, K., Dabigatran etexilate: a review of its use in the treatment of acute venous thromboembolism and prevention of venous thromboembolism recurrence. *Drugs* **2014,** *74* (15), 1785-800.
3. Hauel, N. H.; Nar, H.; Priepke, H.; Ries, U.; Stassen, J. M.; Wienen, W., Structure-based design of novel potent nonpeptide thrombin inhibitors. *Journal of medicinal chemistry* **2002,** *45* (9), 1757-66.
4. . Clinical Pharmacology and Biopharmaceutics Reviews, Application Number 22-512 2010. http://www.accessdata.fda.gov/drugsatfda_docs/nda/2010/022512Orig1s000ClinPharmR.pdf.
5. . Controlled PI template - Pradaxa 2014. http://files.boehringer.com.au/files/PI/Pradaxa%20PI.pdf.
6. Ishiguro, N.; Kishimoto, W.; Volz, A.; Ludwig-Schwellinger, E.; Ebner, T.; Schaefer, O., Impact of endogenous esterase activity on in vitro p-glycoprotein profiling of dabigatran etexilate in Caco-2 monolayers. *Drug metabolism and disposition: the biological fate of chemicals* **2014,** *42* (2), 250-6.
7. Incecayir, T.; Tsume, Y.; Amidon, G. L., Comparison of the permeability of metoprolol and labetalol in rat, mouse, and Caco-2 cells: use as a reference standard for BCS classification. *Molecular pharmaceutics* **2013,** *10* (3), 958-66.
8. Tsume, Y.; Mudie, D. M.; Langguth, P.; Amidon, G. E.; Amidon, G. L., The Biopharmaceutics Classification System: subclasses for in vivo predictive dissolution (IPD) methodology and IVIVC. *European journal of pharmaceutical sciences : official journal of the European Federation for Pharmaceutical Sciences* **2014,** *57*, 152-63.
9. Blech, S.; Ebner, T.; Ludwig-Schwellinger, E.; Stangier, J.; Roth, W., The metabolism and disposition of the oral direct thrombin inhibitor, dabigatran, in humans. *Drug metabolism and disposition: the biological fate of chemicals* **2008,** *36* (2), 386-99.
10. Takeuchi, S.; Tsume, Y.; Amidon, G. E.; Amidon, G. L., Evaluation of a three compartment in vitro gastrointestinal simulator dissolution apparatus to predict in vivo dissolution. *Journal of pharmaceutical sciences* **2014,** *103* (11), 3416-22.
11. Stangier, J.; Stahle, H.; Rathgen, K.; Roth, W.; Shakeri-Nejad, K., Pharmacokinetics and pharmacodynamics of dabigatran etexilate, an oral direct thrombin inhibitor, are not affected by moderate hepatic impairment. *Journal of clinical pharmacology* **2008,** *48* (12), 1411-9.
12. Stangier, J.; Eriksson, B. I.; Dahl, O. E.; Ahnfelt, L.; Nehmiz, G.; Stahle, H.; Rathgen, K.; Svard, R., Pharmacokinetic profile of the oral direct thrombin inhibitor dabigatran etexilate in healthy volunteers and patients undergoing total hip replacement. *Journal of clinical pharmacology* **2005,** *45* (5), 555-63.
13. Hartter, S.; Sennewald, R.; Nehmiz, G.; Reilly, P., Oral bioavailability of dabigatran etexilate (Pradaxa((R))) after co-medication with verapamil in healthy subjects. *British journal of clinical pharmacology* **2013,** *75* (4), 1053-62.
14. Delavenne, X.; Ollier, E.; Basset, T.; Bertoletti, L.; Accassat, S.; Garcin, A.; Laporte, S.; Zufferey, P.; Mismetti, P., A semi-mechanistic absorption model to evaluate drug-drug interaction with dabigatran: application with clarithromycin. *British journal of clinical pharmacology* **2013,** *76* (1), 107-13.
15. Backman, J. T.; Kivisto, K. T.; Olkkola, K. T.; Neuvonen, P. J., The area under the plasma concentration-time curve for oral midazolam is 400-fold larger during treatment with itraconazole than with rifampicin. *European journal of clinical pharmacology* **1998,** *54* (1), 53-8.

16. Hartter, S.; Koenen-Bergmann, M.; Sharma, A.; Nehmiz, G.; Lemke, U.; Timmer, W.; Reilly, P. A., Decrease in the oral bioavailability of dabigatran etexilate after co-medication with rifampicin. *British journal of clinical pharmacology* **2012,** *74* (3), 490-500.
17. Kishimoto, W.; Ishiguro, N.; Ludwig-Schwellinger, E.; Ebner, T.; Schaefer, O., In vitro predictability of drug-drug interaction likelihood of P-glycoprotein-mediated efflux of dabigatran etexilate based on [I]2/IC50 threshold. *Drug metabolism and disposition: the biological fate of chemicals* **2014,** *42* (2), 257-63.
18. Bruyere, A.; Decleves, X.; Bouzom, F.; Ball, K.; Marques, C.; Treton, X.; Pocard, M.; Valleur, P.; Bouhnik, Y.; Panis, Y.; Scherrmann, J. M.; Mouly, S., Effect of variations in the amounts of P-glycoprotein (ABCB1), BCRP (ABCG2) and CYP3A4 along the human small intestine on PBPK models for predicting intestinal first pass. *Molecular pharmaceutics* **2010,** *7* (5), 1596-607.
19. Laizure, S. C.; Parker, R. B.; Herring, V. L.; Hu, Z. Y., Identification of carboxylesterase-dependent dabigatran etexilate hydrolysis. *Drug metabolism and disposition: the biological fate of chemicals* **2014,** *42* (2), 201-6.
20. Adam, G. C.; Burbaum, J.; Kozarich, J. W.; Patricelli, M. P.; Cravatt, B. F., Mapping enzyme active sites in complex proteomes. *Journal of the American Chemical Society* **2004,** *126* (5), 1363-8.
21. Galia, E.; Nicolaides, E.; Horter, D.; Lobenberg, R.; Reppas, C.; Dressman, J. B., Evaluation of various dissolution media for predicting in vivo performance of class I and II drugs. *Pharmaceutical research* **1998,** *15* (5), 698-705.
22. Badawy, S. I.; Gray, D. B.; Zhao, F.; Sun, D.; Schuster, A. E.; Hussain, M. A., Formulation of solid dosage forms to overcome gastric pH interaction of the factor Xa inhibitor, BMS-561389. *Pharmaceutical research* **2006,** *23* (5), 989-96.
23. Hartter, S.; Sennewald, R.; Schepers, C.; Baumann, S.; Fritsch, H.; Friedman, J., Pharmacokinetic and pharmacodynamic effects of comedication of clopidogrel and dabigatran etexilate in healthy male volunteers. *European journal of clinical pharmacology* **2013,** *69* (3), 327-39.
24. Shi, D.; Yang, J.; Yang, D.; LeCluyse, E. L.; Black, C.; You, L.; Akhlaghi, F.; Yan, B., Anti-influenza prodrug oseltamivir is activated by carboxylesterase human carboxylesterase 1, and the activation is inhibited by antiplatelet agent clopidogrel. *The Journal of pharmacology and experimental therapeutics* **2006,** *319* (3), 1477-84.
25. Tully, S. E.; Cravatt, B. F., Activity-based probes that target functional subclasses of phospholipases in proteomes. *Journal of the American Chemical Society* **2010,** *132* (10), 3264-5.
26. Mahony, C.; Wolfram, K. M.; Cocchetto, D. M.; Bjornsson, T. D., Dipyridamol kinetics. *Clinical pharmacology and therapeutics* **1982,** *31* (3), 330-8.
27. Woolf, E. J.; Matuszewski, B. K., Simultaneous determination of unlabeled and deuterium-labeled indinavir in human plasma by high-performance liquid chromatography with tandem mass spectrometric detection. *Journal of pharmaceutical sciences* **1997,** *86* (2), 193-8.
28. Tremblay, D.; Dupront, A.; Ho, C.; Coussediere, D.; Lenfant, B., Pharmacokinetics of cefpodoxime in young and elderly volunteers after single doses. *The Journal of antimicrobial chemotherapy* **1990,** *26 Suppl E*, 21-8.
29. Colombo, S.; Buclin, T.; Cavassini, M.; Decosterd, L. A.; Telenti, A.; Biollaz, J.; Csajka, C., Population pharmacokinetics of atazanavir in patients with human immunodeficiency virus infection. *Antimicrobial agents and chemotherapy* **2006,** *50* (11), 3801-8.
30. Aungst, B. J., P-glycoprotein, secretory transport, and other barriers to the oral delivery of anti-HIV drugs. *Advanced drug delivery reviews* **1999,** *39* (1-3), 105-116.
31. Di Gion, P.; Kanefendt, F.; Lindauer, A.; Scheffler, M.; Doroshyenko, O.; Fuhr, U.; Wolf, J.; Jaehde, U., Clinical pharmacokinetics of tyrosine kinase inhibitors: focus on pyrimidines, pyridines and pyrroles. *Clinical pharmacokinetics* **2011,** *50* (9), 551-603.

32. Frohna, P.; Lu, J.; Eppler, S.; Hamilton, M.; Wolf, J.; Rakhit, A.; Ling, J.; Kenkare-Mitra, S. R.; Lum, B. L., Evaluation of the absolute oral bioavailability and bioequivalence of erlotinib, an inhibitor of the epidermal growth factor receptor tyrosine kinase, in a randomized, crossover study in healthy subjects. *Journal of clinical pharmacology* **2006,** *46* (3), 282-90.